N O T I C E

THIS DOCUMENT HAS BEEN REPRODUCED FROM MICROFICHE. ALTHOUGH IT IS RECOGNIZED THAT CERTAIN PORTIONS ARE ILLEGIBLE, IT IS BEING RELEASED IN THE INTEREST OF MAKING AVAILABLE AS MUCH INFORMATION AS POSSIBLE

9950-592

FINAL REPORT

Contract 955100

THERMACORE, INC.
LANCASTER, PENNSYLVANIA

N82-10110

(NASA-CR-164878) HEAT PIPE HEAT REJECTION SYSTEM AND DEMONSTRATION MODEL FOR THE NUCLEAR ELECTRIC PROPULSION (NEP) SPACECRAFT Final Report (Thermacore, Inc.) 135 p HC A07/MF A01 CSCL 21F G3/20 Unclas 27647

# HEAT PIPE HEAT REJECTION SYSTEM AND DEMONSTRATION MODEL FOR THE NUCLEAR ELECTRIC PROPULSION (NEP) SPACECRAFT

March 1981

Principal Investigator

Donald M. Ernst

Prepared for:

Jet Propulsion Laboratory

California Institute of Technology

Pasadena, California

RECEIVED NASA STI FACILITY ACCESS DEPT.

"This work was performed for the Jet Propulsion Laboratory, California Institute of Technology sponsored by the National Aeronautics and Space Administration under Contract NAS7-100."

## TECHNICAL CONTENT STATEMENT

"This report contains information prepared by Thermacore, Inc. under JPL sub-contract. Its content is not necessarily endorsed by the Jet Propulsion Laboratory, California Institute of Technology, or the National Aeronautics and Space Administration."

## ABSTRACT

This report covers the critical evaluation and subsequent redesign of the power conversion subsystem of the Nuclear Electric Propulsion (NEP) Spacecraft. As part of that evaluation and redesign, prototype heat pipe components for the heat rejection system were designed fabricated and tested. Based on the results of these tests in conjunction with changing mission requirements and changing energy conversion devices, new system designs were investigated.

The initial evaluation and redesign was based on state-of-the-art fabrication and assembly techniques for high temperature liquid metal heat pipes and energy conversion devices. The hardware evaluation demonstrated the validity of several complicated heat pipe geometries and wick structures, including an annular-to-circular transition, bends in the heat pipe, long heat pipe condensers and arterial wicks. Additionally, a heat pipe computer model was developed which describes the end point temperature profile of long radiator heat pipes to within several degrees celsius.

An ongoing evaluation and redesign, coupled with new concepts, generated computer programs for radiation coupled heat source to power conversion devices. Also a radiator design program was written from which an optimum mass heat pipe radiator can be generated. These computer programs and the heat pipe modeling program were transferred to the ongoing JPL Subcontract 955935 where they are being upgraded.

## TABLE OF CONTENTS

## FIGURES

## TABLES

# 1. INTRODUCTION

This report covers work done by Thermacore, Inc., Lancaster, PA under JPL Contract 955100, Heat Pipe Heat Rejection System and Demonstration Model for the Nuclear Electric Propulsion (NEP) Spacecraft. The work was performed between August 1978 and November 1980.

The work effort had several distinct phases and are presented as sections of this report. They are 1) initial system design evaluations and recommendations, 2) system redesign, 3) collector heat pipe demonstration model design, fabrication and test, 4) system evaluation and redesign, 5) radiator heat pipe design, fabrication and test, and 6) new concepts. These phases evolved as a result of ongoing interaction between JPL, Thermacore, and other JPL Contractors. Accordingly, this report does not present a final NEP System design or radiator heat pipe design, since the metamorphosis of the NEP spacecraft continues. Thermacore's continuing effort is being carried out under JPL Contract 955935.

## 2. INITIAL SYSTEM DESIGN EVALUATION

The NEP system design as of October 1977 is seen in Figure 1. The net electrical output at the end of a twelve year mission was to be 400 kW. The energy conversion devices were thermionic operating at a 15% conversion efficiency. The reactor power was 3,068 $kW_{th}$ and the heat rejection system was to remove 2600 $kW_{th}$ at 920°K.

The design had a 15 x 6 x 6 rectangular matrix of thermionic converters. There were ninety reactor core - emitter heat pipes, each having six thermionic converters. There were thirty-six collector heat pipes removing heat from each row of fifteen thermionic converters. These collector heat pipes were subsequently attached to twenty-four distributive heat pipes in two sets of six layers of a 3 x 4 matrix. These heat pipes distributed the heat to the radiator heat pipes for rejection of the 2600 kW of waste heat. The number of radiator heat pipes ranged from 200 continuous "hoola hoop" heat pipes, 14.13 meters in lengths, to 6000 straight heat pipes one-half meter in length.

This design was evaluated with respect to heat pipe capability, thermal performance of mechanical interfaces and their implication on the radiator's performance and mass, meteoroid protection, and assembly of pretestable arrays.

### 2.1. Materials Evaluation

The evaluation of materials of the heat rejection system must take several aspects into consideration. They are meteoroid protection, compatibility with potassium or sodium working fluids at 920°K, fabrication techniques for hermetically sealing similar and possible dissimilar materials in the presence of sodium or potassium, the

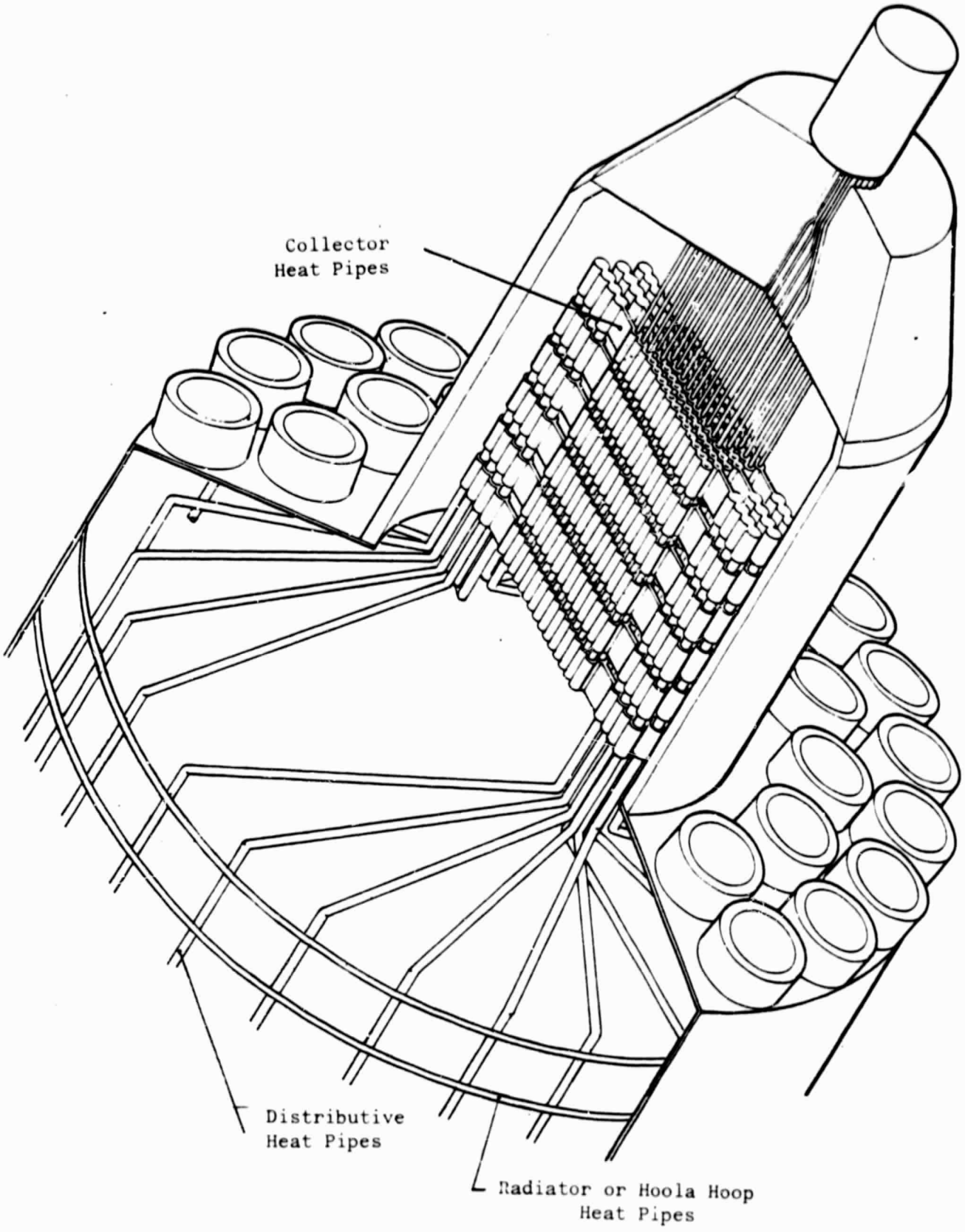


Figure 1

Cut-away View - Thermionic Matrix and
Heat Pipe Heat Rejection System -
October 1977

mechanical thermal interface between different materials, and the ability of the material to withstand the shock and vibration of launch.

2.1.1. Beryllium

Beryllium is recognized as one of the best materials for meteoroid protection because of its high puncture strength to mass ratio. However, using beryllium as an add-on armor plate to a conventional heat pipe material such as niobium or stainless steel may not be mass effective. Likewise, the ability to bond beryllium to stainless steel or niobium and that bonds thermal and mechanical integrity under thermal loading and cycling when added to the higher mass makes add-on armor look unattractive. Accordingly, the potential use of beryllium as a heat pipe envelope material was investigated.

The compatibility of beryllium with sodium and potassium has been investigated at various temperatures with similar results. Brett and Draycott[1] found no significant corrosion after 1000 hours at 700 C in distilled sodium with an argon cover gas under conditions favoring mass transfer. When oxygen was present (as $Na_2O$) corrosion occurred and fine gray beryllia powder was recovered from the specimen and the loop; however, no mass transfer of beryllium metal was observed. It was concluded that beryllium has a negligible solubility in sodium or potassium, but that corrosion occurs when oxygen is present by the formation and removal of beryllia.

Knolls Atomic Power Laboratory[2] has shown the various grades of beryllium to be resistant to attack in oxygen-free sodium ($> 0.01\%$) at 500 C, under static and dynamic conditions. In very pure sodium, observed weight changes have been within the experimental error, leading to the conclusion that beryllium is probably almost completely insoluble in sodium at 500 C.

To provide an indication of stress corrosion and also yield useful data on elevated temperature strength, a series of stress-rupture tests were performed at the Knolls Atomic Power Laboratory in sodium at 540 C. The results are seen in Table I and Figure 2. From metallographic examination, it was determined that there was no stress corrosion or intergranular penetration.

From this information, one concludes that since a sodium or potassium heat pipe is a self-contained, vacuum tight vessel which is fabricated and processed to exclude any possibility of oxygen contamination, then the use of beryllium as a containment vessel is possible from a corrosion point of view and may be worth pursuing experimentally.

The ability to obtain pure sodium or potassium by distillation can be enhanced by the use of calcium chips within the distillation pot and the heat pipe. Calcium forms more stable oxides than beryllium, and since calcium is appreciably soluble in sodium or potassium, calcium has a kinetic advantage in de-oxidation over beryllium. The use of calcium as a getter in purifying sodium and potassium in beryllium heat pipes is similar to the use of yttrium and hafnium in molybdenum or niobium-1 Zr heat pipes and zirconium in sodium and potassium in superalloy, niobium-1 Zr, or molybdenum heat pipes.

Los Alamos[3] tested a Nb-1% Zr potassium heat pipe, which had a beryllium liner placed between the heat pipe wall and wick. This pipe was operated for 1208 hours at 750 C with no evidence of mass transport. This data may be applicable to beryllium heat pipes. However, the gettering effect of the Nb-1% Zr container may have influenced the results. Also the ability to hermetically seal a beryllium vessel, which was not the case in the Los Alamos experiment, needs investigation.

## Table 1

**Stress Rupture Tests of Beryllium in Sodium at 1000 °F (538 °C)**

| Method of Fabrication | Tensile Stress (psi) | Time to Rupture (hrs.) | % Elong. |
|---|---|---|---|
| Hot-Pressed | 5000 | 1274 | 4 |
| | 7000 | 858 | 4 |
| | 8000 | 378 | 5 |
| | 9000 | 50 | — |
| | 10,000 | 221 | — |
| | 11,000 | 87 | — |
| Hot-Pressed and Extruded at 800 °F (425 °C) | 2000 | 955 | 2 |
| | 2500 | 285 | 4 |
| | 3000 | 148 | 0 |
| Hot-Pressed and Extruded at 2000 °F (1100 °C) | 2000 | 4536 | 2 |
| | 2500 | 5724 | 4 |
| | 3000 | 584 | 6 |
| | 4000 | 235 | 4 |
| | 6000 | 15 | 10 |
| | 10,000 | 4 | 8 |

Note: All specimens annealed and etched to remove machined surface before testing.

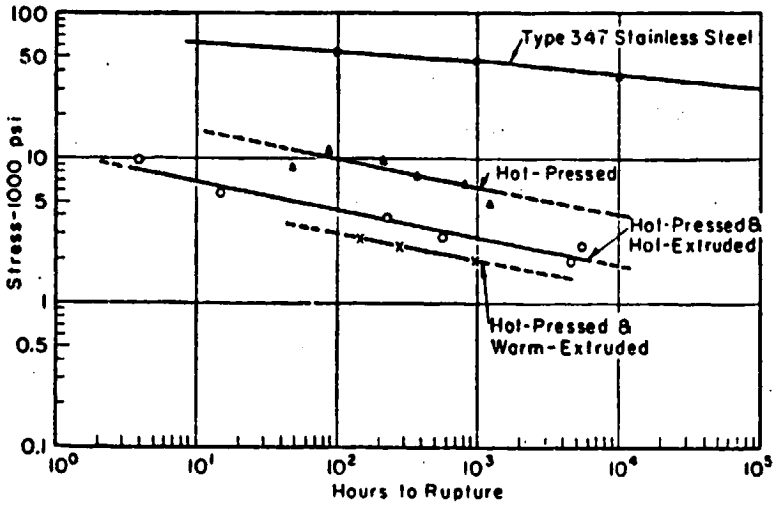


Rupture Strength of Beryllium. Temperature, 1000 °F (510 °C); atmosphere, sodium. (General Electric Co., Knolls Atomic Power Laboratory.)

Figure 2

Beryllium can be welded; however, the weldment is very brittle and as a result probably not acceptable for use with heat pipes that must survive launch. Other conventional sealing methods include a silver brazing alloys and the aluminum brazing alloys. While this may produce a hermetically sealed heat pipe, the compatibility of the brazing alloys is suspect and accordingly needs a thorough investigation with experimental testing of the more promising candidates.

One aspect of the use of beryllium which must be considered is its low creep strength at elevated temperature, and its ductility at room temperature conditions. The latter is of importance during launch when shock and vibration are greatest. The former will limit long life at elevated temperatures. Beryllium is currently being used as structural members in spacecraft thereby implying that the ductility at room temperature is sufficiently high. The high temperature, long term creep which would result from the internal pressure of the sodium or potassium working fluid is a problem of major concern and must be reckoned with if beryllium is to be considered as a heat pipe vessel material. Figure 3 shows the creep strength of beryllium at various temperatures.

If beryllium is to be used for the radiator heat pipes a beryllium-niobium joint is required at the niobium collector heat pipe. If the joint is external to the heat pipes then a high temperature braze material could be used. However, if either heat pipe is to be penetrated by the other, then the same problem exists as in the case of hermetically sealing a beryllium heat pipe.

The fact that beryllium has approximately twice the thermal expansion of niobium makes joining beryllium to niobium difficult and limits the prospects of pressure bonding, unless a graded type joint could be employed.

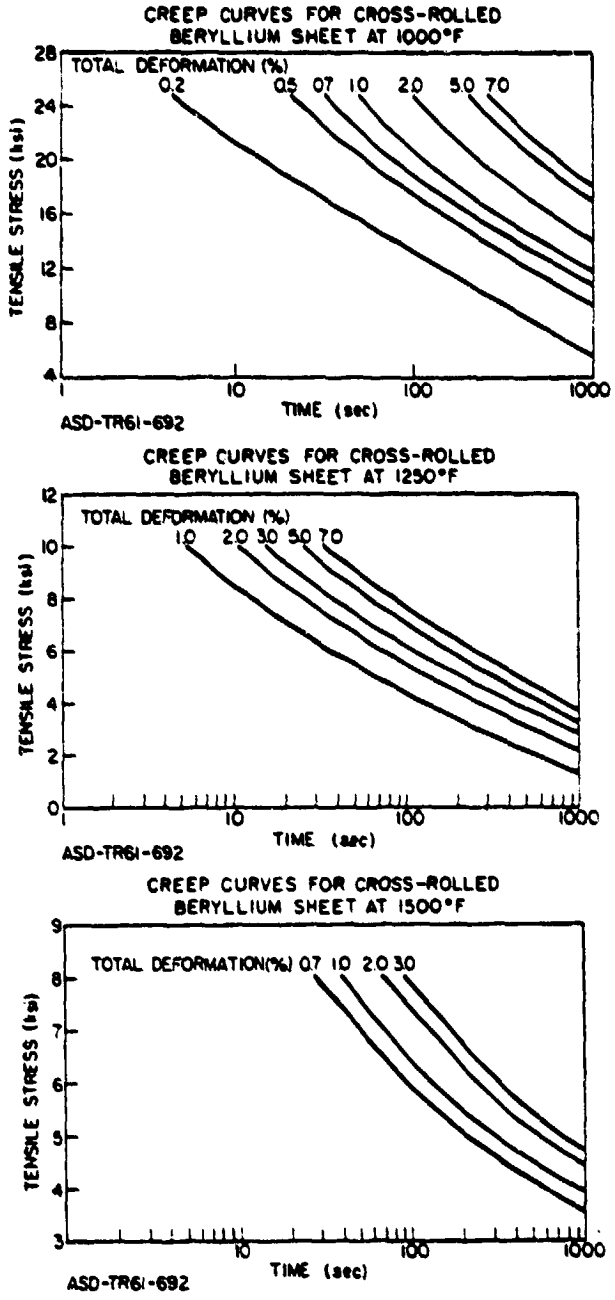
CREEP CURVES FOR CROSS-ROLLED
BERYLLIUM SHEET AT 1000°F
TOTAL DEFORMATION (%)
0.2
0.5
0.7
1.0
2.0
5.0
7.0
TENSILE STRESS (ksi)
28
24
20
16
12
8
4
10
100
1000
TIME (sec)
ASD-TR61-692
CREEP CURVES FOR CROSS-ROLLED
BERYLLIUM SHEET AT 1250°F
TOTAL DEFORMATION (%)
1.0
2.0
3.0
5.0
7.0
TENSILE STRESS (ksi)
12
10
8
6
4
2
0
10
100
1000
TIME (sec)
ASD-TR61-692
CREEP CURVES FOR CROSS-ROLLED
BERYLLIUM SHEET AT 1500°F
TOTAL DEFORMATION(%)
0.7
1.0
2.0
3.0
TENSILE STRESS (ksi)
9
8
7
6
5
4
3
10
100
1000
TIME (sec)
ASD-TR61-692

Figure 3

From this short investigation it apperas that there are many reasons which may preclude the use of beryllium as a heat pipe vessel material. However, additional investigation may warrant some experimental verification.

2.1.2. Titanium

The potential use of titanium or a titanium alloy as a low mass heat pipe material was investigated. Long term creep data indicated that the strength would be marginal at 920 K for a twelve year life. Data on the compatibility of sodium and potassium with titanium and its alloys was researched. Preliminary information showed long term stability at temperatures up to 875 K with possible limited life above 875 K.

Further research into the use of titanium, and its alloys at 920 K revealed that they cannot be considered because their microstructure is not stable above 810 K (537 C, 1000 F). As summarized in the Metals Handbook[4]:

> "Thermal stability is the ability of alloys to retain their original mechanical properties after prolonged service at elevated temperatures. An alloy is thermally unstable if it undergoes microstructural changes during use at elevated temperatures that affect its properties adversely. Instability may cause either embrittlement or softening, depending on the nature of the microstructural changes.
>
> Titanium alloys are generally stable over the temperature ranges where they resist oxidation and retain their useful strength. The alpha alloys are generally stable up to 1000 F for exposure periods of 1000 hours or more, except alloys high in Al."

The creep strength of the strongest titanium alloy is 2000 psi at 1000 F for a 1% creep in 1000 hours, which if extrapolated to 100,000 hours at 920 K (1200 F) shows virtually zero creep strength. This is also verified from a Larson-Miller plot at 0.1% creep. The L-M Parameter T (20 + log t)/1000 is 41.5 for 1200 F and 105,120 hours, and the titanium alloys show virtually zero strength at a L-M Parameter of 33.

### 2.1.3. Heat Resistant and Refractory Alloys

Having shown that beryllium and titanium alloys are not suitable for long term use at 920 K, the material search turned to the heat resisting alloys and the refractory metals and their alloys. Table II shows the maximum hoop stress developed in the heat pipe wall for the operating pressure of 200 Torr (3.87 psi) which corresponds to potassium's vapor pressure at 900 K.

Table III summarizes the mechanical properties of 12 metals and alloys which have been researched for potential heat pipe envelopes. Also shown in Table III is the armor thickness multiplier which was calculated in accordance with Haller and Lieblein's meteoroid armor equation, as described by Dauterman and Montgomery[5] and as modified by JPL[6]. If a hoop stress of 3000 psi is used as the lower limit for long term creep, one sees from Table III that Be, Ti, Ni and pure Nb do not have sufficient strength to be considered for use at 920 K for 105, 120 hours. (12 years)

In addition to creep strength, and of greater significance in choosing a heat pipe material, is the possibility of buckling of the thin walled evacuated heat pipe by atmospheric pressure at room temperature. Roark[7] shows the following formula:

$$P = \frac{1}{4} \frac{E}{1-\nu^2} \frac{t^3}{r^3}$$

P = External pressure where buckling occurs - psi
E = Young's Modulus - psi
v = Poisson's ratio
t = Wall thickness - inches
r = Pipe radius - inches

TABLE II

Hoop Stress vs Wall Thickness and Pipe Diameter

for Potassium at 900 K.

$$S = \frac{PD}{2t}$$

S = Maximum hoop stress
D = Pipe diameter
t = Wall thickness

$P_{K\ @\ 900^{o}K}$ = 200 Torr = 3.87 psi

| Wall Thickness Mils | Pipe Diameter - Inches 1 | 2 | 3 | 4 | 5 |
|---|---|---|---|---|---|
| 1 | 1934 psi | 3868 psi | 5802 | 7736 | 9670 |
| 3 | 645 | 1289 | 1934 | 2578 | 3223 |
| 5 | 387 | 774 | 1160 | 1547 | 1934 |
| 10 | 193 | 387 | 580 | 774 | 967 |
| 15 | 129 | 258 | 387 | 516 | 645 |
| 20 | 97 | 193 | 290 | 387 | 484 |
| 25 | 77 | 155 | 332 | 309 | 387 |
| 30 | 64 | 129 | 193 | 258 | 322 |

| Material | RT 0.2% Offset Y.S. lbs/In$^2$ | Stress To Produce Stated Condition For $10^5$ Hours lbs/In$^2$ | Density lbs/In$^3$ | Armor Factor Thickness Multiplier For Penetration Lockalloy = 1 | Poisson's Ratio $\sigma$ | Young's 75 C - lbs/In$^2$ | Modulus 1200 F - lbs/In$^2$ |
|---|---|---|---|---|---|---|---|
| **Low Density Metals** | | | | | | | |
| Beryllium | 27,000-69,000 | ≃ 250 0.1% Creep @ 1150 F | 0.067 | 1.01 | ----- | -------- | -------- |
| Titanium | >120,000 | ≃ 100 0.1% Creep @ 1200 F | 0.163 | ---- | ----- | -------- | -------- |
| **Iron Alloys** | | | | | | | |
| 316 SS | 35,000 | 6,000 0.1% Creep @ 1150 F | 0.290 | 0.53 | 0.3 | $28 \times 10^6$ | -------- |
| 286 | 105,000 | 38,000 0.1% Creep @ 1100 F | 0.286 | 0.52 | ----- | -------- | -------- |
| **Nickel Alloys** | | | | | | | |
| 70 Ni | 13,000 | 1,200 1.0% Creep @ 1200 F (201 Ni) | 0.322 | ---- | ----- | -------- | -------- |
| Inconic 80A | 90,000 | 10,000 50% of Rupture Stress @ 1200 F | 0.298 | 0.52 | ----- | $32 \times 10^6$ | $26 \times 10^6$ |
| **Niobium Alloys** | | | | | | | |
| Pure Nb | 20,000 | 2,000 0.1% Creep @ 1200 F | 0.31 | 0.52 | .38 | $15 \times 10^6$ | $14 \times 10^6$ |
| Nb-1% Zr | > 50,000 | 12,500 0.5% Creep @ 1800 F | 0.31 | 0.52 | ----- | -------- | -------- |
| FS-82 | <89,000 | 65,000 1.0% Creep Larson Miller Parameter | 0.367 | ---- | ----- | -------- | -------- |
| C-31 | ------ | 29,000 1.0% Creep Larson Miller Parameter | 0.292 | ---- | ----- | -------- | -------- |
| **Molybdenum Alloys** | | | | | | | |
| Arc Cast Mo | 80,000 | >15,000 50% of Rupture Strength Larson Miller PM | 0.369 | 0.52 | .324 | $45 \times 10^6$ | $38 \times 10^6$ |
| TZM | 110,000 | >50,000 0.5% Creep Larson Miller Parameter | 0.363 | 0.52 | ----- | -------- | -------- |

| Alloy | C | Mn | Si | Cr | Mo | Ti | Co | Al | Fe | Ni |
|---|---|---|---|---|---|---|---|---|---|---|
| 316-286 | .08 | 1.35 | .5 | 15 | 1.25 | 2.0 | --- | ---- | Rem | 26 |
| Inconic 80A | .1 | 1.0 | 1.0 | 20 | ---- | 2.25 | 2.0 | 1.25 | 5.0 | Rem |

FS-82 Nb - 32Ta - 1Zr

C-31 Nb - 10Ti - 10Mo - 0.1C

920°K = 1197°F

TABLE III

Figure 4 is a plot of the buckling pressure P versus the ratio of wall thickness to pipe radius for four values of Young's modulus. The value of Poisson's ratio was taken as 0.3.

Since the equation implies uniform external stress, a safety factor of 2 must be used to account for non-uniform loading. Accordingly, a lower limit of 30 psi for the buckling pressure shows a t/r of 0.014 to 0.02 for moduli of 45 to 15 million psi respectively. From Table III it is seen that these moduli correspond to molybdenum and its alloys ($45 \times 10^6$) and niobium and its alloys ($15 \times 10^6$) which bracket the remaining materials.

Figure 5 is a plot of heat pipe diameter versus wall thickness for various (t/r). Of particular interest are t/r's of 0.0135, 0.0155 and 0.0195 which correspond to moduli for molybdenum and its alloys, stainless alloys, and niobium and its alloys respectively. From Figure 5 one sees that a wall thickness to radius ratio of 0.02 is a conservative value to withstand buckling of heat pipes due to the earth's atmospheric pressure. This value, which is 1% of the diameter, is small; however, it may make larger diameter heat pipes too massive, thus pointing the direction toward a larger number of smaller diameter heat pipes.

## 2.2. Mechanical Interfaces

The design of Figure 1 has numerous interfaces. They include heat pipe-to-heat pipe, and heat pipe-to-thermionic converters. The following concepts were evaluated in varying degrees of detail, the results of which played an important role in the system redesign.

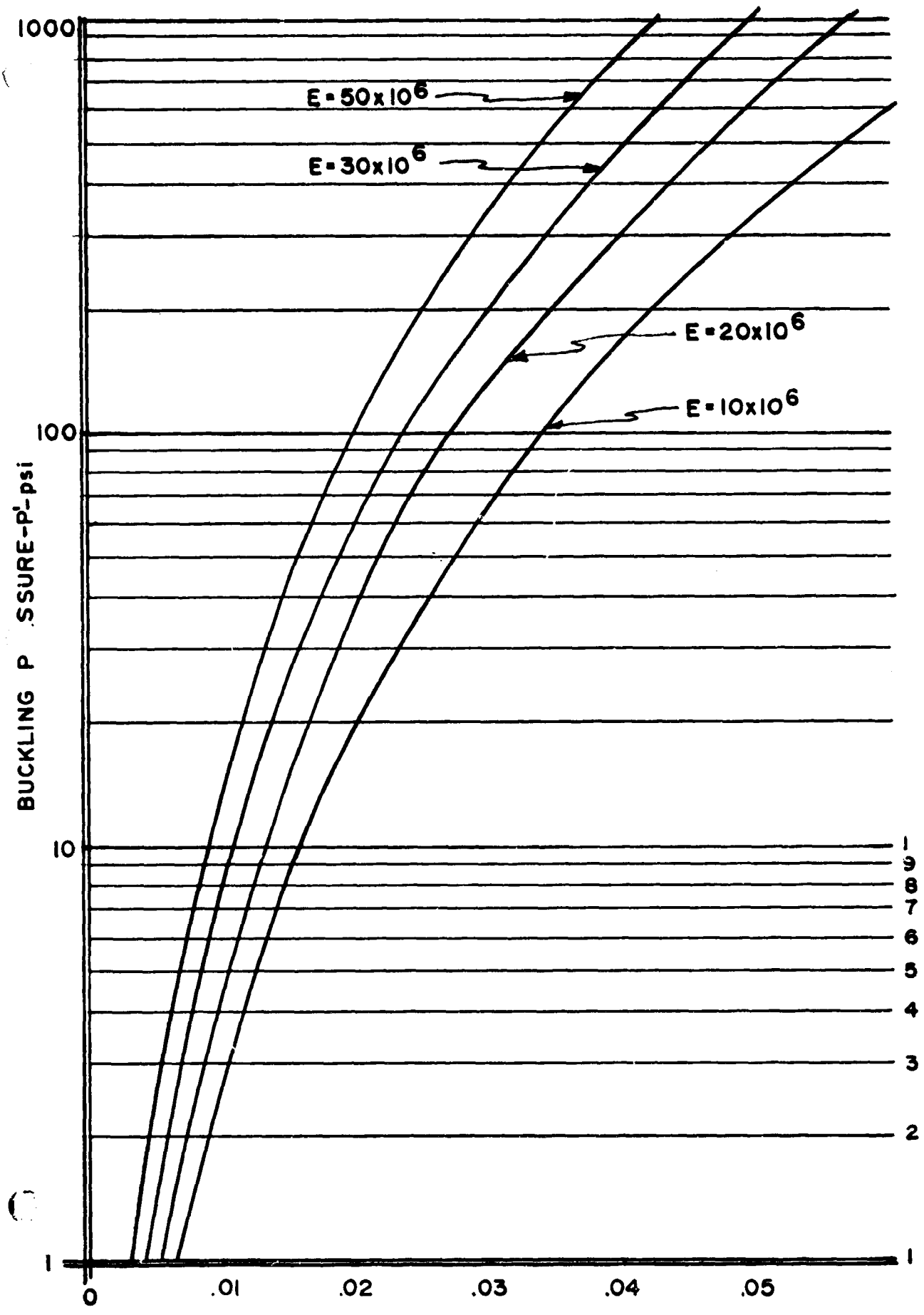
1000
100
10
1
E = 50x10^6
E = 30x10^6
E = 20x10^6
E = 10x10^6
BUCKLING PRESSURE - P' - psi
1
9
8
7
6
5
4
3
2
1
0
.01
.02
.03
.04
.05
THICKNESS / RADIUS - (t/r)

FIGURE 4

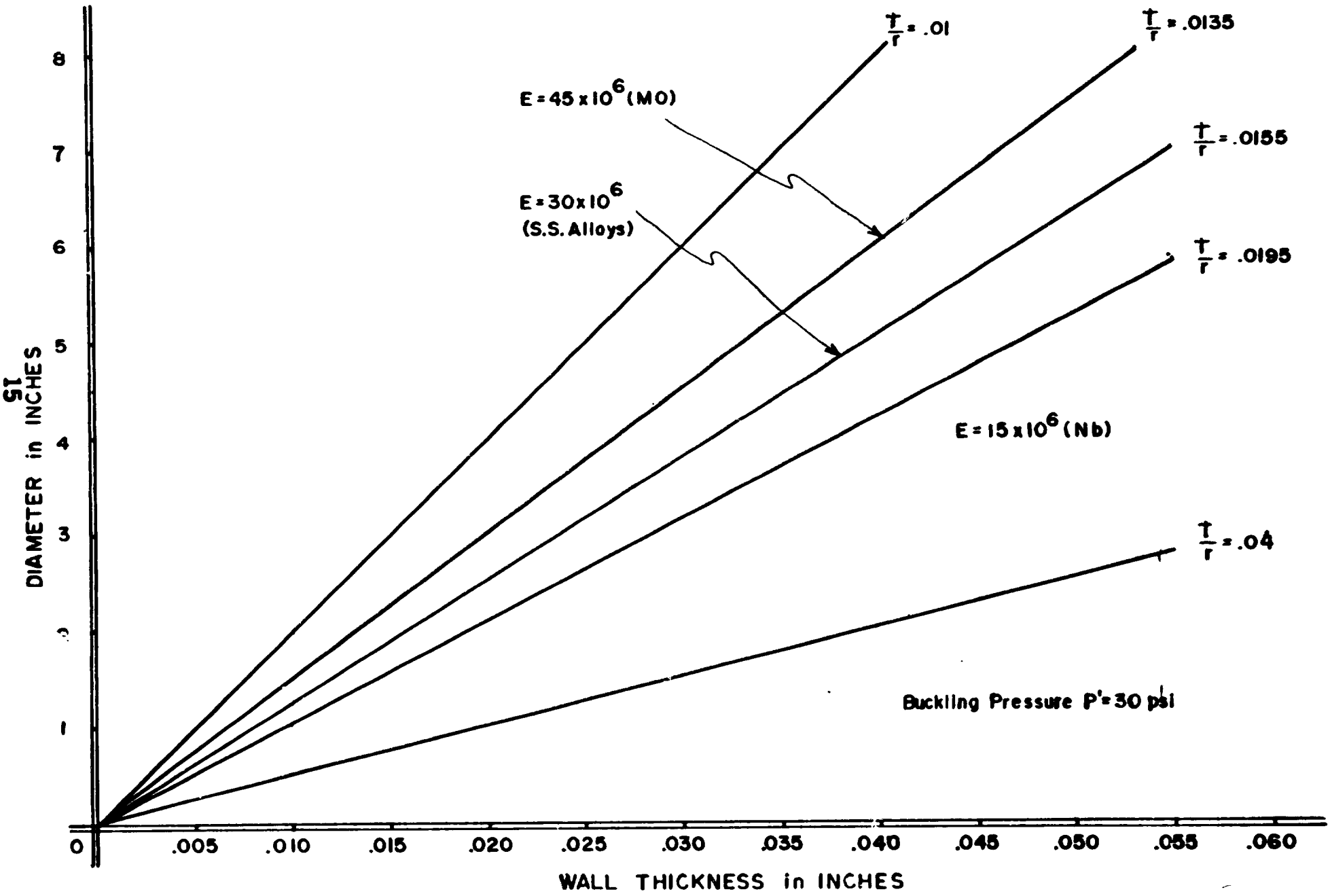
$\frac{t}{r}$ = .01
$\frac{t}{r}$ = .0135
E = 45 x 10^6 (MO)
$\frac{t}{r}$ = .0155
E = 30x10^6
(S.S. Alloys)
$\frac{t}{r}$ = .0195
E = 15 x 10^6 (Nb)
$\frac{t}{r}$ = .04
Buckling Pressure P' = 30 psi
DIAMETER in INCHES
SI
0
1
2
3
4
5
6
7
8
.005
.010
.015
.020
.025
.030
.035
.040
.045
.050
.055
.060
WALL THICKNESS in INCHES

FIGURE 5

### 2.2.1. Heat Pipe to Heat Pipe Interface Concepts

There are several methods by which two heat pipes can be joined together:

1. One heat pipe penetrates the wall of the other, i.e. only one wall separates the working fluids of the two heat pipes.
2. A mechanical transition between the walls of the two heat pipes which is welded, brazed, bonded, threaded, or slip fitted.
3. Heat pipes external to each other but sharing a common wall within the transition. Several concepts are seen in Figures 6, 7, 8 and 9.

Table IV shows the relative merits of the six different heat pipe to heat pipe interfaces.

TABLE IV

RELATIVE MERITS OF HEAT PIPE INTERFACES

| Figure Number | | Circular | Rectangular | Assembly | $\triangle T$ | Pretestable | Thermal Stress |
|---|---|---|---|---|---|---|---|
| 6 | Screw thread/ slip fit | X | | Easy | High | Yes | Low |
| 6 | Integral fabrication | X | | Hard | Low | No | Low |
| 6 | Slip fit with Na interface | X | | Med. | Med. | Partial | Low |
| 7 | Single integral interface | | X | Med. | Med. | No | Med. |
| 8 | Multiple integral interface | | X | Hard | Low | No | High |
| 9 | Integral/external interlocking | | X | Impractical | | | |

From Table IV one concludes that cylindrical heat pipe fabrication with a sodium filled interface or integral fabrication of the heat pipes are the most practical for good heat pipe to heat pipe interfaces. Also the total

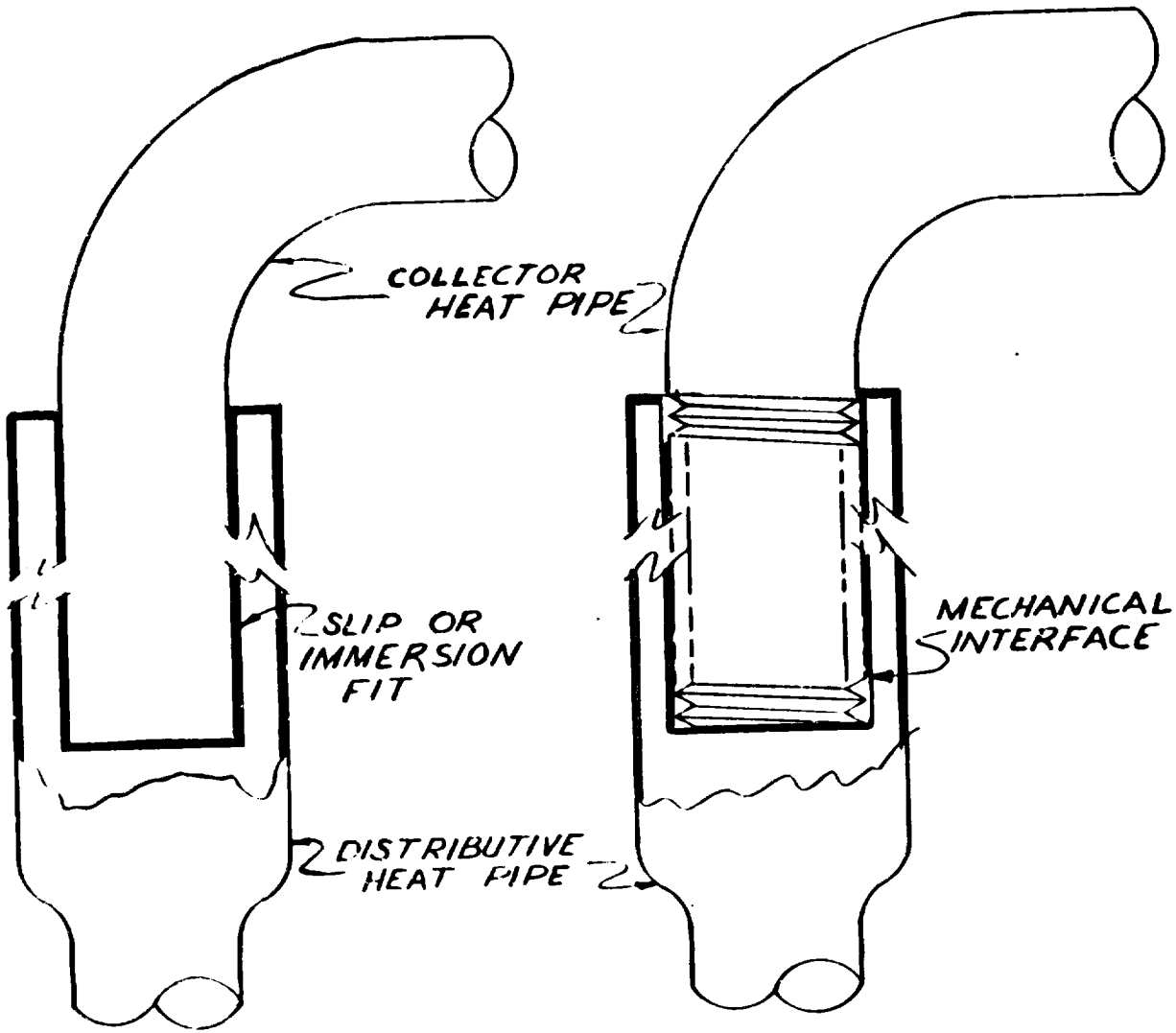


Figure 6

CYLINDRICAL INTERFACE DESIGNS

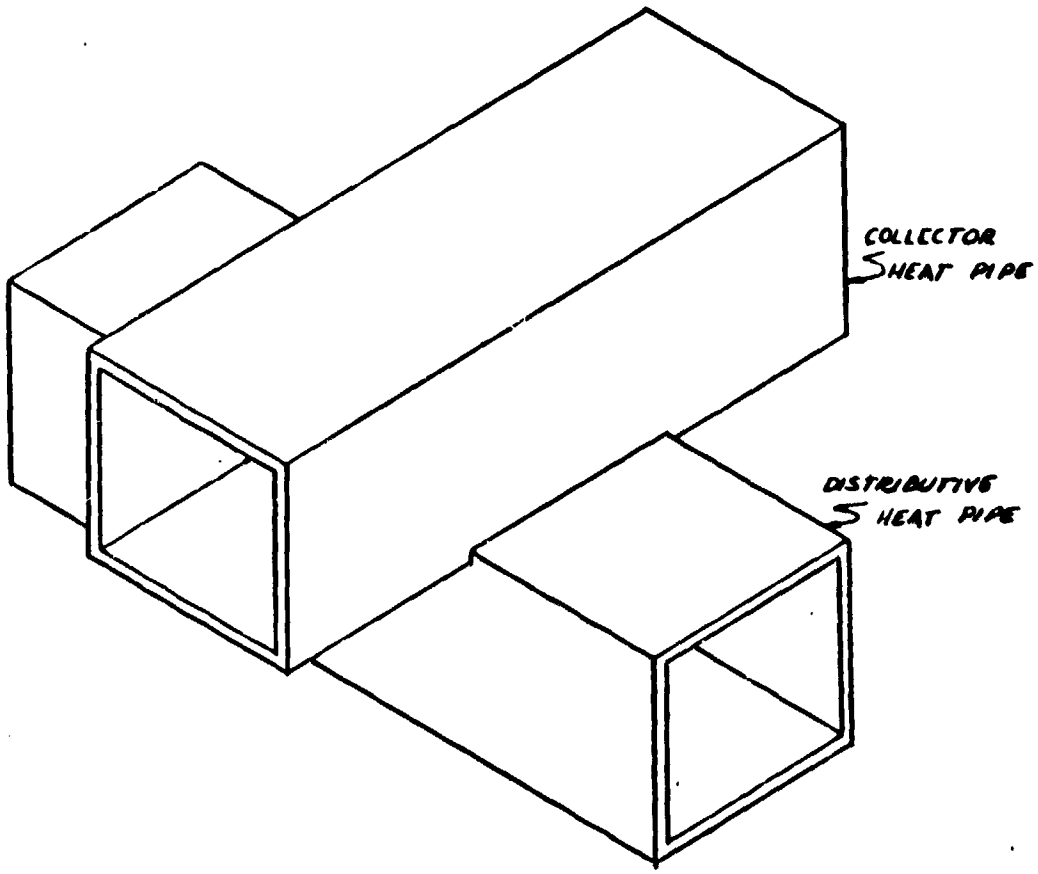


Figure 7

INTEGRAL INTERFACE

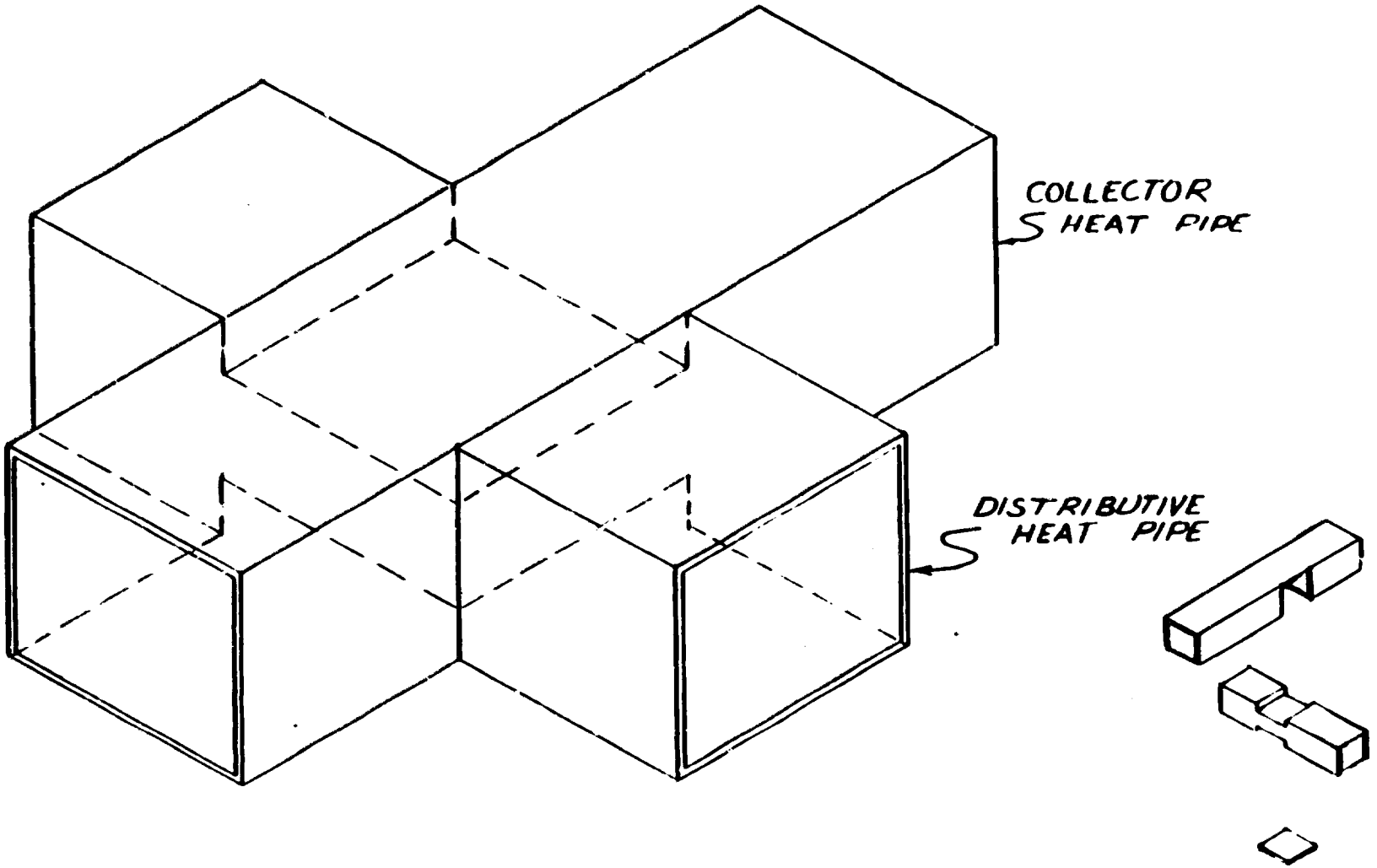


Figure 8

DOUBLE INTEGRAL INTERFACE

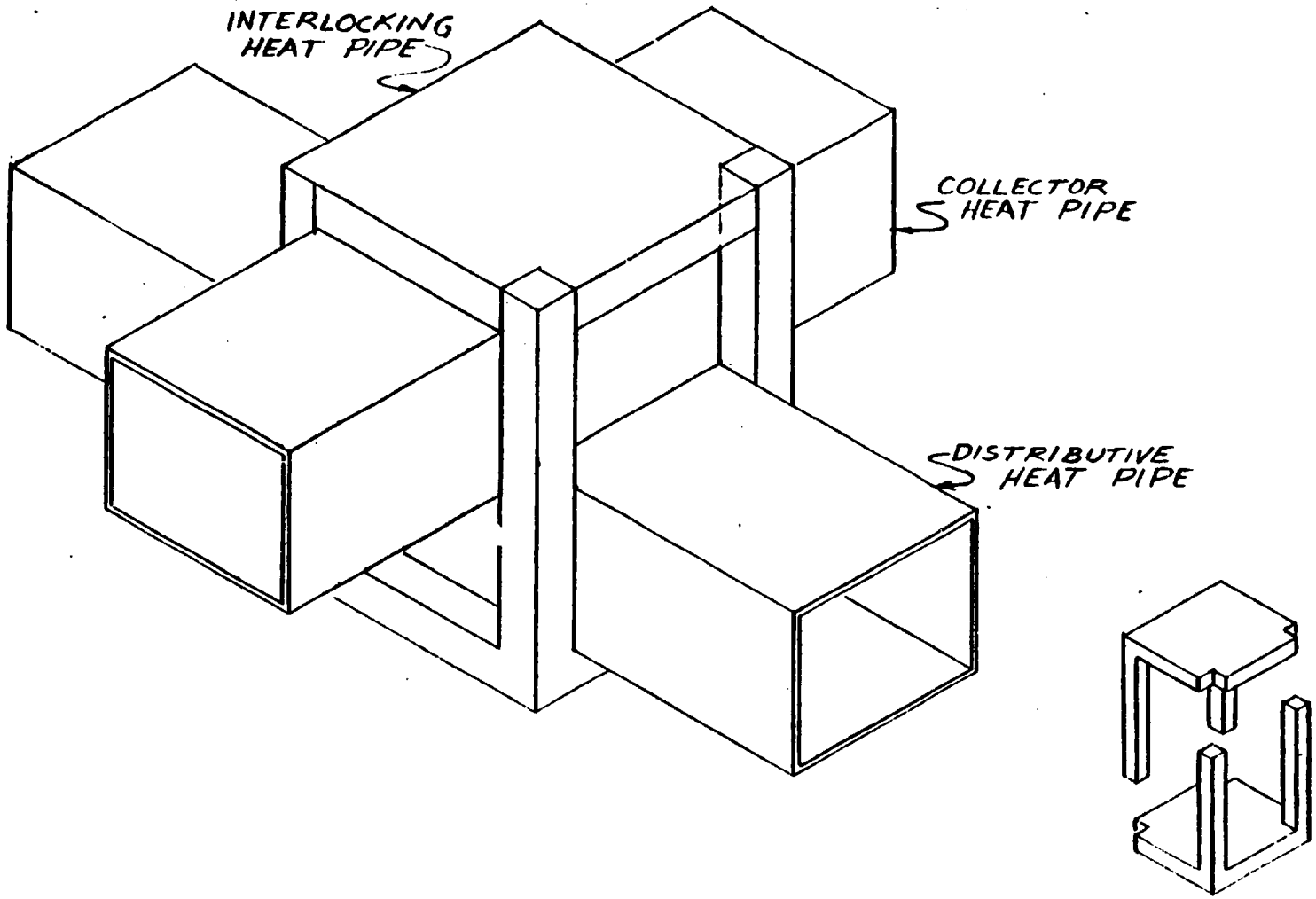


Figure 9

INTERLOCKING EXTERNAL

HEAT PIPES

number of interfaces must be kept to a minimum to reduce the overall system $\Delta T$.

2.2.2. Heat Pipe to Thermionic Collector Interface Concepts

In a converter matrix of 6 x 15 x 6, the heat removal from the collectors can be accomplished by joining each string of 15 converters together with one collector heat pipe. However, fabricating heat pipes in place around the collectors presents several interesting challenges. Of major concern is the amount of an on-site welding, which will be difficult to Non Destructive Test (NDT). Conversely, it is desirable to fabricate and NDT as much of the heat pipe as feasible.

Several concepts are seen in Figures 10, 11, 12 and 13. Figure 10 shows two completely prefabricated heat pipes which have mechanical interfaces with the collector. This concept, while exhibiting a large interface $\Delta T$, will be the most reliable as there is redundancy in having two collector heat pipes per string of fifteen converters; and of greater importance is the fact that the heat pipes can be fabricated and pretested as heat pipes prior to installation.

Figure 11 shows the converters with self-contained annular collector heat pipes which are then welded as part of the sealing envelope completing the transverse collector heat pipe. This concept could use one transverse collector heat pipe for every other converter in the string as shown, or it could accept heat from every converter.

Figure 12 shows a concept by which two separate transverse collector heat pipes can be welded in place where the collector sheath is used to complete the transverse collector heat pipe envelope. Figure 13 shows an alternate method of fabricating the concept of two separate transverse heat pipes.

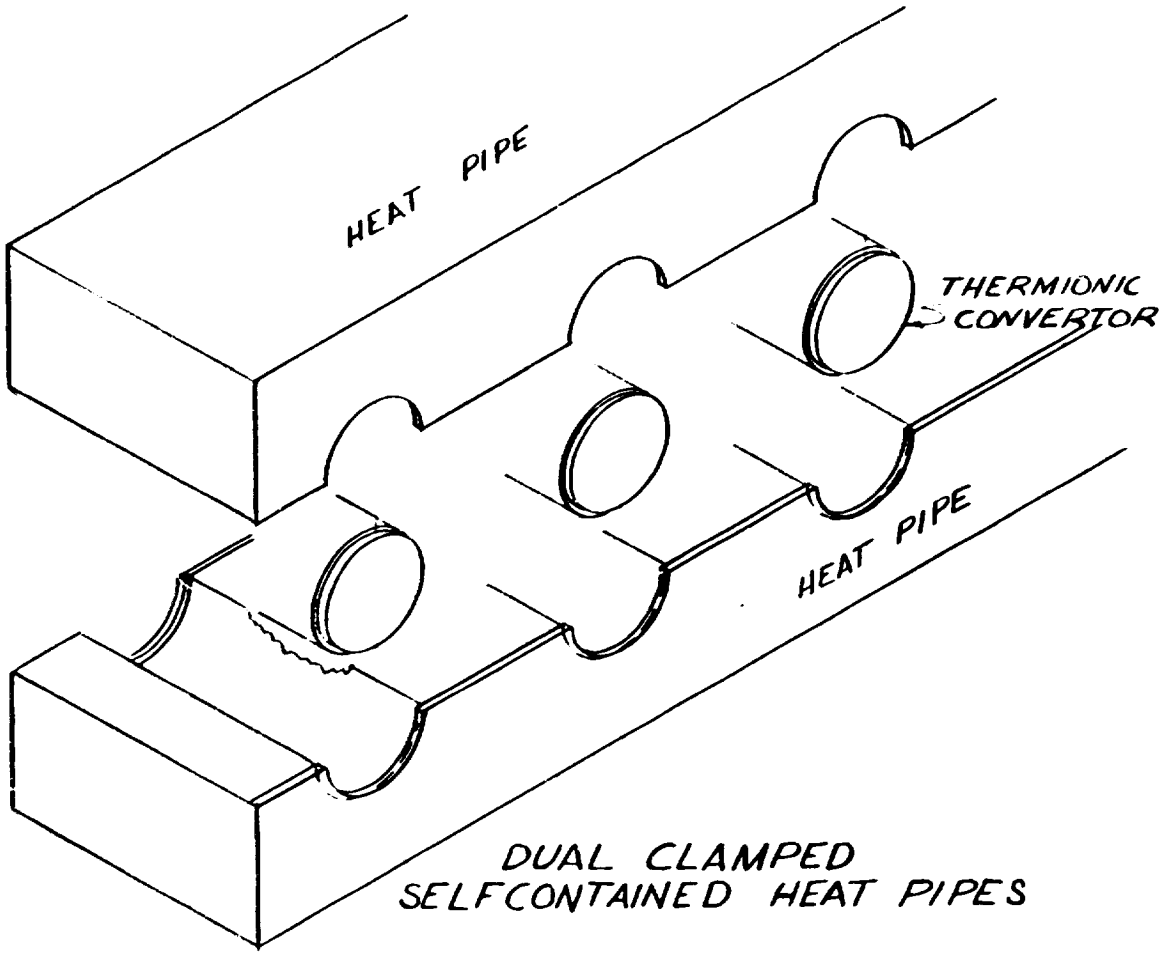
HEAT PIPE
THERMIONIC CONVERTOR
HEAT PIPE
DUAL CLAMPED
SELFCONTAINED HEAT PIPES

Figure 10

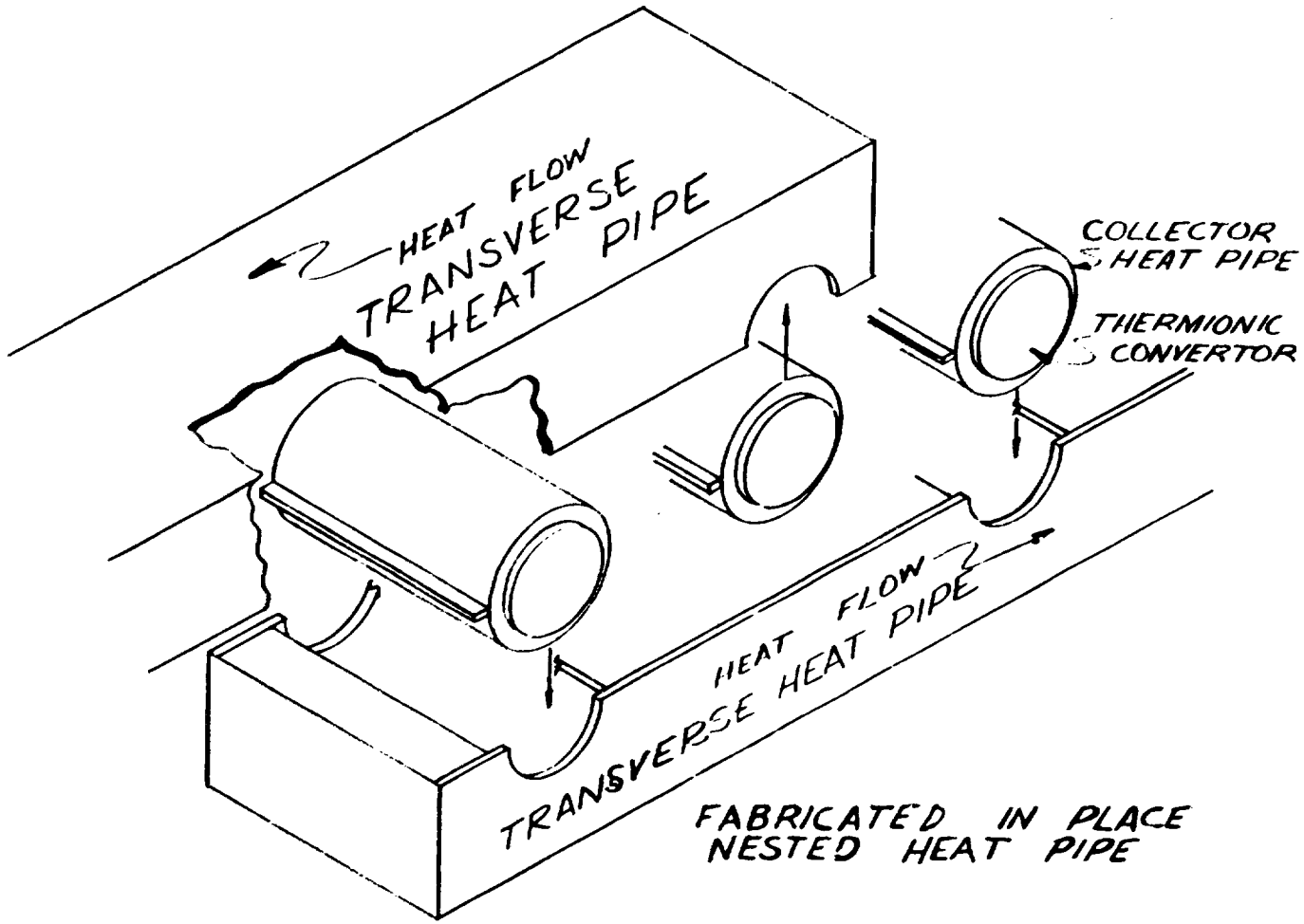
HEAT FLOW
TRANSVERSE
HEAT PIPE
COLLECTOR
HEAT PIPE
THERMIONIC
CONVERTOR
HEAT FLOW
TRANSVERSE HEAT PIPE
FABRICATED IN PLACE
NESTED HEAT PIPE

Figure 11

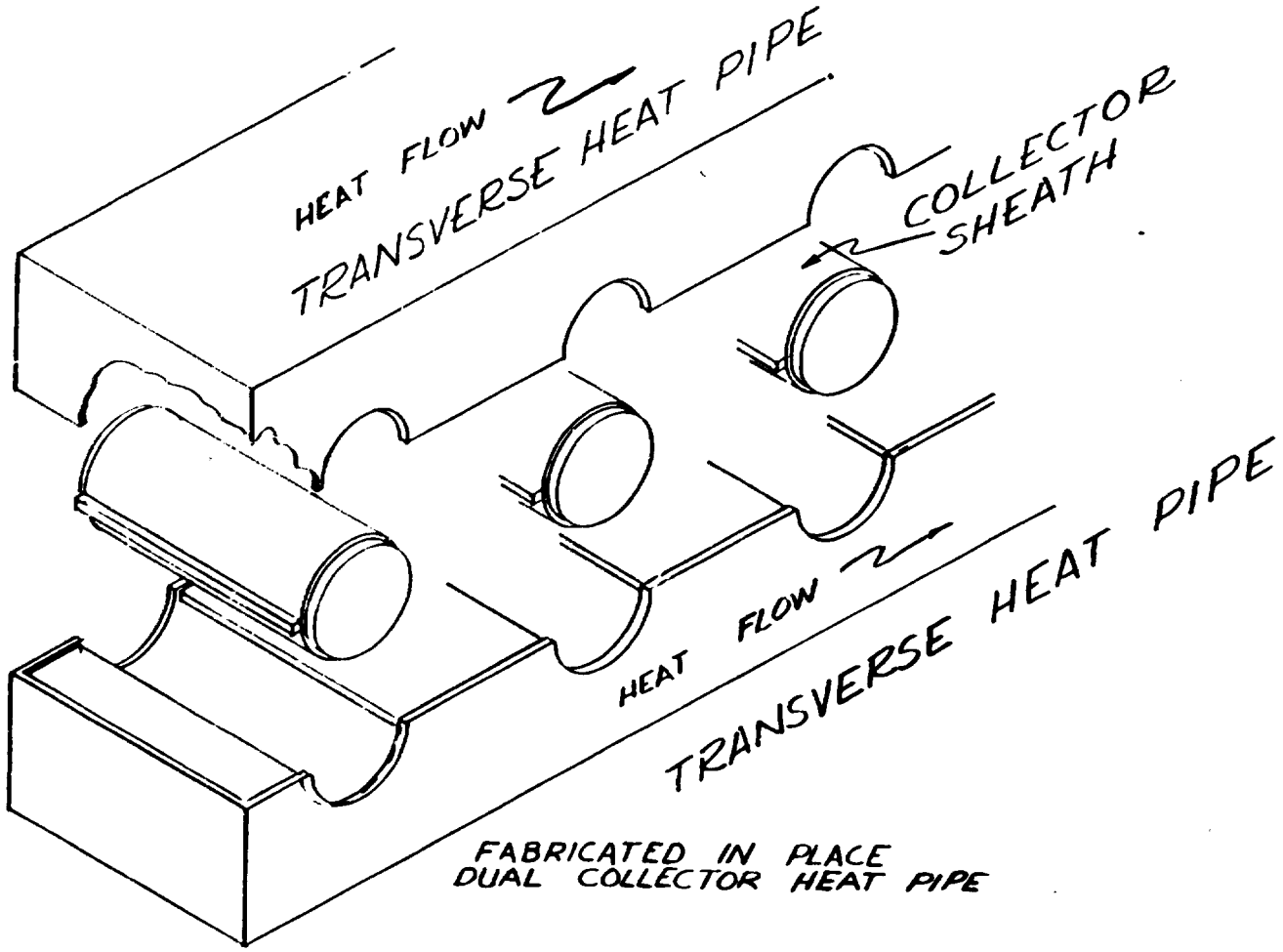
HEAT FLOW
TRANSVERSE HEAT PIPE
COLLECTOR SHEATH
HEAT FLOW
TRANSVERSE HEAT PIPE
FABRICATED IN PLACE
DUAL COLLECTOR HEAT PIPE

Figure 12

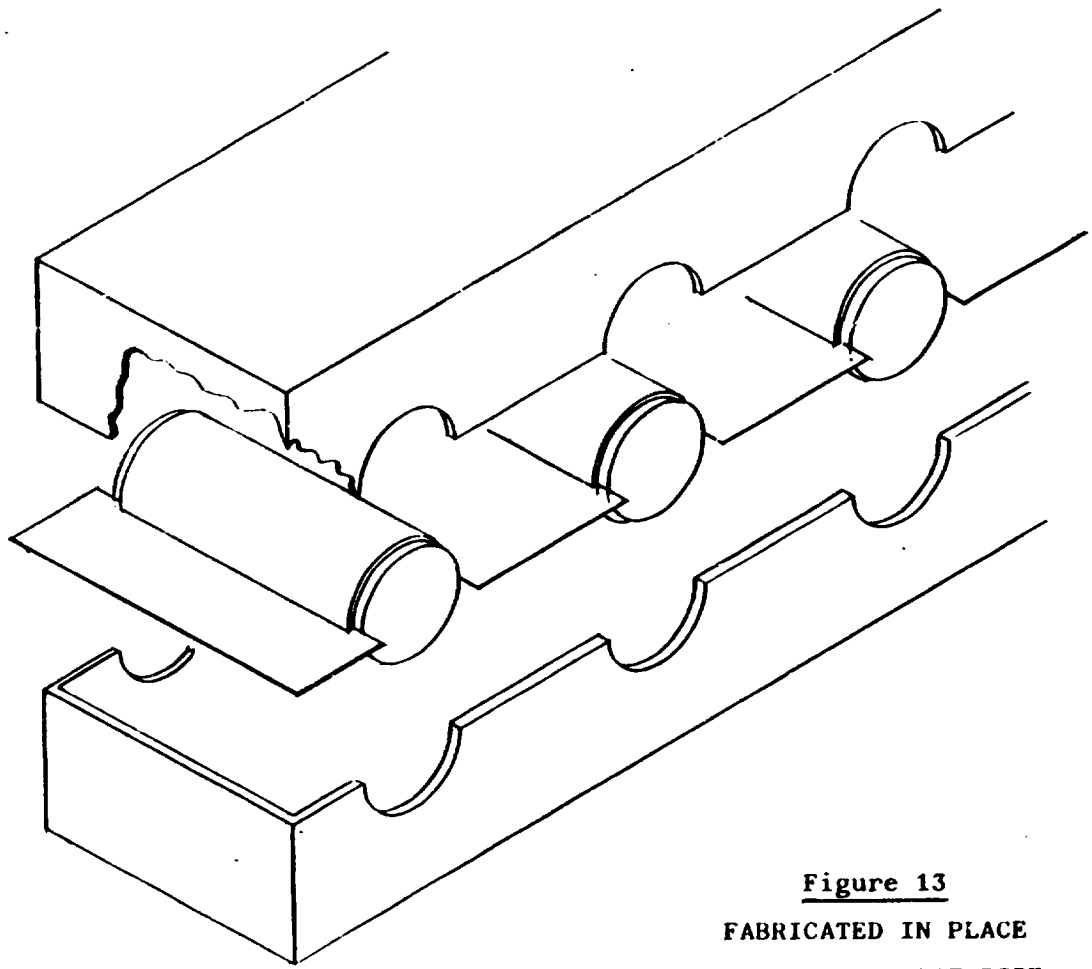

Figure 13

FABRICATED IN PLACE

DUAL COLLECTOR HEAT PIPE

Each concept has its good and bad points. Of major concern in evaluating the concepts are 1) the interface $\Delta T$ and 2) the ability to pre-test the heat pipes or pre-test as many linear feet of weld as possible, which has the corollary of keeping the actual amount of welding in place to a minimum.

The mechanical attachment of the heat rejection system heat pipes to the thermionic converter is seen to be a difficult if not impossible job, and in fact was one of the reasons why a fresh look at the system design was undertaken.

## 2.3. Heat Pipe Heat Rejection System Performance and Mass

During the course of the initial evaluation of the NEP heat rejection system, a second generation rectangular matrix of thermionic converters and radiator design concepts was generated by JPL. This matrix had eighteen converters in a series string, all connected to a single collector-distributive heat pipe. This eliminated the collector heat pipe to distributive heat pipe interface, which would be difficult to fabricate and exhibit a high $\Delta T$. Accordingly, the system's thermal performance and mass was calculated based on the use of thirty collector-distributive heat pipes and 6000 individual radiator heat pipes, and is seen in Table V.

The following constraints were used in generating Table V:

1. The interface at the thermionic collector is mechanical and exhibits a 10 C $\Delta T$.
2. The entire system including armor is niobium - 1% Zr. This circumvents thermal expansion and joining problems.
3. The radiator is 5.53 meters long x 4.5 meters in diameter and has 6000 individual heat pipes attached to the 30 collector-distributive

heat pipes via a braze joint. This joint exhibits a 5 C $\Delta$T.

4. Buckling as a constraint dictates the required wall thickness.
5. The armor thickness is 0.095 cm niobium (1% Zr) and affords an individual survival probability of 0.8 for a 126 $cm^2$ area in 105,120 hours. This armor exhibits a $\Delta$T of 0.7 C and has a total mass of 616 kg.
6. The radiator heat pipes are 2.67 cm in diameter with an 0.028 cm wall. They have one layer of 80 mesh screen which is 30% dense and 0.028 cm thick. The heat pipes are 47 cm long. The total mass of the heat pipes is 815 kg.
7. The braze joints between the collector-distributive heat pipes and the radiator heat pipes have a 10 gm of braze material each, having a total mass of 60 kg.
8. The mechanical interface at the collector has a 0.01 cm thick foil of niobium which has 20 gm mass for a total of 10 kg.

Several items of Table V bear investigating. The overall $\Delta$T of 28-32 C when subtracted from the 920 K assumed radiator temperature has the effect of reducing the radiant power from the radiator by 11.6% and 13.2% respectively. Accordingly, the mass of the entire system will increase proportionally as shown.

Of major concern with the collector-distributive heat pipe heat rejection concept is the joining of the collector-distributive heat pipes to the thermionic converters within the 5 x 6 x 6 rectangular matrix. The total linear feet of untested welding for an integral attachment method is at least 0.5 M per thermionic converter which for the entire matrix amounts to 220 meters. Each converter will have at least eight welds for a total of 4320 welds. Each collector-distributive

## TABLE V

MASS OF 2600 kW HEAT PIPE HEAT REJECTION SYSTEM
WITH A BASE LINE RADIATING TEMPERATURE OF 920 K
WITH AN EMISSIVITY OF 0.9

| | COLLECTOR-DISTRIBUTIVE HEAT PIPE DIAMETER | | | | | | | |
|---|---|---|---|---|---|---|---|---|
| | 5" (127 mm) | | 4.5" (114 mm) | | 4.0" (102 mm) | | 3.5" (89 mm) | |
| | Mass Kg | $\Delta T$ °C | Mass Kg | $\Delta T$ °C | Mass Kg | $\Delta T$ °C | Mass Kg | $\Delta T$ °C |
| Collector Interface | 10 | 10.0 | 10 | 10.0 | 10 | 10.0 | 10 | 10.0 |
| Collector-Distributive HP | 1766 | 8.4 | 1386 | 9.1 | 1027 | 9.9 | 930 | 11 |
| C-D HP-Rad. HP Interface | 60 | 5.0 | 60 | 5.0 | 60 | 5.0 | 60 | 5.0 |
| Radiator Heat Pipe | 815 | 3.9 | 815 | 4.3 | 815 | 4.8 | 815 | 5.4 |
| Armor | 616 | 0.7 | 616 | 0.7 | 616 | 0.7 | 616 | 0.7 |
| TOTAL | 3267 | 28 | 2887 | 29.1 | 2535 | 30.4 | 2431 | 32.1 |
| % and Mass Increase On - | 11.6% | | 12.1% | | 12.6% | | 13.2% | |
| Radiator Portion Due To $\Delta T$ | 281 | | 269 | | 256 | | 261 | |
| TOTAL MASS | 3548 | | 3156 | | 2881 | | 2692 | |

heat pipe will have a minimum of 144 untested welds. Therefore, a failure rate of 0.69% would produce a bad weld in each collector-distributive heat pipe.

If the collector-distributive heat pipe is made in two halves and mechanically clamped to the collector, then the interface $\Delta T$ becomes a major problem as does the clamping mechanism, which was not considered in the above mass calculation. The 10 C interface $\Delta T$ which was assumed for the calculations of Table V is a minimum and will probably be upwards of 20 C. An additional 10 C $\Delta T$ will increase the mass of the radiator portion of the heat rejection system by another 4.4%, which makes the masses of Table V become 3704, 3295, 3008, and 2745 kg for the 5, 4.5, 4.0 and 3.5 inch diameter collector-distributive heat pipes.

The reference design[8] used 2763 kg for the heat rejection system, which showed a specific mass of 19.9 kg/kWe system) for a 30° cone angle. Thus, it appears that only the 3.5" diameter (89 mm) collector-distributive heat pipe design would fall within the design limits.

Notwithstanding the results of the above mass and $\Delta T$ analysis, it is beyond reasonable technological advancement to assume that the 30 collector-distributive heat pipe design with 6000 radiator heat pipes can be built with a high probability of success. Accordingly, a recommendation was made to look at the overall NEP system design. These concepts and redesigns are presented in Section 3.

## 3. SYSTEM REDESIGN

As the NEP heat rejection system design was being evaluated, it became increasingly evident, as borne out by the recommendation in Section 2, that in order to have a buildable system the entire NEP system design must be re-evaluated. Accordingly, new concepts were generated which evolved into a new system design.

### 3.1. New Concepts

The initial design concept as evaluated had the power conversion radiator axially displaced from the conversion devices. If for the moment, all constraints are removed and only the radiator's criteria are considered, then placing the radiator radially outward from the conversion devices is an attractive design. Figures 14 and 15 show two possible concepts.

Figure 14 illustrates individual spiral heat pipes connected to each converter. The 540 heat pipes then become the radiator elements and must be sized to carry the power, radiate the heat and have a high survival probability. Figure 15 illustrates a concept which has only collector and radiator heat pipes. Here the collector heat pipes would require additional armor because they have a surface exposed to space. It is this design concept which was eventually evaluated in Section 2 and led the way to a full scale redesign.

Figures 16 and 17 are an annular arrangement of 540 and 600 converter matrices. Here again, each converter has a single collector heat pipe, and when assembled in an array, the surface at the OD (4.5 meters) looks like a black body radiator. (Black body radiator has an emissivity $\epsilon = 1$)

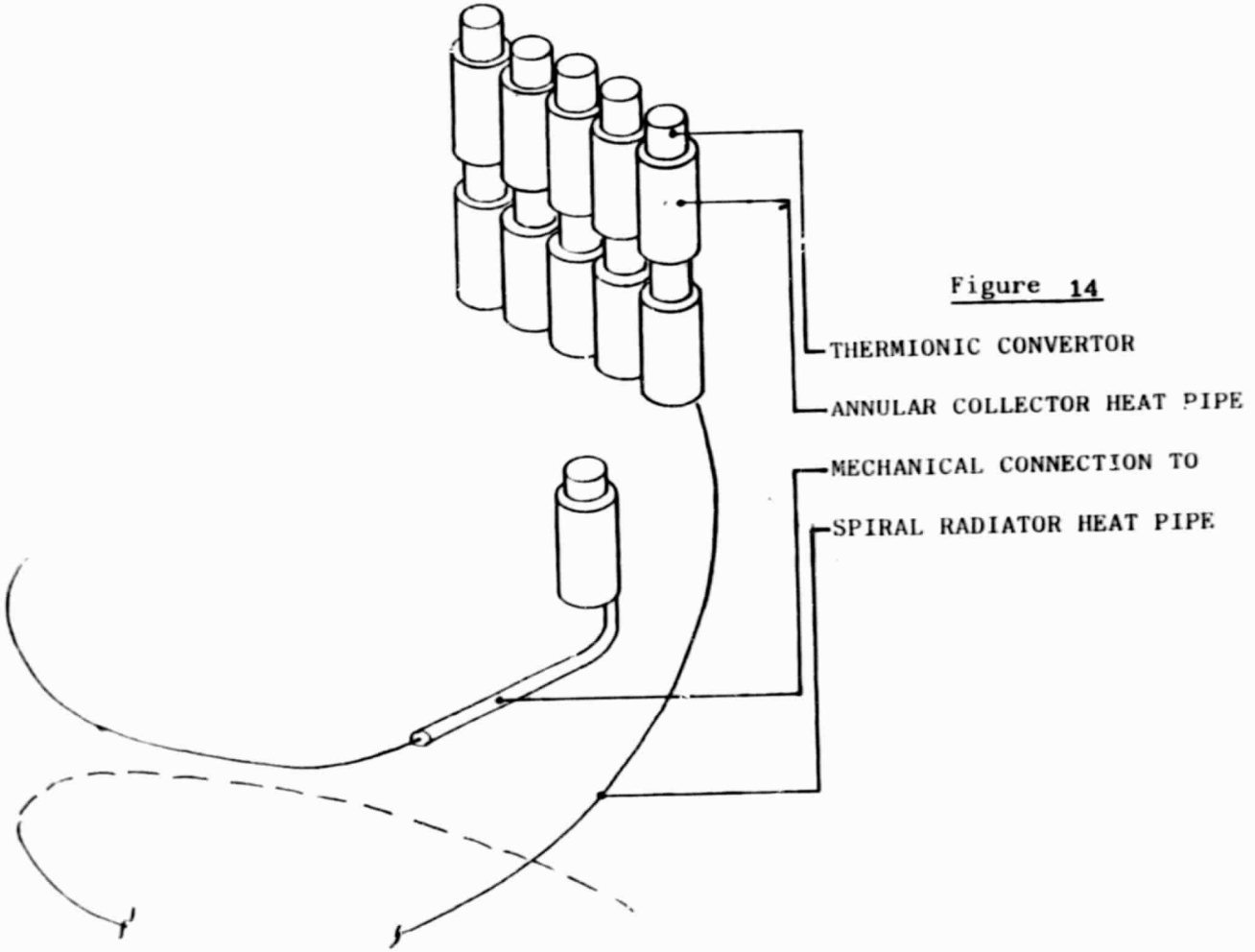


Figure 14

| KEY | REVISION NOTE | INITIAL | DATE |
|---|---|---|---|
| | | | |

TITLE MECHANICAL CONNECTION

NAME SPIRAL HEAT PIPE

DRAWN DATE

APPROVED

SCALE MATL.

ASS'Y or BILL

STD. TOLERANCES
DECIMAL .xx ± .010, .xxx ± .005
FRACTION ± 1/64
ANGULAR ± .083 PER INCH OF LENGTH

THERMACORE, INC.
HEAT TRANSFER SPECIALISTS

DWG. NO. B-59-69

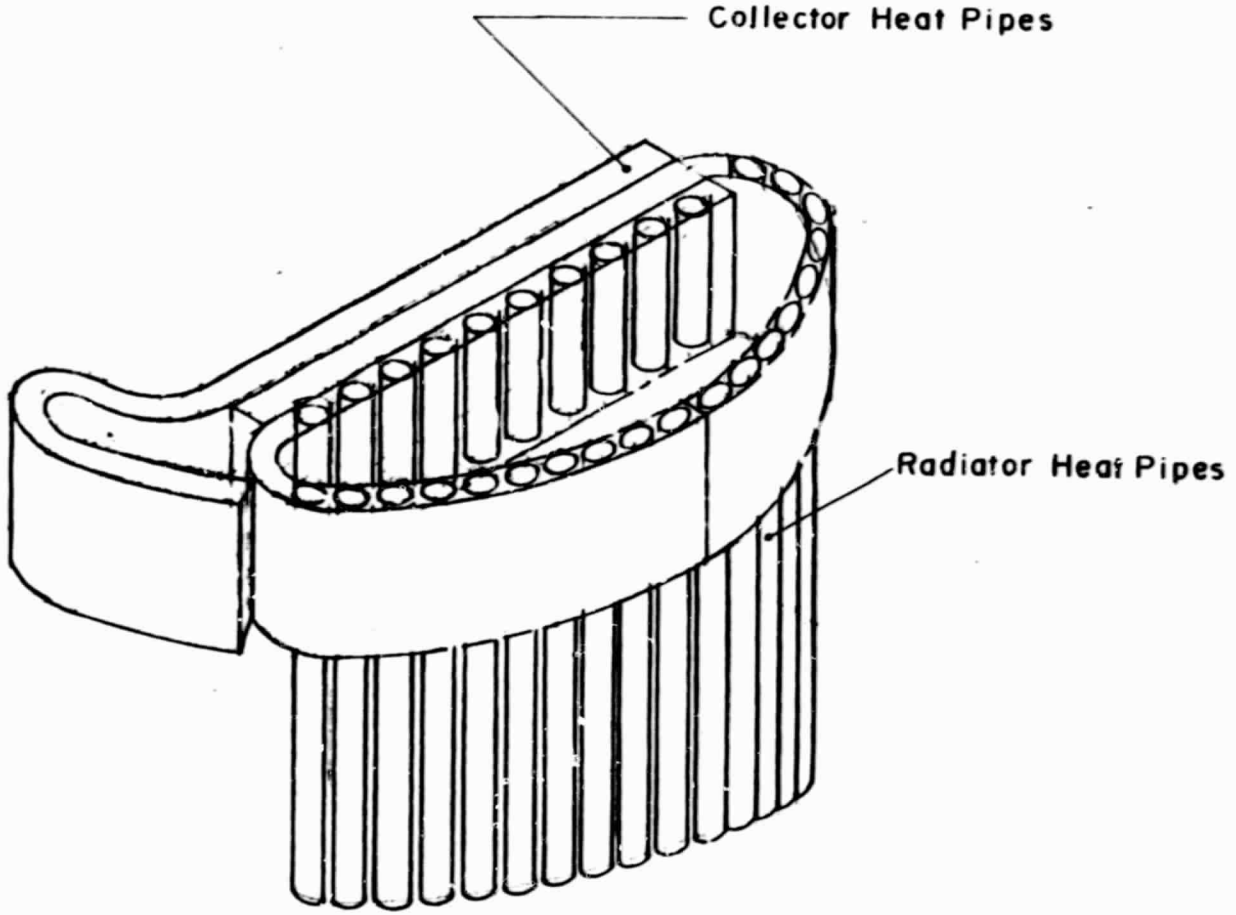
Collector Heat Pipes
Radiator Heat Pipes
DUAL HEAT PIPE CONCEPT

Figure 15

PLAN VIEW OF SELF-CONTAINED
BLACK BODY RADIATOR CONCEPT

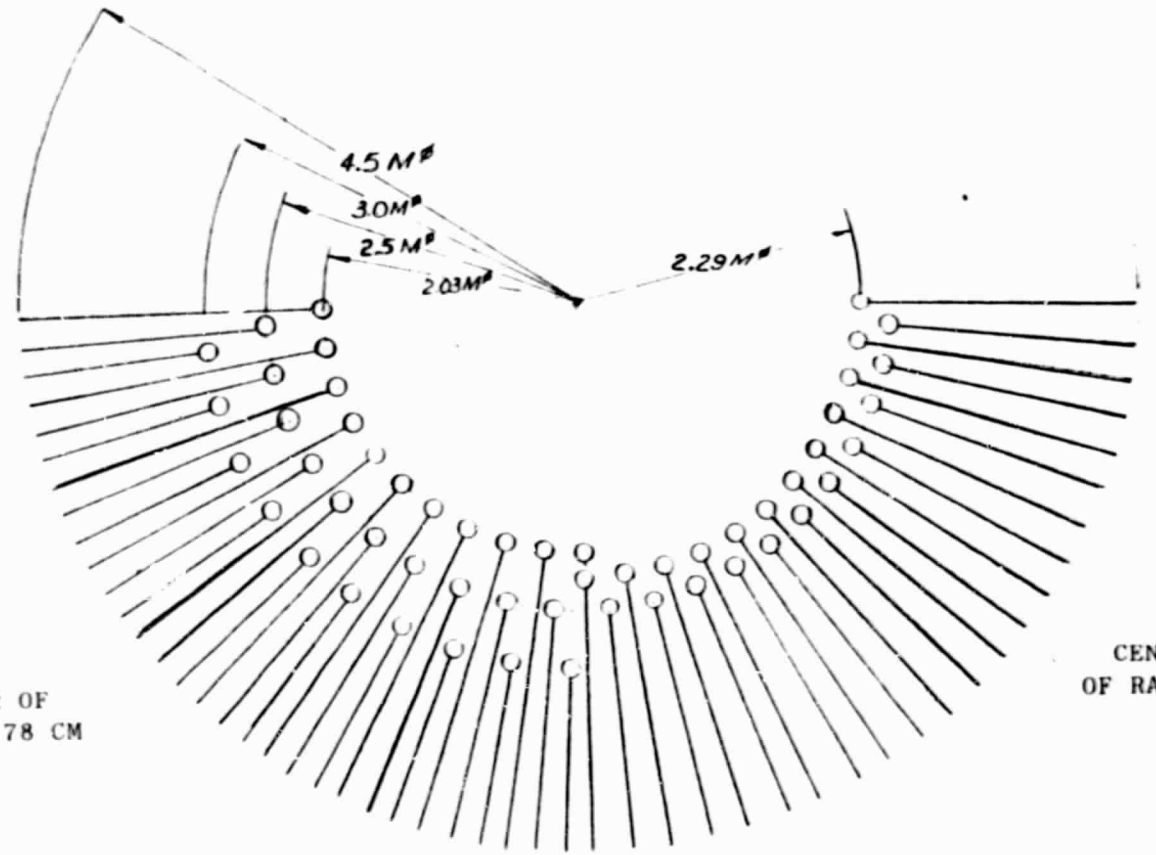


Figure 16



ORIGINAL PAGE IS
OF POOR QUALITY

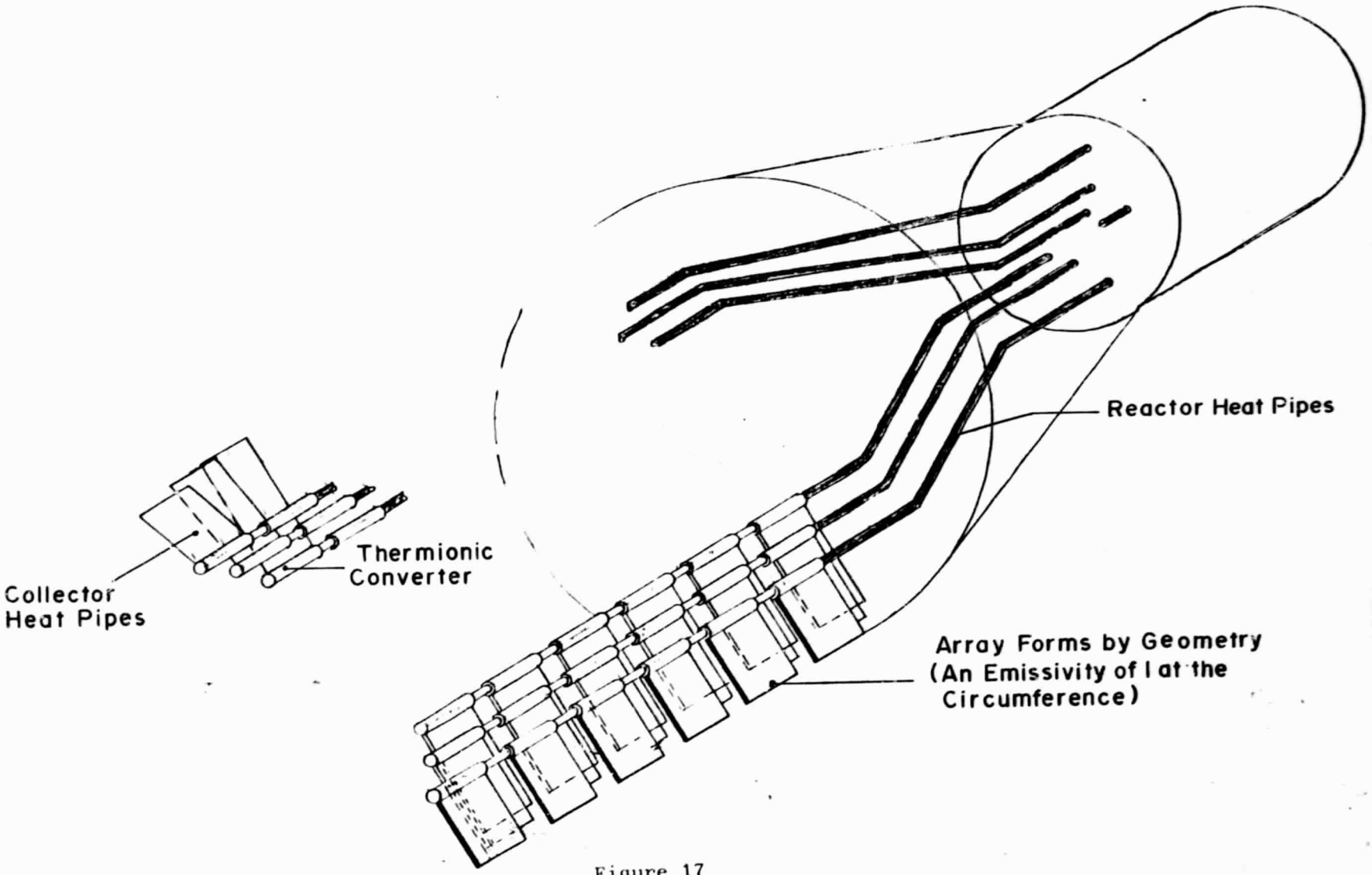


Figure 17

SELFCONTAINED BLACK BODY
RADIATOR CONCEPT

ORIGINAL PAGE IS
OF POOR QUALITY

For redundancy, a minimum of four converters are to be placed in parallel which implies two or four converters per radius.

All of these concepts were ruled out because of system constraints, but were the basis for the design concept which evolved and is presented below.

## 3.2. Individual Collector-Radiator Heat Pipe Concept

The design which was felt most likely to be fabricable and have a reasonable chance of success is seen in Figure 18. This concept has five layers of 108 thermionic converters. Each layer has four concentric rows of 27 converters on 88, 104, 120 and 136 cm diameter circles.

Each converter collector is 4.5 cm OD x 15 cm long. The total length of a converter cell is 25 cm. Each collector is enclosed by an integral annular heat pipe of 6.8 cm OD. These annular heat pipes are joined by a 2.6 cm diameter tangential arm which becomes an individual radiating element (for each collector) when it reaches the 4.5 M diameter radiator. (Note: $540 \times 2.6 \approx 450\pi$, i.e, the 540 heat pipes nest perfectly on the 4.5 M diameter). The radiator portion of the heat pipe has niobium - 1% Zr armor and will be discussed below.

Four converters on a radius are connected electrically in parallel. Additional series-parallel connections are made inside the innermost row of converters. Looking at an emitter heat pipe, each one has five converters on it. Placing four of these on a radius allows the reactor heat exchanger to be assembled in groups of four emitter heat pipes to six reactor heat pipes as is being considered by LASL.

Therefore, it is possible to build up each emitter heat pipe with its five converters and assemble them into groups of four as a major sub-assembly. Accordingly, 27 of these sub-assemblies make up the entire matrix.

Figure 18 shows the collector-radiator heat pipe as a single pipe. It is obvious that the annular heat pipe with a straight arm section is quite buildable along with the thermionic converters, thus any potential on-site welding is readily accessible.

The power requirement for the individual collector-radiator heat pipe is 4815 watts. Various computer runs on TG-1 and TUNNEL 22 were performed with the results seen in Figures 18, 20 and 21. The heat pipe dimensions are seen in Table VI.

TABLE VI

HEAT PIPE DIMENSIONS USED IN

FIGURES 18, 20 & 21

Temperature - 920 K

Fluid - Potassium

Evaporator Length - 15 cm

Adiabatic Length - 230 cm

Condenser Length - 555 cm

Total Length - 800 cm

O.D. - 2.62 cm

Wall Thickness - 0.25 cm

Groove Covering - 200 mesh

Powder Metallurgy Wick - 325 mesh

Figures 19 and 21 show that a heat pipe with 20 grooves 0.025 inch deep has a 7500 watt capability and has a 3.75 kg mass. Figures 20 and 21 show that a heat pipe with eight tunnels, 0.06 inch in diameter has a 14,500 watt capability and has 4.25 kg mass. The overall heat pipe $\triangle$T's are 7.52 C for the grooved design and 6.36 C for the tunnel

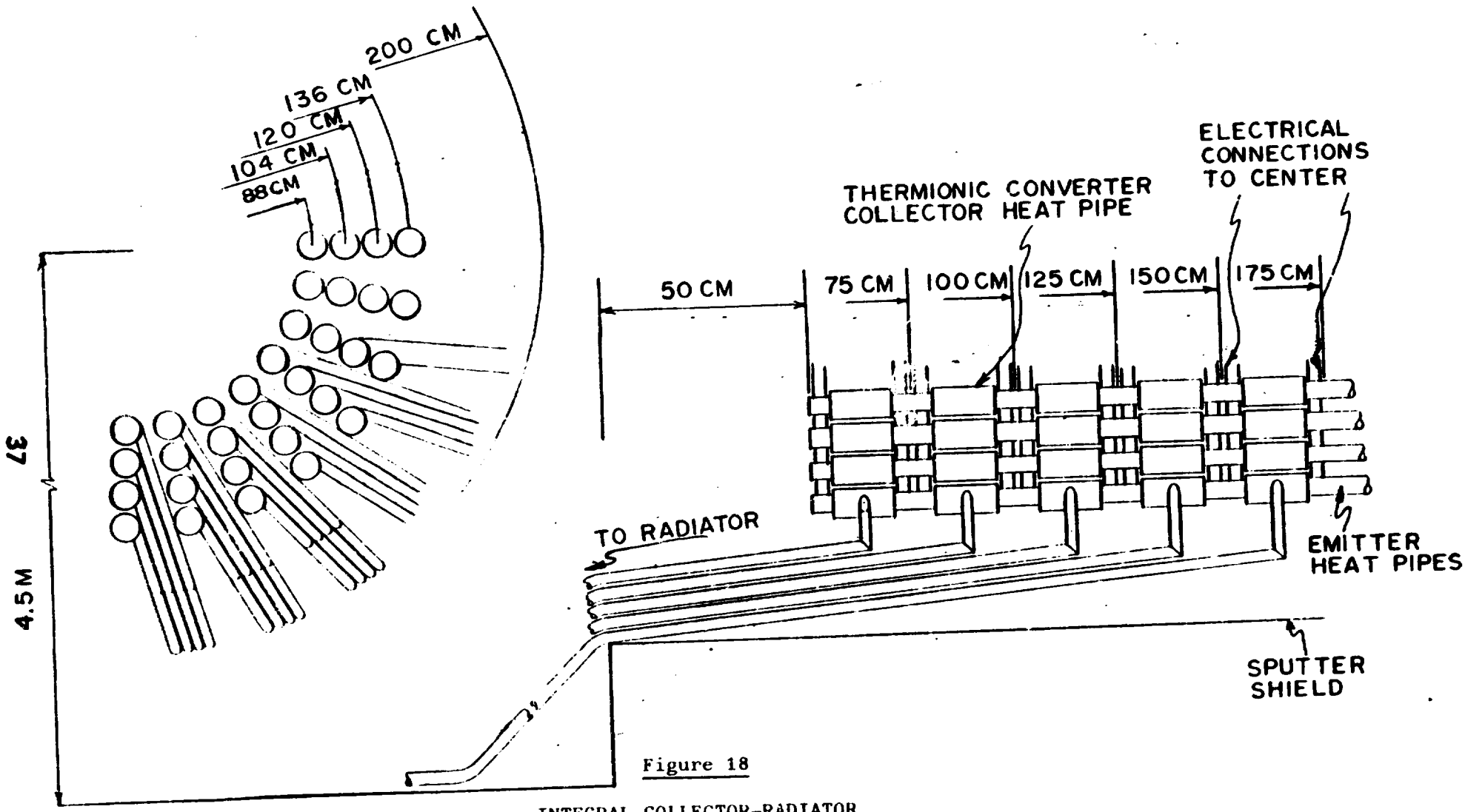


Figure 18

INTEGRAL COLLECTOR-RADIATOR

HEAT PIPE CONCEPT

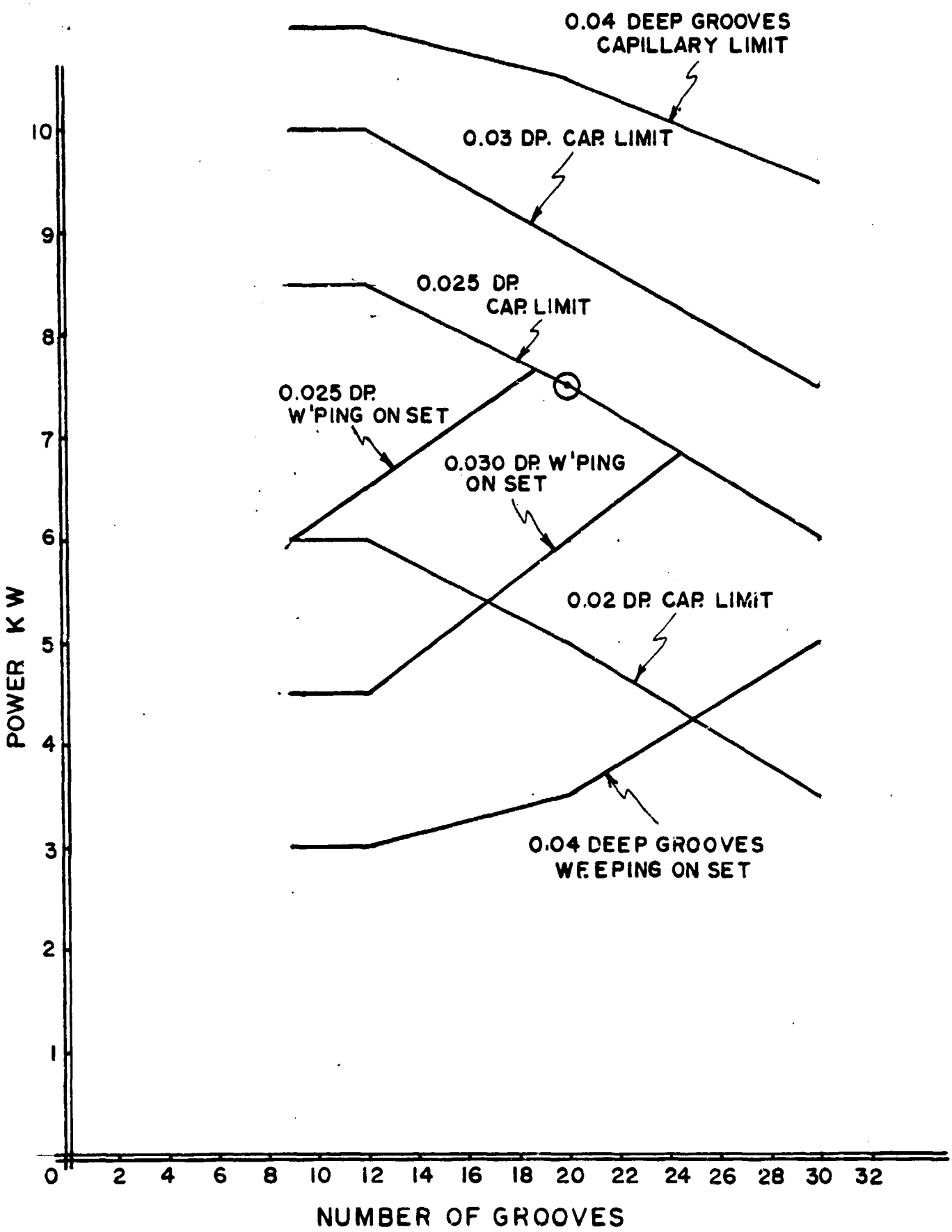
0.04 DEEP GROOVES
CAPILLARY LIMIT
0.03 DP. CAP. LIMIT
0.025 DP.
CAP. LIMIT
0.025 DP.
W'PING ON SET
0.030 DP. W'PING
ON SET
0.02 DP. CAP. LIMIT
0.04 DEEP GROOVES
WEEPING ON SET
POWER K W
1
2
3
4
5
6
7
8
9
10
0
2
4
6
8
10
12
14
16
18
20
22
24
26
28
30
32
NUMBER OF GROOVES

FIGURE 19

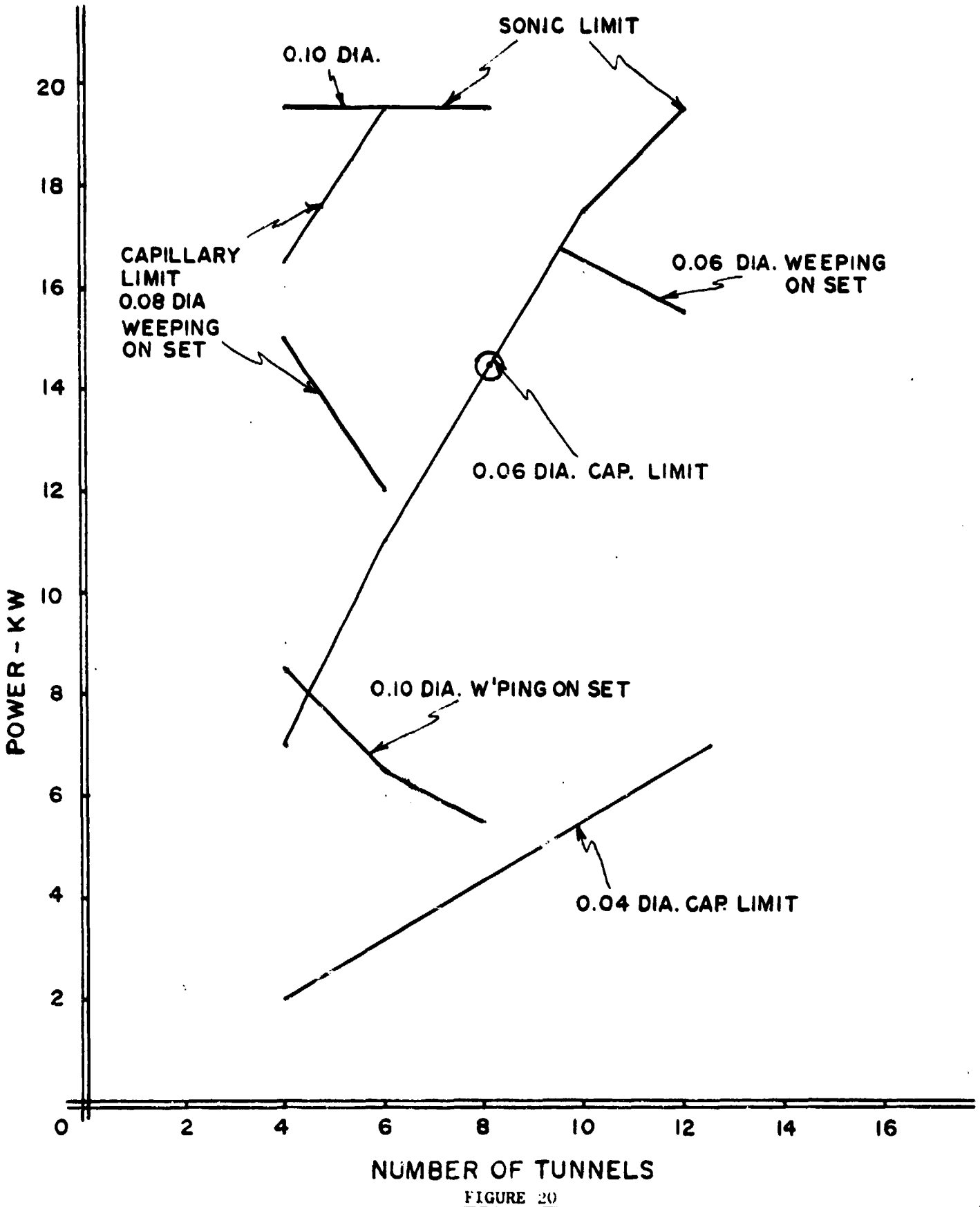
SONIC LIMIT
0.10 DIA.
CAPILLARY LIMIT 0.08 DIA WEEPING ON SET
0.06 DIA. WEEPING ON SET
0.06 DIA. CAP. LIMIT
0.10 DIA. W'PING ON SET
0.04 DIA. CAP. LIMIT
POWER - KW
NUMBER OF TUNNELS
0
2
4
6
8
10
12
14
16
18
20

FIGURE 20

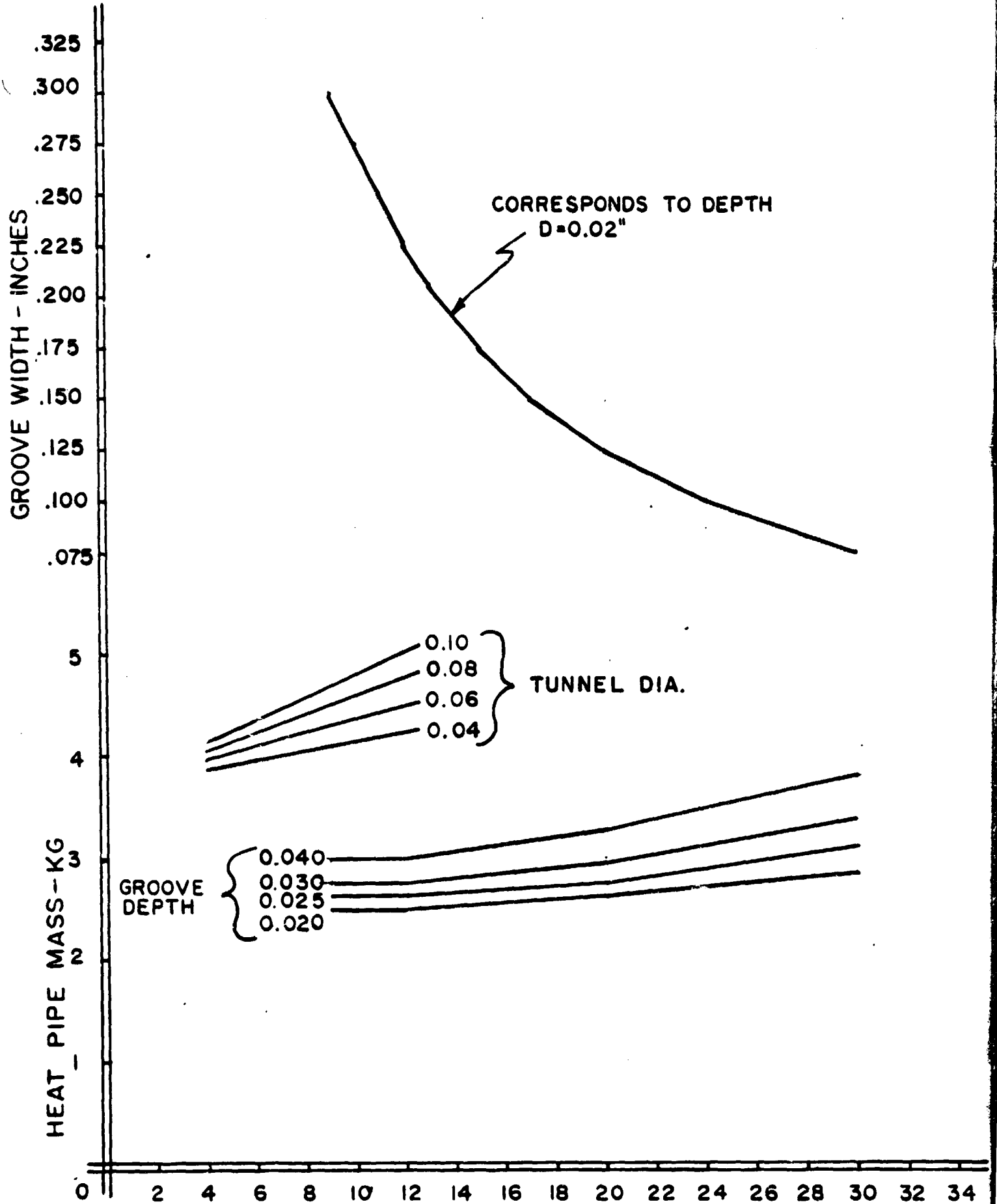
GROOVE WIDTH - INCHES
.325
.300
.275
.250
.225
.200
.175
.150
.125
.100
.075
CORRESPONDS TO DEPTH
D=0.02"
0.10
0.08
0.06
0.04
TUNNEL DIA.
HEAT PIPE MASS - KG
5
4
3
2
1
0
GROOVE DEPTH
0.040
0.030
0.025
0.020
2 4 6 8 10 12 14 16 18 20 22 24 26 28 30 32 34
NUMBER OF GROOVES/TUNNELS

FIGURE 21

design. These $\Delta$T's are from the OD of the collector to the OD of the radiator portion of the heat pipe.

3.3. Meteoroid Protection

When the collector heat pipe becomes a radiator element, it needs meteoroid protection. Initially, a solid niobium - 1% Zr armor was considered. The individual survival probability for each collector-radiator heat pipe was assumed to be 0.9. A computer program was written to predict the probability requirement,

using $P = 0.9$. $T = 105{,}120$ hr. $A = 1448$ cm$^2$

$$t = 0.52 \times 0.0010144 \left(\frac{AT}{-\ln P}\right)^{.2902}$$

The thickness for niobium - 1% Zr was found to be $t = 0.24$ cm, which if used as armor, has a mass of 2.98 kg per heat pipe.

Assuming the use of the 3.75 kg grooved heat pipe and 2.98 kg armor, each collector-radiator heat pipe has a mass of 6.73 kg for a total mass of the heat rejection system of 3634 kg. The armor is an integral part of the heat pipe and exhibits a 1.7 C $\Delta$T so the entire heat rejection system has a $\Delta$T of 9.22 C.

The thermal performance of the individual collector-radiator heat pipe concept is good in that the total $\Delta$T is less than 10 C. However, its mass is somewhat high. This design is considered to be buildable. In an effort to reduce the mass of the armor, the idea of using bumpers was considered. AI[5] shows that a mass reduction of 50-65% is possible. The major problem with the use of bumpers is that it also acts as a radiation shield.

Concurrent with the armor mass reduction thoughts, some consideration was given to methods of obtaining stable emissivities of 0.9 at 920 K. Since no coating is known which is stable for 12 years, the thinking

turned to sand-blasted or grit-blasted surfaces which exhibit emissivities of 0.5 to 0.6. The use of niobium oxide ( $\epsilon$ = 0.8) was considered; however, it was felt that the oxygen would diffuse into the heat pipe and react with the working fluid.

The method which was selected was the use of "black body fins". It is commonly known that holes which have a 6:1 depth to diameter ratio exhibit black body characteristics. This concept has been extended to fins with a 6:1 to 10:1 depth to spacing ratio and has produced emissivities in excess of 0.99.

The actual configuration of the fins can be straight along the length of the heat pipe radiator. They may take a Honeycomb configuration, and it may be possible to use a powder metallurgy matrix similar to a powder metal wick to achieve the effect. Figure 22 shows the three different concepts.

Figure 22 also implies that the 25-50% dense black body radiator will function properly as armor, and, in fact, with the same effectiveness as a 25-50% dense bumper shield. Only those meteors which are perpendicular to the axis of the heat pipe have a high probability of not encountering the armor shield. The shielding offered by porous armor needs further investigation. (See Thermacore Final Report, July 1979, JPL Contract 955108).

If a 25% dense Honeycomb armor 0.48 cm thick offers the same protection as 100% dense 0.24 cm thick armor, the mass of the armor is reduced by 50% and the $\Delta T$ of the armor is increased by approximately a factor of four. Then the mass of the heat rejection system is 2830 kg and has a total $\Delta T$ of 14.3 C.

The 14.3 C $\Delta T$ will increase the radiator portion of heat rejection

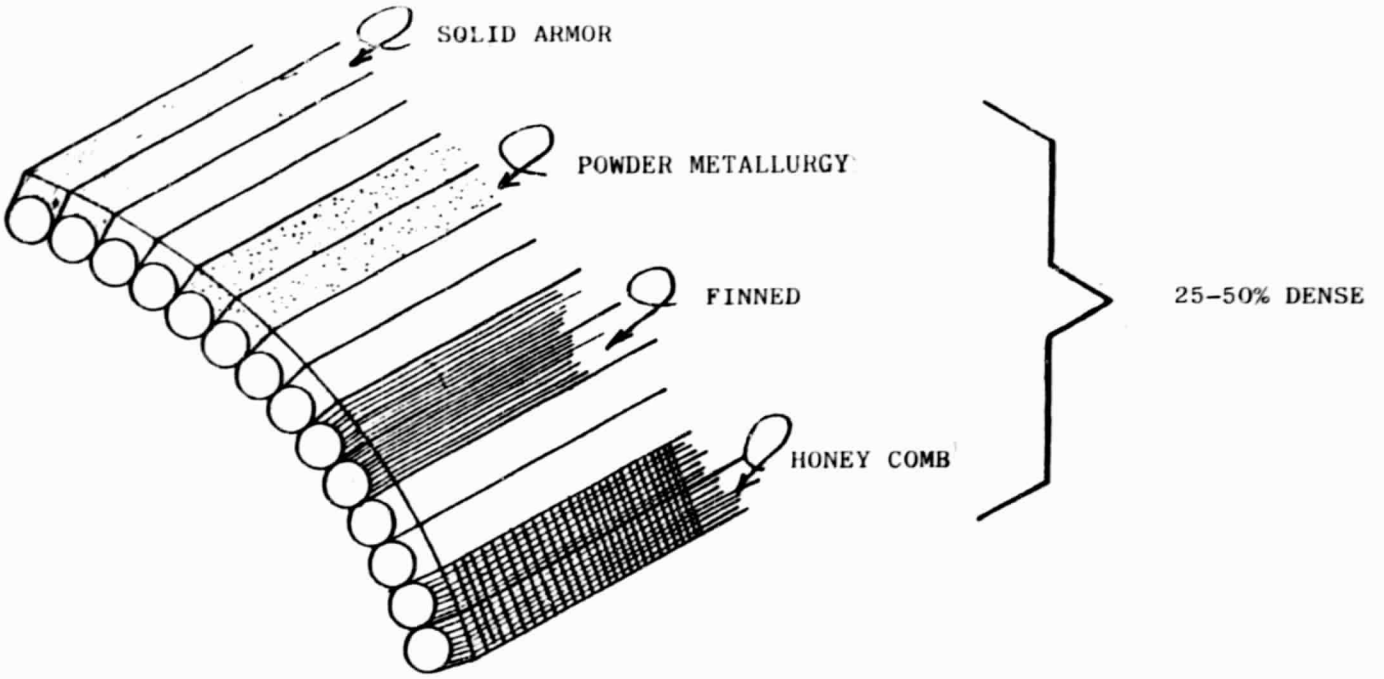


Figure 22

METEOROID PROTECTION CONCEPTS FOR HEAT PIPE RADIATOR

system by 6%. This increases the mass of the system to 2962 kg which is within 7% of the 2763 kg mass of the reference design.

## 3.4. Interim System Design

The heat rejection system as shown in Figure 18 was altered as shown in Figure 23. This design reflects a collector heat pipe-to-radiator interface to improve fabrication and assembly, and a coupling heat pipe to provide some redundancy between the various collector and radiator heat pipes.

The tangential portion of the collector heat pipe was redesigned to emanate from the "top" of the collector rather than the mid plane. The diameter of the collector heat pipe arm was reduced from 2.65 cm to 1.5 cm. This reduction in diameter allows for closer nesting of the heat pipe-thermionic cells. The thermionics are now on concentric circles with diameters of 62, 76, 90 and 104 cm. In addition, the 1.5 cm diameter heat pipe now terminates at the "lower" plane of the cell. This permits the assembly of the thermionic converter after the collector heat pipe has been built and tested. Thus, the thermionics can be tested prior to installation into the system.

The 2.65 cm diameter radiator heat pipe is built over the 1.3 cm diameter heat pipe after the thermionics have been tested. Several interface designs were considered and are seen in Figures 24 and 25. This interface is an additional thermal resistance within the overall heat rejection system and must be reckoned with.

The thermal resistance of the collector-radiator interface is a function of the length of the interface, which is a function of the length of the emitter and the intercell spacing. Current thermionic performance and design calls for an emitter length of 30 cm with a

B59-6

FIGURE 23

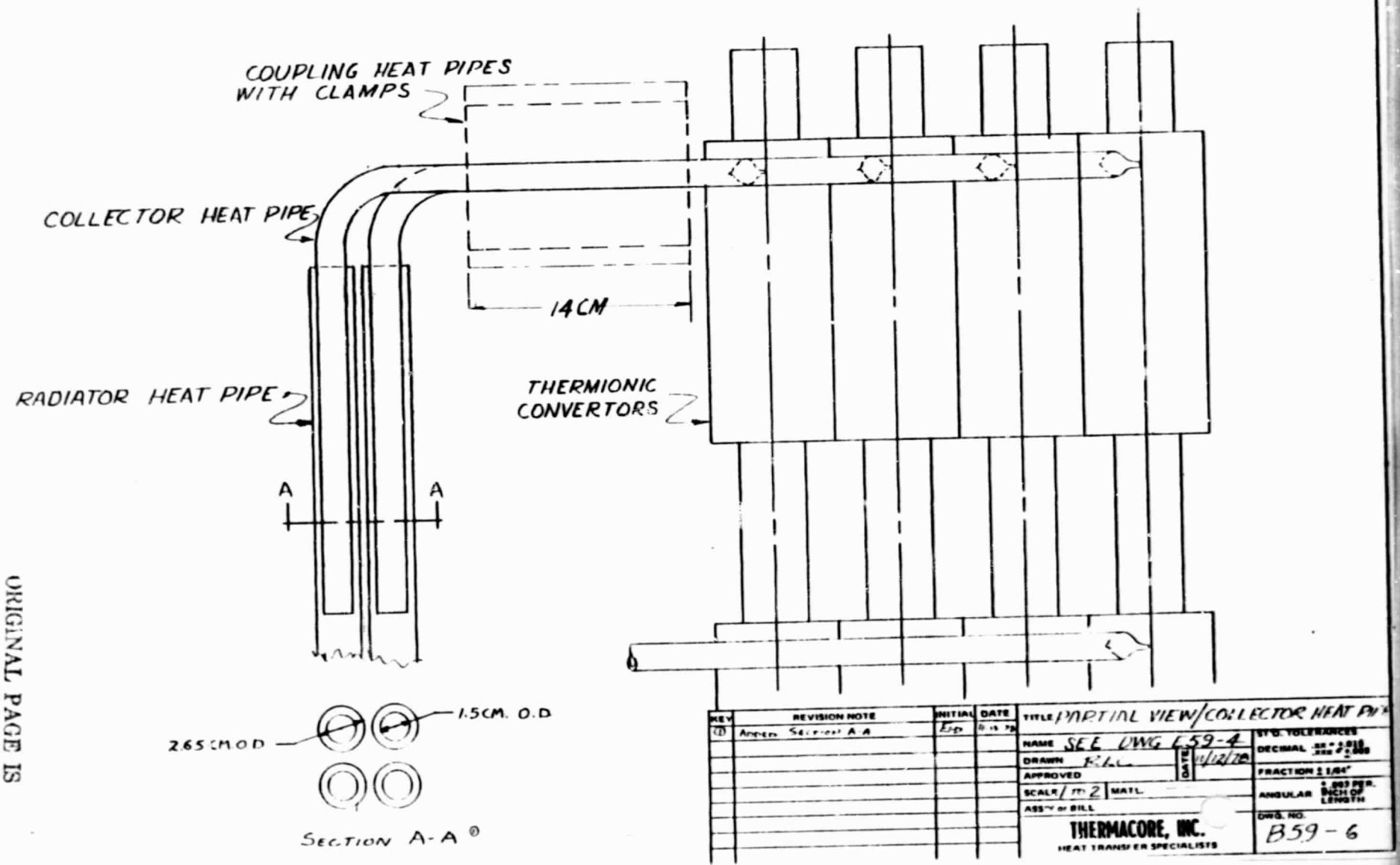




ORIGINAL PAGE IS
OF POOR QUALITY

DWG. NO. B59-5

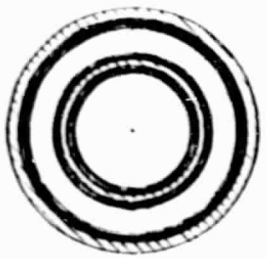

SECT B-B①

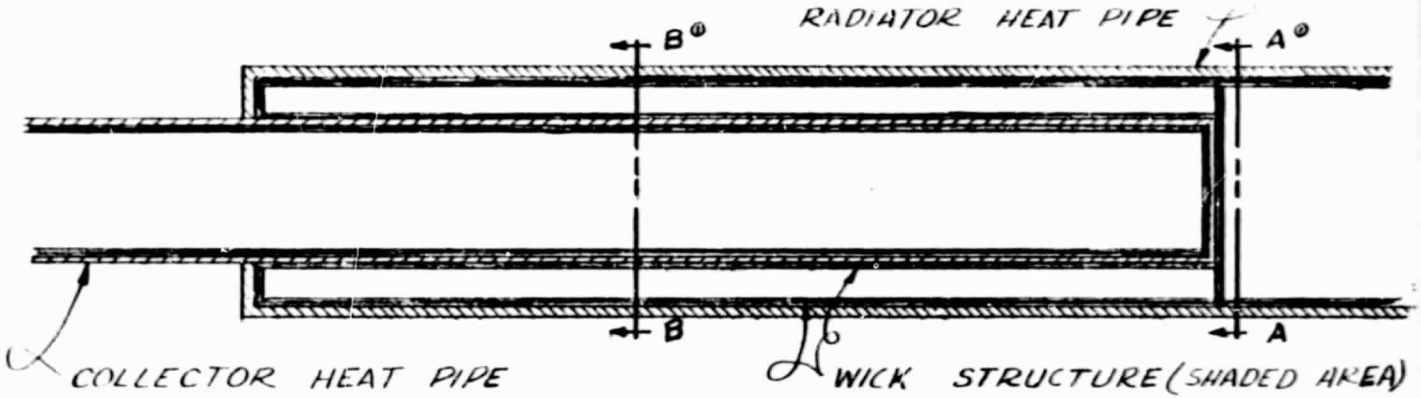


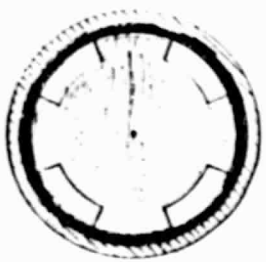

SECT A-A①

| KEY | REVISION NOTE | INITIAL | DATE |
|---|---|---|---|
| ① | Rev. B.S. Added A-A | EPD | 11/13/78 |

TITLE JOINT - COLLECTOR / RADIATO

NAME

DRAWN RLC DATE 11/17/78

APPROVED

SCALE 2 TO 1 MATL. —

ASS'Y or BILL

THERMACORE, INC.
HEAT TRANSFER SPECIALISTS

STD. TOLERANCES

DECIMAL .xx ± .010 .xxx ± .005

FRACTION ± 1/64

ANGULAR ± .005 INCH OF LENGTH

DWG. NO. B59-5



Figure 24

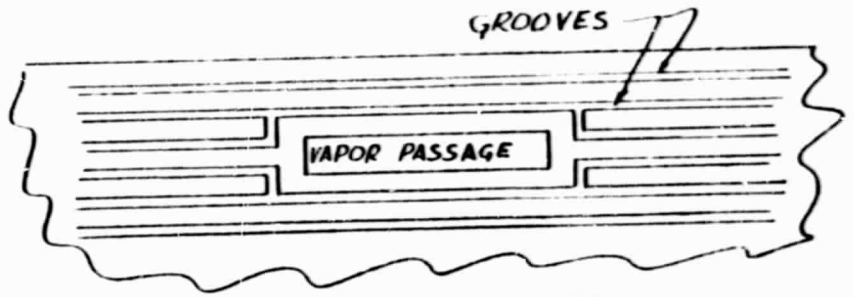


DETAIL OF GROOVES
AROUND VAPOR PASSAGE

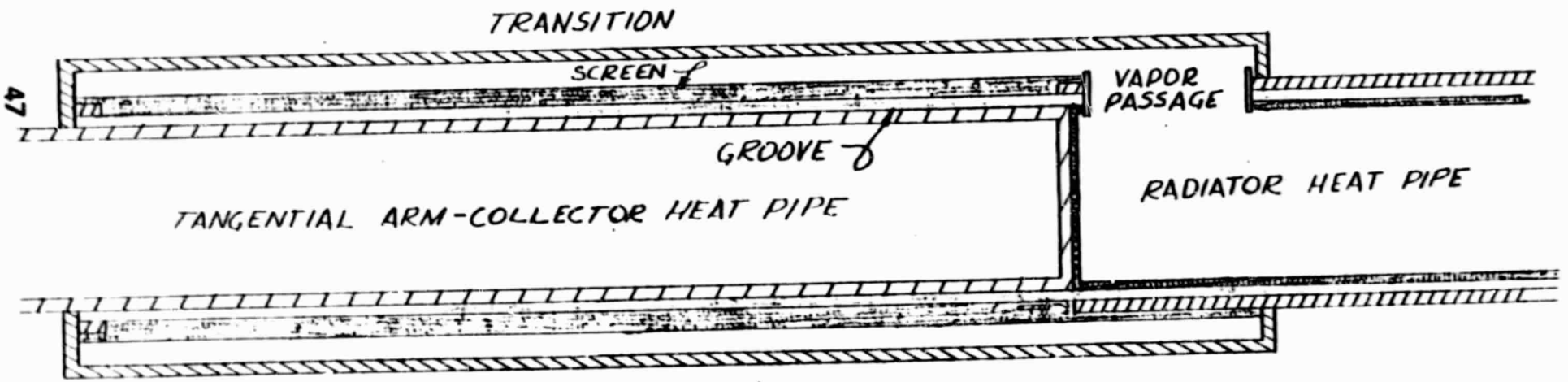


Figure 25

HEAT PIPE GROOVE GEOMETRY

IN TRANSITION ZONE

10 cm intercell length. This provides a 32 cm heat pipe interface. Design goals for the flight hardware are 16.7 cm emitter length with a 10 cm intercell length which makes the heat pipe interface 18.7 cm length. The interface temperature drop is estimated as 22 C for potassium-niobium heat pipes with a 1.5 cm diameter x 18.7 cm length interface. The 37 cm length interface shows an 11 C $\Delta$T. Thus, from the heat rejection point of view, a longer thermionic emitter at the same power per emitter is beneficial in reducing the total temperature drop within the system.

The coupling heat pipe which thermally connects four tangential collector heat pipes together is seen in Figure 26. The cylindrical shape was chosen to take advantage of its inherent strength. The multi-foil thermal insulation is employed within a load bearing shell, which transmits the force from the spring to the coupling heat pipe to assure good thermal contact. Internal struts will transmit the load from the outer shell of the heat pipe to the inner scalloped member. The multifoil is used to keep the temperature of the spring low enough so it is not annealed over the mission lifetime.

## 3.5. Final System Design

The final "snap shot" system design for the NEP spacecraft is seen in Figures 27 and 28. This design has fewer converters and larger radiator heat pipes. There are 480 thermionic converters distributed in a cylindrical array of six layers. Each layer has four concentric circles of 20 diodes on 44, 51, 58 and 65 cm diameters.

The new design requires 5312 watts dissipation per heat pipe radiator versus 4815 in the interim design. The diameter of the collection heat pipe remains at 7 cm. However, the outer sheath diameter of the converter

B59-7

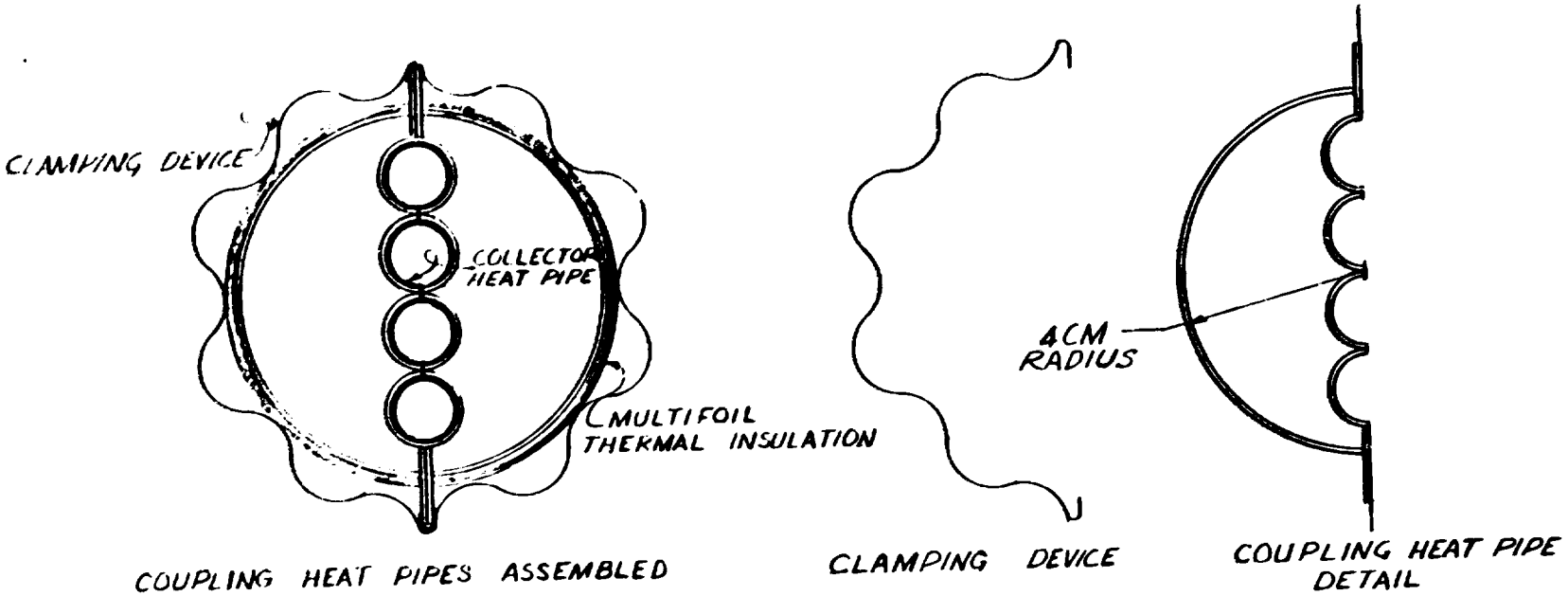


COUPLING HEAT PIPES ASSEMBLED

CLAMPING DEVICE

COUPLING HEAT PIPE DETAIL

Figure 26

| REV | REVISION NOTE | INITIAL | DATE |
|---|---|---|---|
| | | | |

TITLE DETAILS FOR COUPLING HEAT PIPE

NAME

DRAWN F.C. DATE 11/12/76

APPROVED

SCALE /0 / MATL. ---

ASS'Y or DILL

THERMACORE, INC.
HEAT TRANSFER SPECIALISTS

DWG. NO. B59-7

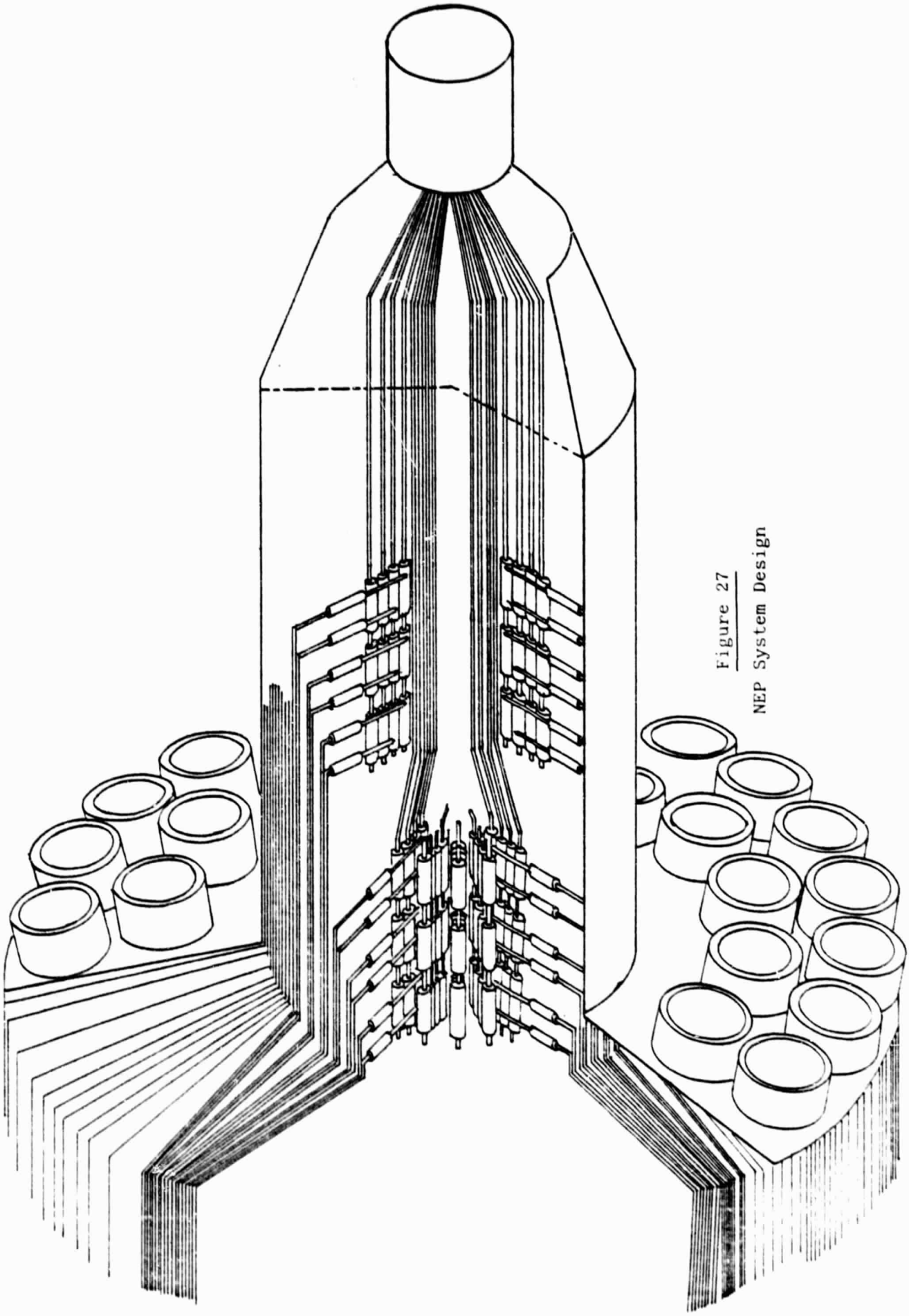

Figure 27

NEP System Design

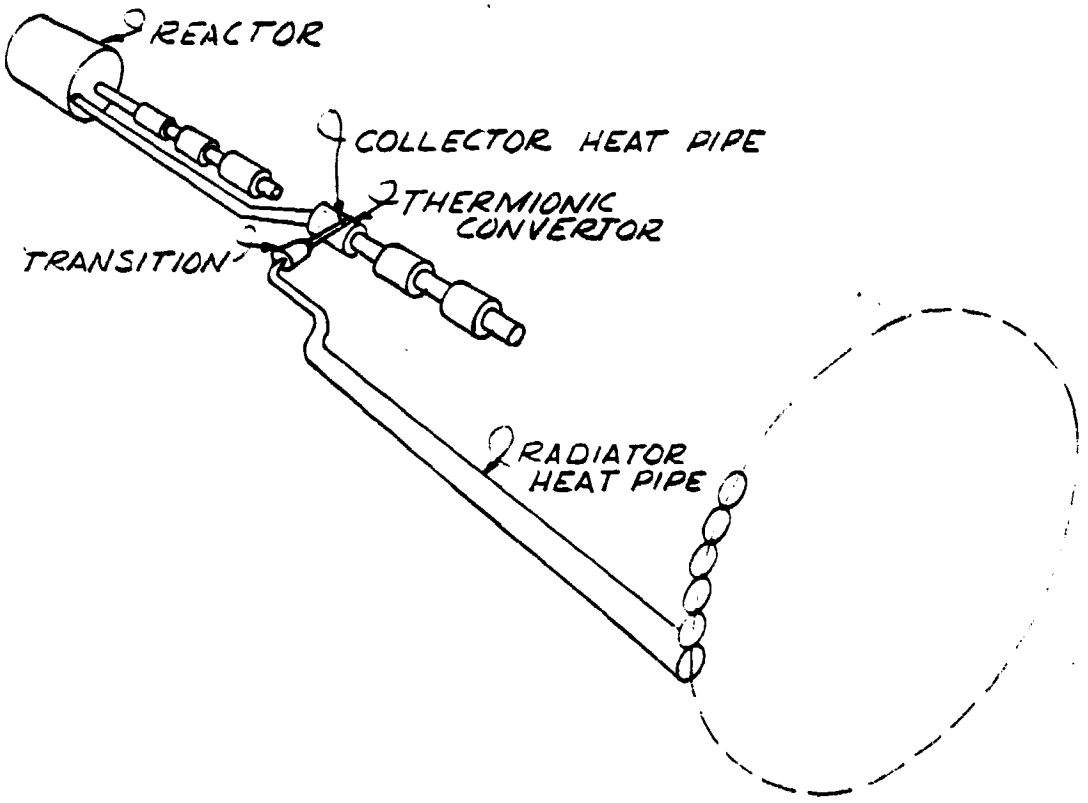


Figure 28

NEP HEAT REJECTION CONCEPT

was reduced to 3.6 cm. The thermionic emitter length is 22.2 cm and the thermionic cell length is 30 cm.

The tangential arm heat pipe is increased in size from 1.6 cm to 2.0 cm and the radiator heat pipe is increased in size from 2.6 cm to 2.9 cm.

The lengths of all of the heat pipes were calculated, from which an "average heat pipe" was calculated to determine thermal performance and mass calculations. The results are seen in Table VII.

A mass of 5.97 kg per heat pipe amounts to 2866 kg for the entire radiator system. These mass calculations assume a 603 cm long radiator heat pipe, which is radiating at the root of the black body cavity at a temperature of 900 K and off the ends of armor fins at 896 K. From Table VII the actual temperatures are 904.55 K and 898.32 K respectively. Thus a small safety factor (1.7%) is built in which is in addition to the 4.3 % safety factor built into the 603 cm length.

If the 6% safety factor is removed from the mass of the radiator heat pipes and armor, then the individual heat pipe has a mass of 5.72 kg with a system mass of 2745 kg.

Appendix A contains a detailed package of drawings reflecting the system design. An explanation of the drawings follows:

C-59-500

An isometric view of the NEP heat rejection concept showing the reactor, emitter heat pipes, converters, collector heat pipes and radiator heat pipes.

B-59-501

The design has 480 diodes on four concentric rings on six levels. The upper three levels are fed by one group of emitter heat pipes. The

## TABLE VII

### HEAT PIPE RADIATOR SPECIFICATIONS AND PERFORMANCE FOR A 480 THERMIONIC DIODE CYLINDRICAL ARRAY

| | |
|---|---|
| Power Dissipation per Element | 5312.5 watts |
| Total Radiator Power | 2550 Kg |
| Annular Collector Heat Pipe (Evaporator) | |
| 6.8 cm O.D. x 3.6 cm I.D. x 22.2 cm long | 0.311 Kg |
| Tangential Arm of Collector Heat Pipe | |
| Adiabatic - 2 cm O.D. x 54.5 cm long | 0.11 Kg |
| Condenser - 2 cm O.D. x 37.3 cm long | |
| Radiator Heat Pipe | 0.26 Kg |
| Evaporator - 4 cm O.D. x 2 cm I.D. x 37.3 cm long | |
| Adiabatic - 2.9 cm O.D. x 293.9 cm long | 1.10 Kg |
| Condenser - 2.9 cm O.D. x 603 cm long (1.043%) | 2.25 Kg |
| Armor - 1.02 cm thick x 25% dense | 1.94 Kg |
| TOTAL - Mass per Heat Pipe | 5.97 Kg |
| Mass per Radiator System | 2866 Kg |

| | |
|---|---|
| Diode Outer Sheath Temperature | $T = 923.00^{\circ}K$ |
| Collector Heat Pipe $\Delta T = 12.17$ | |
| Average Temperature Collector-Radiator Heat Pipe Interface | $T = 910.83^{\circ}K$ |
| Radiator Heat Pipe $\Delta T = 6.28$ K | |
| Average Root Temperature of Armor Fins in Radiating Cavity of ($\epsilon = .9$) - A = 1290 cm | $T = 904.55^{\circ}K$ |
| Armor Fins $\Delta T = 6.23$ K | |
| Fin Tip Temperature - ($\epsilon = .7$) - A = 486 $cm^2$ | $T = 898.32^{\circ}K$ |

lower three levels are fed by a second set of emitter heat pipes. Thus, if one takes out an equal radial segment, there are twenty such segments with twenty-four diodes per segment. This drawing defines the numbering system for each of the twenty segments in the overall matrix.

D-59-502

This is a plan view of the collector heat pipes showing the 30 cm transition zone to the radiator heat pipes.

D-59-503

This is an alternate plan view of the collector heat pipe arrangement in an attempt to lengthen the transition zone.

D-59-504

This is an elevation of the matrix of the base line design. (D-59-502)

C-59-505

This is a typical view of one level showing the arrangement of the tangential arm-collector heat pipe confluence.

B-59-506

This drawing shows physical dimensions required for $30^{\circ}$ and $60^{\circ}$ bends in the emitter heat pipes for the lower three levels.

C-59-507

Details of the groove wick design within the transition of the radiator heat pipe to the tangential arm heat pipe.

B-59-508

A listing of the length and diameters of the twenty-four different heat pipe systems.

## 4. COLLECTOR HEAT PIPE DEMONSTRATION MODEL

While the system design evolved, as presented in Section 3, the collector heat pipe design also evolved. This annular to tangential heat pipe transition was selected for the demonstration heat pipe model, and is seen in Figure 29.

The demonstration model was two heat pipes, one built around the other, thus sharing a common wall. The first, or driver heat pipe, simulated a thermionic converter. The second or collector heat pipe was of annular construction and built around the condenser of the first. The annular portion of the collector heat pipe had a tangential arm emenating from its outer wall. This tangential arm was of circular construction and consisted of a condenser attached to an adiabatic section, which contained a 45° bend just beyond its attachment to the outer envelope of the annular section.

The design and fabrication are presented together because they are inter-related in the fact that several design modifications were invoked as a result of fabrication procedures. The design covered is the final version. Intermediate designs are discussed only to the extent they provide insight to the fabrication techniques or final design.

### 4.1. Design

The collector heat pipe demonstration model is seen in Figures 29. The materials of construction were 316 L stainless steel for the envelopes and 304 L or 316 L for the wire mesh wicks. Both heat pipes used sodium as the working fluid. The nominal temperature of operation was 920° K. The required power was 5312 watts.

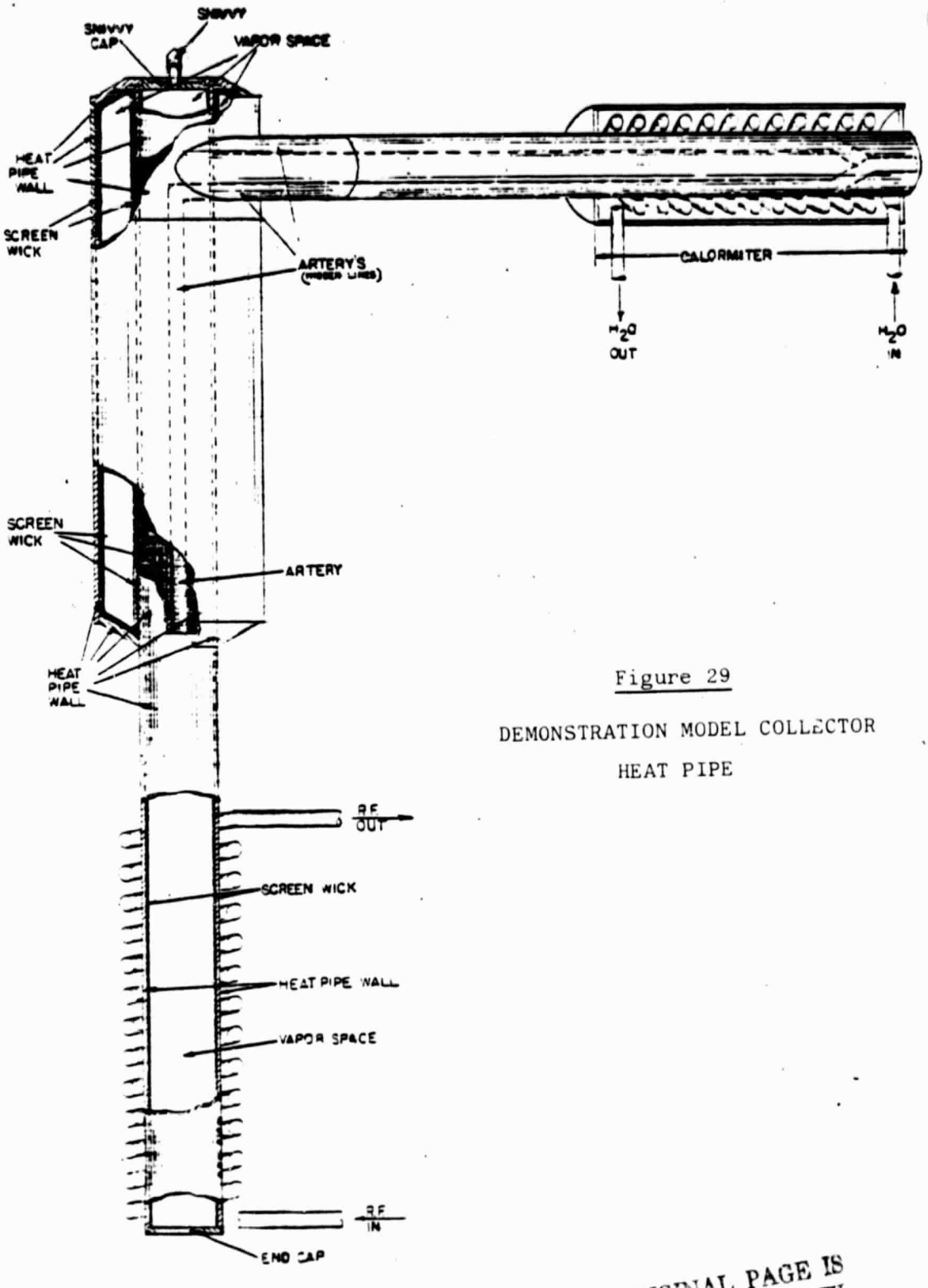


Figure 29

DEMONSTRATION MODEL COLLECTOR HEAT PIPE

ORIGINAL PAGE IS OF POOR QUALITY

### 4.1.1. Driver Heat Pipe

The driver heat pipe was 1" IPS Sch. 5 (1.315" OD x 0.065 wall) pipe 18 inches long. The evaporator was 9 inches long, the condenser 8 inches long, and the adiabatic zone was 1 inch long. The wick was chosen such that the heat pipe was capable of operating either in the horizontal position or with gravity assistance.

The initial wick design was four wraps of 40 x 40 mesh for use with potassium. Several potassium heat pipes were fabricated and tested with the same results: hot spots in the evaporator at relatively low powers. An analysis of the test data showed that the limiting power was inversely proportional to the temperature, i.e. the higher the operating temperature the lower the limiting power. This type of limitation is indicative of the boiling or super heat limit of the working fluid. This limit is well known and recognizable, however, the ability to predict the onset of boiling, without pretesting of the actual device is limited. Accordingly, the driver heat pipe was redesigned for use with sodium.

The wick design for the driver heat pipe with sodium working fluid was two layers of 40 x 40 mesh. The reduction of the wick thickness by 50%, coupled with sodium's increased ability to withstand super heat, was felt to be sufficient to assure the performance of the sodium driver heat pipe.

A theoretical treatment of the super heat limit has been presented by several authors.[10,11] The essence of these treatises equate the $\Delta T$ through the liquid filled wick to be the super heat driving force to promote boiling, and the bubble radius to have an upper limit equal to the mesh opening half width.

Appendix B contains the several equations and calculations for the driver heat pipe with sodium and potassium at 920°K. The results are seen in Table VIII for the two driver heat pipe designs.

From Table VIII one sees, within the accuracy of the correlation, that the sodium driver heat pipe should perform satisfactorily. However, since the super heat limit is very temperature sensitive and inversely proportional to the temperature, the temperature of the driver heat pipe must be kept near the design point of 920°K.

Figure 30 shows the driver heat pipe operating at the design temperature. This test was performed with the evaporator elevated to force the heat pipe to operate against gravity. Thus, the capability of the heat pipe (except for super heat limit) could be determined without the need to provide the full thermal load. These tests were performed at 950°K and 1100°K.

TABLE VIII

SUPER HEAT CORRELATIONS

T - 920°K

| | | Correlation | | |
|---|---|---|---|---|
| | | Ernst & Shefsiek[10] (Limits) | Hsu[11] | Requirement |
| Wick Type | Fluid | $\Delta T$ - Q/A °K - W/cm$^2$ | $\Delta T$ - Q/A °K - W/cm$^2$ | Q/A W/cm$^2$ |
| 4 Wraps 40 Mesh | K | 2 - 3 | 25 - 37 | 27 |
| 2 Wraps 40 Mesh | Na | 13 - 71 | 169 - 910 | 27 |

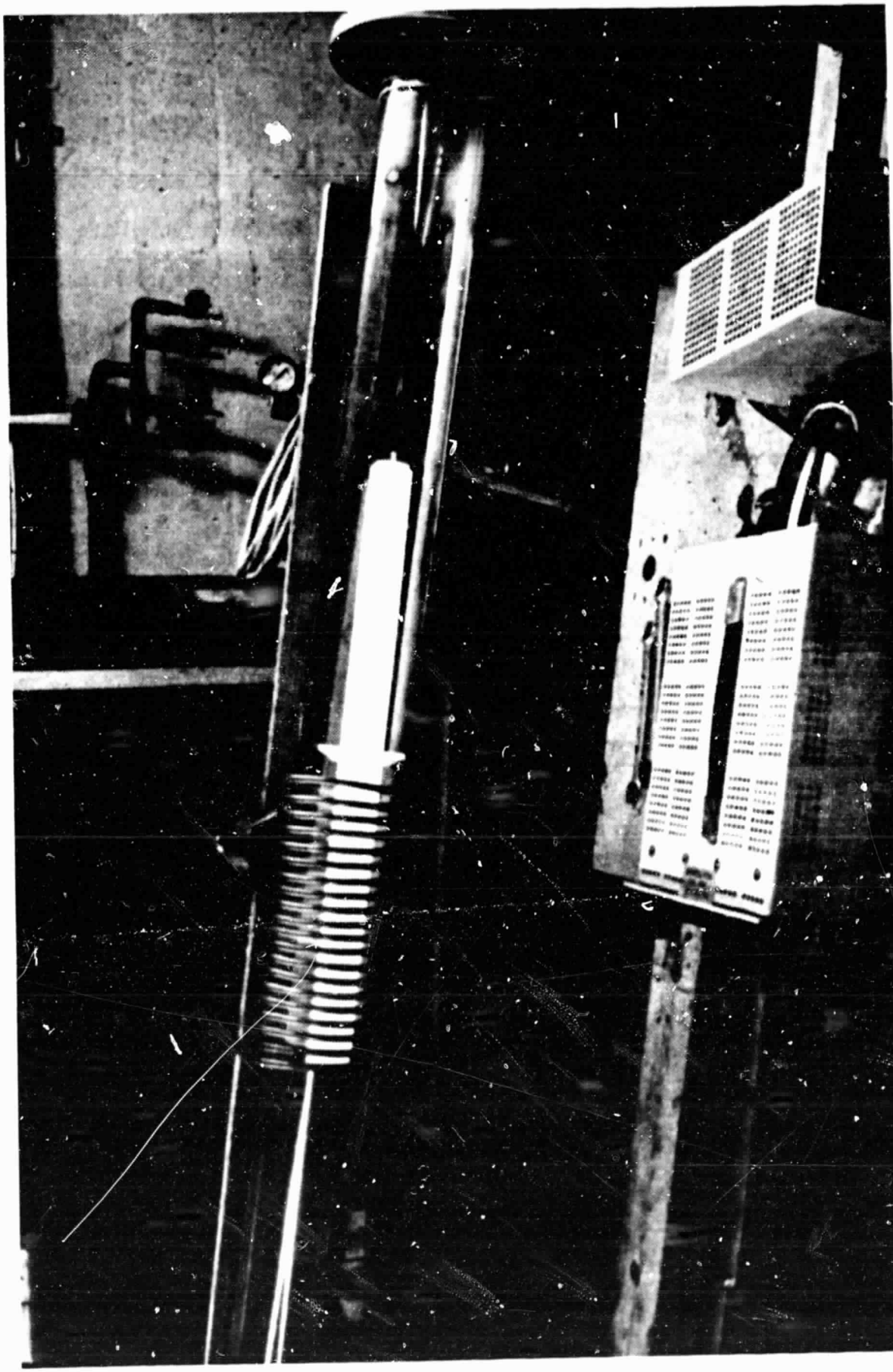

FIGURE 30

DRIVER HEAT PIPE OPERATING AGAINST GRAVITY AT 920°K

ORIGINAL PAGE IS
OF POOR QUALITY

The radiant power of the condenser portion of the heat pipe at 950 and 1100°K is 660 and 1120 watts respectively. The opposing gravity angles which make these a limit for the heat pipe are 12 and 10°. Thus for an 18" long heat pipe the elevation of the condenser above the evaporator is 3.75 and 3.125 inches. Accordingly, the heat pipe was set up with the condenser 3.75" above the evaporator and tested. At no time did the heat pipe show signs of being at a limit.

From the results of these tests, it was concluded that the heat pipe should be capable of transferring the required power of 5300 watts. Accordingly, the assembly of this heat pipe into the collector heat pipe was begun.

4.1.2. Collector Heat Pipe

Initially the collector heat pipe was to use potassium as the working fluid. However, re-evaluation of the design with sodium showed a trade-off between the possibility of reaching the boiling limit in the evaporator with potassium and too large of a vapor pressure drop in the transition from the annular evaporator to circular adiabatic and the bend in the adiabatic zone with sodium. Based on the performance of the driver heat pipe and previous results, sodium was chosen as the working fluid.

The wick structure was made from 100 mesh. The evaporator had three wraps of mesh placed around the OD of the driver heat pipe. These were fed by two wire mesh arteries. The arteries were 0.156" ID x 0.250" OD. Their overall length was 20", and since they were flexible they could easily be fed around the bends in the collector heat pipe.

The condenser wick consisted of two wraps of 100 mesh feeding the two arteries. Figures 31 and 32 show the collector heat pipe in its final stages of assembly. The arteries can readily be seen in Figure 31 and the one layer of mesh on the ID of the outer portion of the annular

ORIGINAL PAGE IS
OF POOR QUALITY

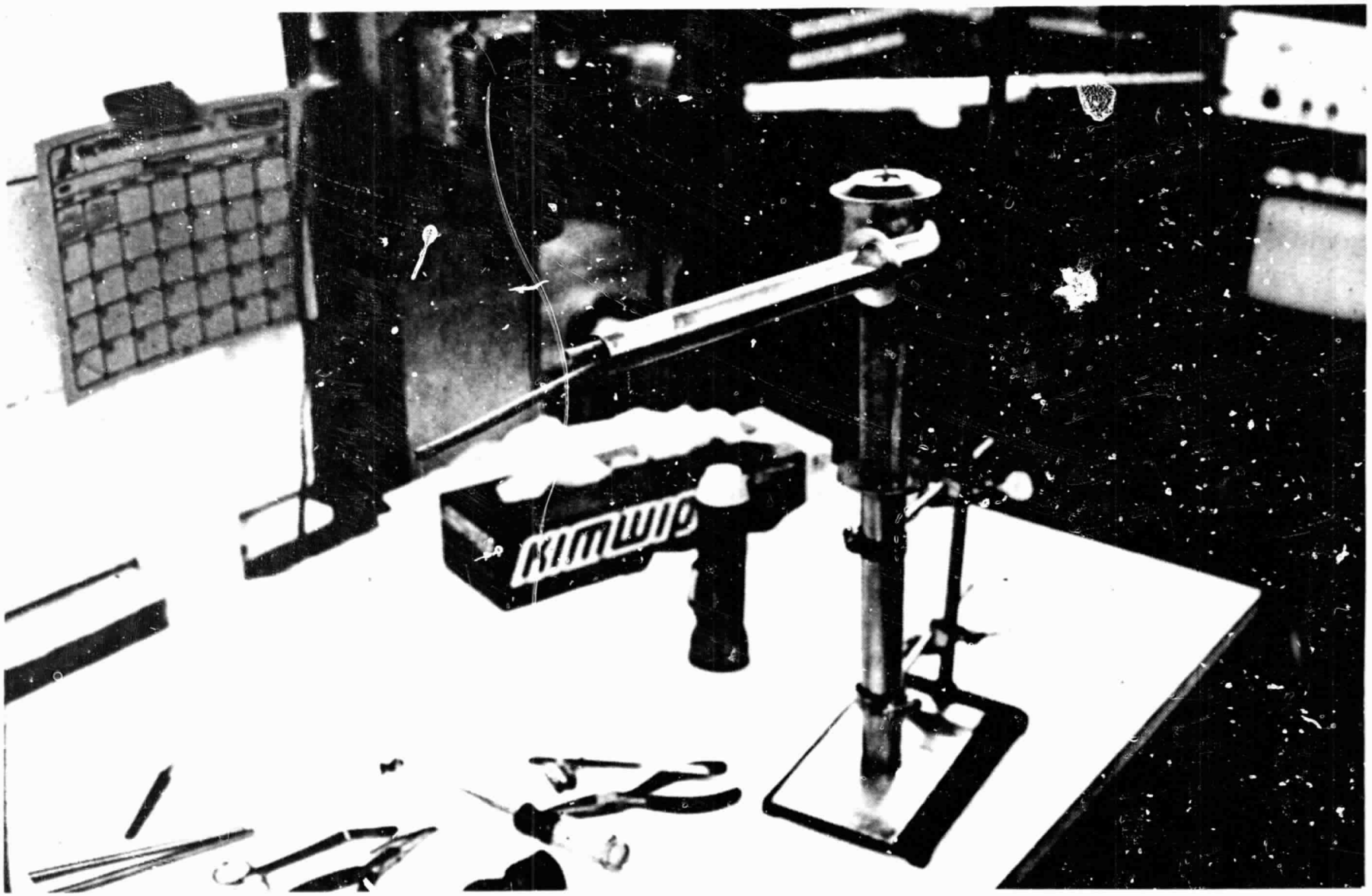

FIGURE 31

COLLECTOR HEAT PIPE DURING ASSEMBLY

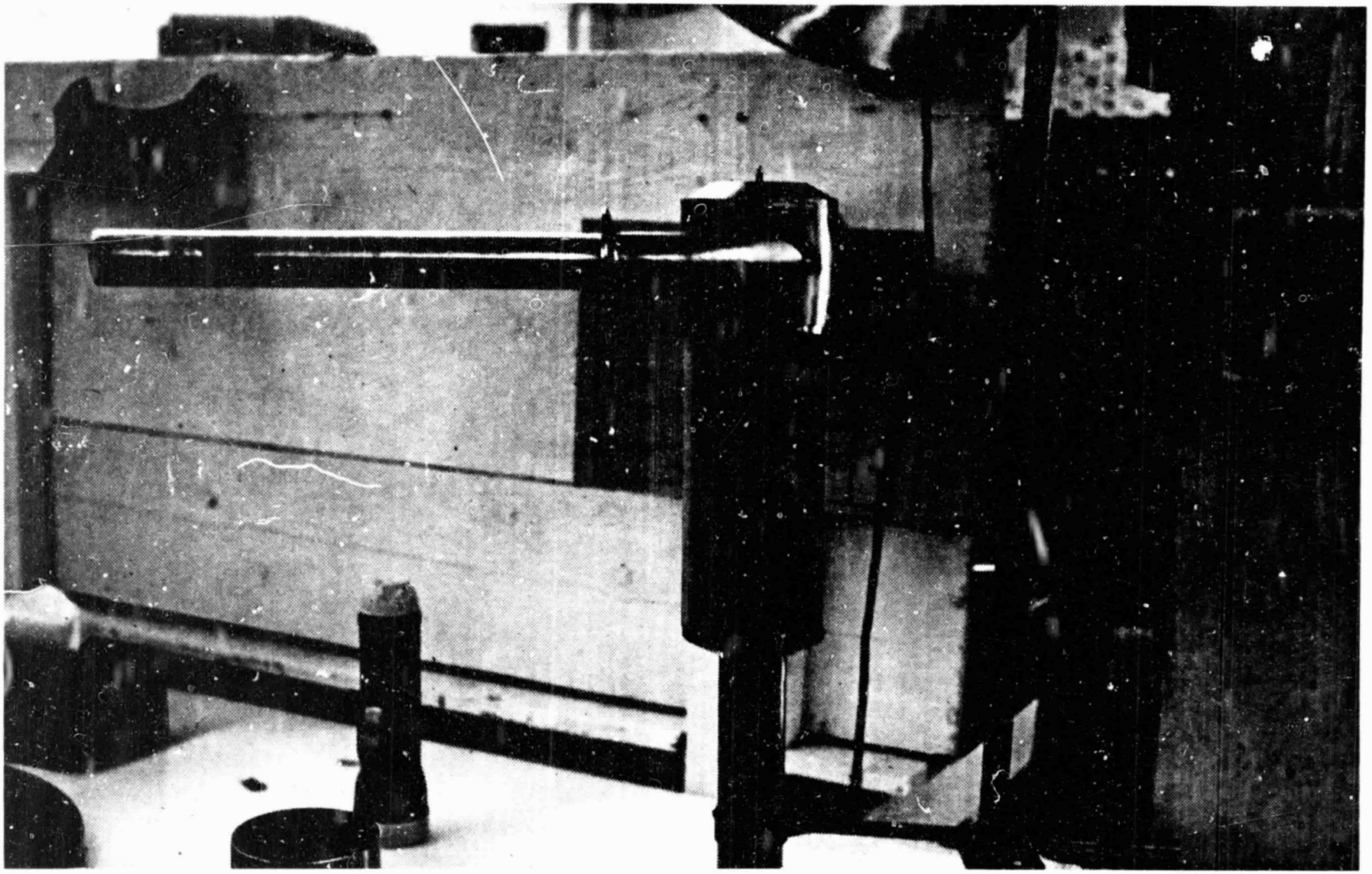

FIGURE 32

COLLECTOR HEAT PIPE DURING ASSEMBLY

collector heat pipe can be seen in Figure 32. Figure 33 shows the collector heat pipe being set up for processing. Figures 34 and 35 show the collector heat pipe operating without the gas gap calorimeter.

Following the processing of the collector heat pipe, it was fitted with a gas gap calorimeter and tested.

4.1.3. Collector Heat Pipe Test

The collector heat pipe assembly was successfully tested to 50% of its designed power of 5312 watts, at a temperature approximately 50°K lower than the 920°K design temperature. The design criteria and test data are seen in Table IX. The operating temperatures of 873°K was an estimate from visual observation and it was impossible to determine the $\Delta$T. Temperature measurements by thermocouples were impeded by the RF field. Shielded thermocouples were ordered and installed upon receipt.

Higher power levels were not achieved in these tests as the driver heat pipe developed a leak. This leak was traced to the seam weld of the 316L SS pipe from which the driver heat pipe was made. Normally, seamless tubing is used for heat pipe fabrication; however, at the time the driver heat pipe was assembled seamless tubing of the proper size was unavailable.

The leaking portion of the driver heat pipe was removed. The opened heat pipe was fitted with a new end cap and processing tube. Following this, it was reprocessed and sealed off. The heat pipe was retested with no evidence of problems associated with reprocessing, i.e. a cold end resulting from non-condensable gases.

Following reprocessing, testing of the heat pipe was limited at higher temperatures due to hot spots which were evident in the driver

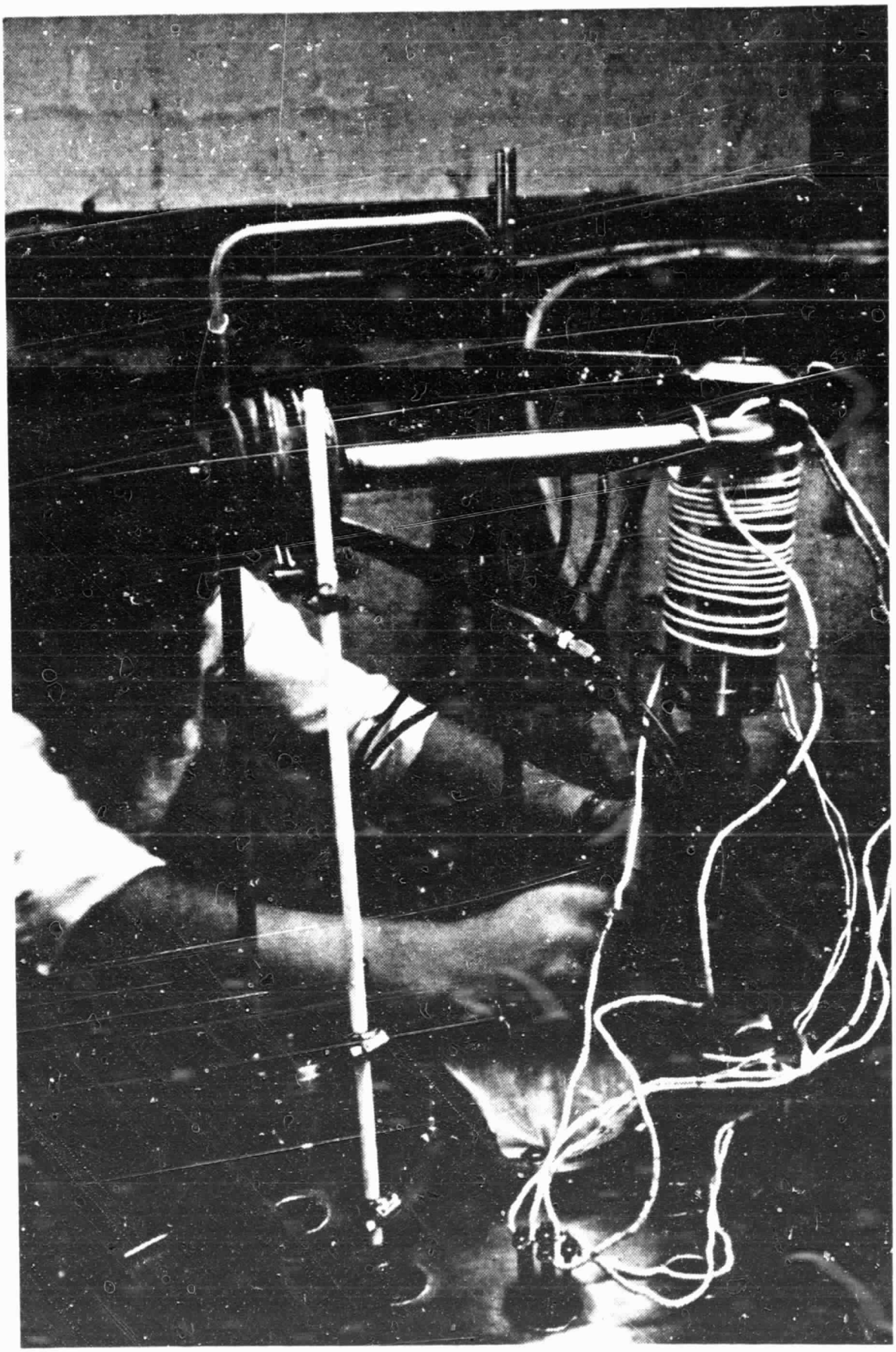

FIGURE 33

COLLECTOR HEAT PIPE BEING PREPARED FOR PROCESSING



ORIGINAL PAGE IS
OF POOR QUALITY

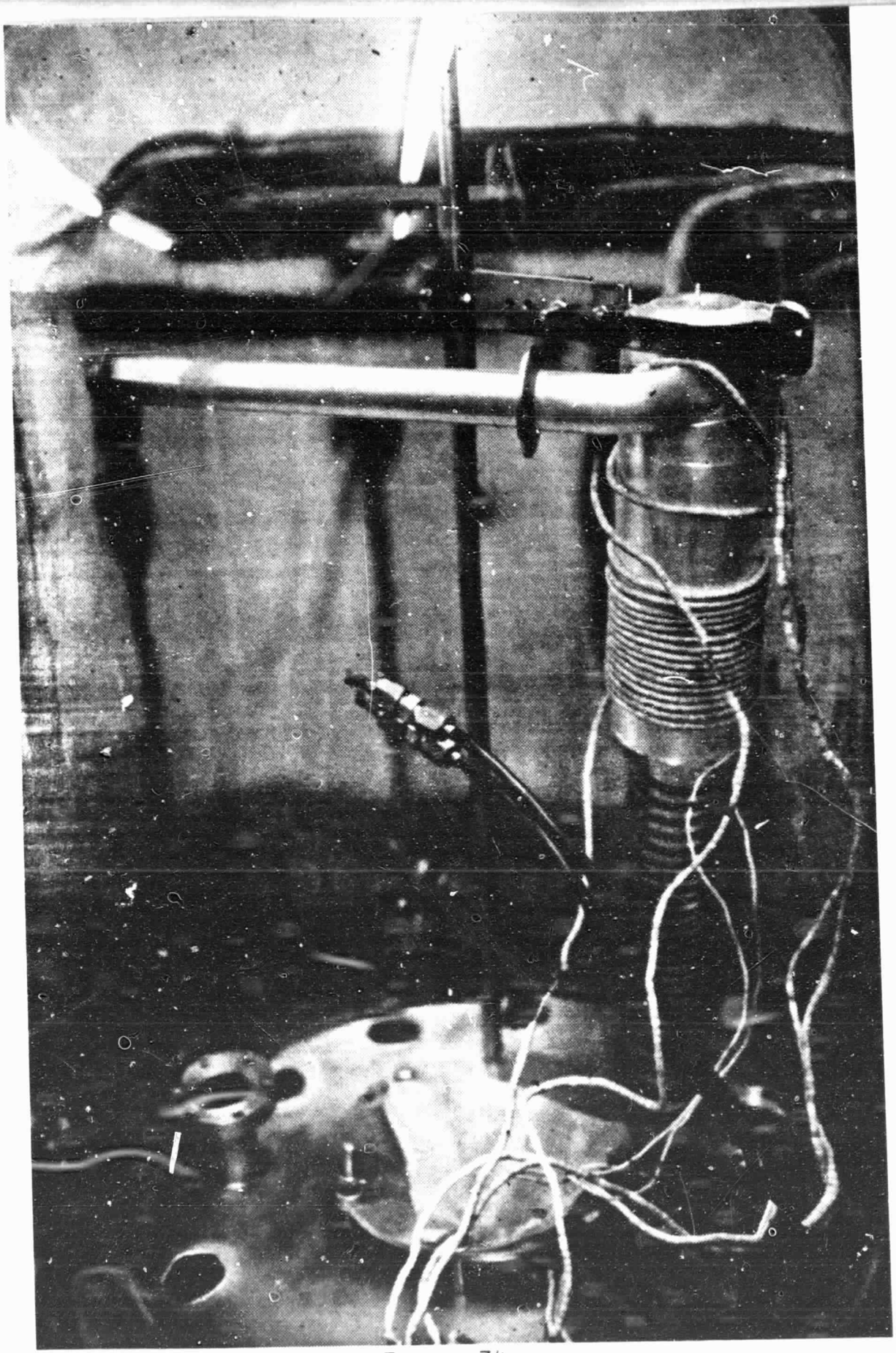

FIGURE 34

COLLECTOR HEAT PIPE OPERATING AT 920°K



ORIGINAL PAGE IS
OF POOR

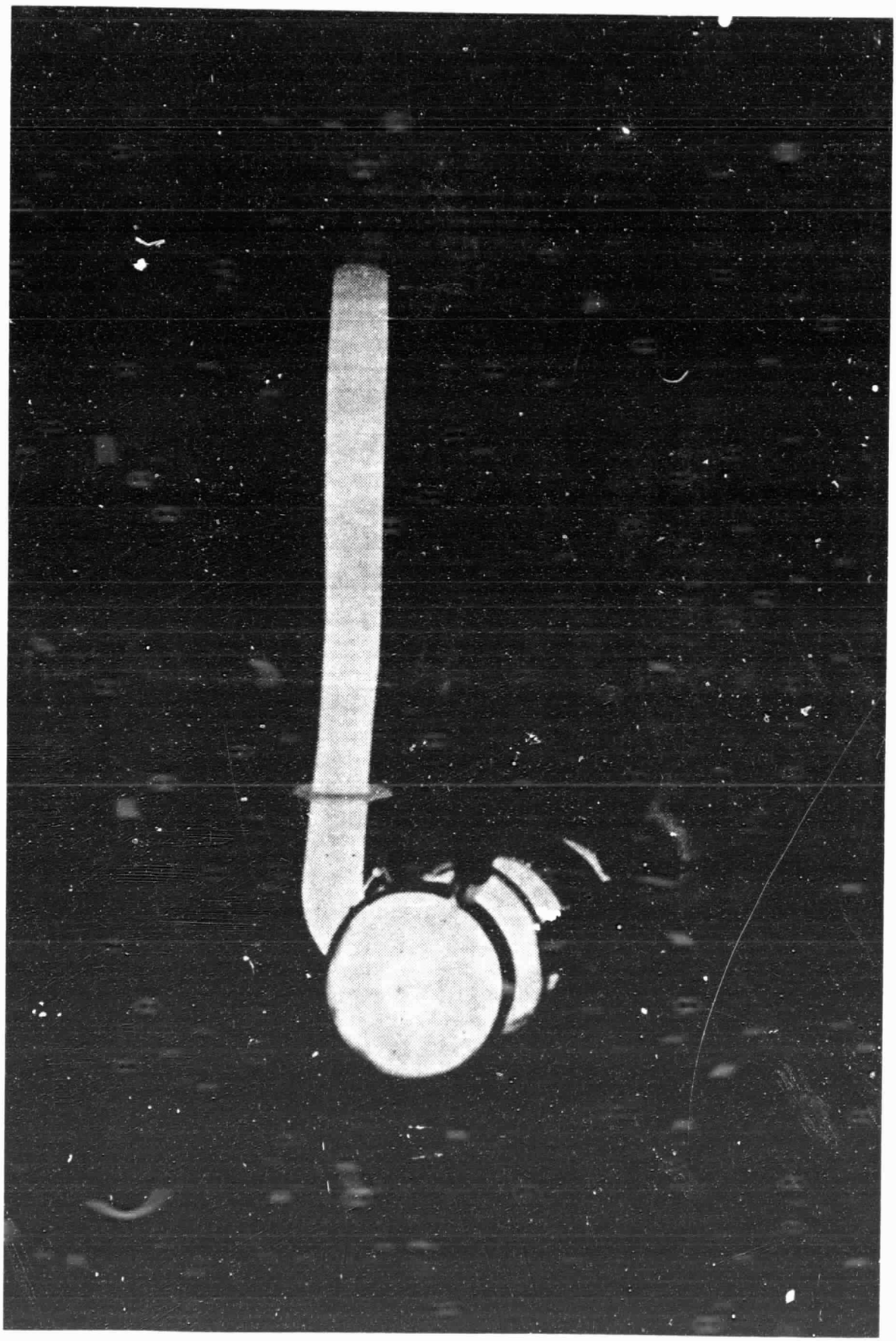

FIGURE 35
COLLECTOR HEAT PIPE OPERATING (TOP VIEW)



ORIGINAL PAGE IS
OF POOR QUALITY

heat pipe. These hot spots were temperature associated rather than power associated. This was observed as the conductance of the calorimeter was varied by going from a vacuum to argon to helium in the gas gap. These data are seen in Table X.

The cause of the hot spots was a matter of concern. The clue to their presence may be the fact that they occurred after the heat pipe was sealed off and had been thermal cycled several times. It may be that the thermal cycles moved the wick in the driver heat pipe away from the wall, thus promoting "boiling" at higher temperatures.

The mechanism by which the wick could be moved away from the wall is as follows. Upon start-up the sodium is in a pool at the bottom of the heat pipe. This pool is about 5 cm long because it contains the sodium which normally fills the wick during operation. As heat is applied a uniform hot spot occurs from the thermal conductance drop through the pool of liquid sodium. When the $\triangle T$ in this pool is sufficient to promote "pool boiling", the pool of sodium erupts in a vigorous "explosion" and the heat pipe becomes isothermal. It is this explosive pool boiling which may have moved the wick away from the wall.

This analysis seems plausible as all of the testing of the driver heat pipe without the collector heat pipe was done with the driver heat pipe operating against gravity, and only after the collector heat pipe was assembled did the driver heat pipe work in the "pool boiler" mode.

TABLE IX

HEAT PIPE PERFORMANCE

| | Temperature | Power | Max. $\triangle T$ |
|---|---|---|---|
| Design | 923°K | 5312 W | 12°K |
| Test Data | 873°K | 2523 W | - |

TABLE X

HEAT PIPE PERFORMANCE VS CALORIMETER CONDUCTANCE

| Calorimeter | RF Current | Temperature | Power | Comments |
|---|---|---|---|---|
| Vacuum | 116 | ≈ 997°K | 1482 W | Large hot spot |
| Argon | 100 | ≈ 923°K | 2143 W | Small hot spot |
| Helium | 95 | ≈ 873°K | 2523 W | No hot spot |

Following the installation of the shielded thermocouples, the collector heat pipe was retested to the limit of the test set up, i.e. the RF coupling to the drive heat pipe and the gas calorimeter. Following these tests the gas calorimeter was found to have a leak between the gas gap and the water passage, and the water passage and the vacuum into the bell jar. These leaks were traced to two welds to a common piece.

The failure of these welds is attributed to embrittlement of the 316L SS from carbide precipation. Normally 316L SS is not prone to carbide precipitation, however, an extensive examination of the end cap of the drive heat pipe which failed, showed marked carbide precipitation and the calorimeter parts were made from the same material stock. The reason for the excessive carbon was not resolved, as the supplier claimed that the carbon content was 0.02%.

The final results of testing the collector heat pipe were varied. Because of the limitation of the test set up, the maximum measured power transfer was 2621 watts at a simulated collector sheath temperature of 946°K. The measured $\Delta T$ between the drive heat pipe and the collector heat pipe was 6°K which gives a thermal resistance of $0.55^{\circ}C/W/cm^2$ for the heat pipe-to-heat pipe transition. The calculated value for this

heat pipe-to-heat pipe transition is 1.4°C/W.cm$^2$. The lower measured value for this one point is attributed to thermocouple error. Subsequent data taken between 850°K to 1000°K at power levels between 1273 watts and 2312 watts showed an average thermal resistance of 1.48° C/W cm$^2$ which agrees with the calculated value.

This thermal resistance is high as an absolute value due to the use of an 1.65 mm wall (.065 inch) as compared to the 0.25 mm wall (.01 inch), which would be employed in a collector heat pipe-to-radiator heat pipe transition. The calculated thermal resistance for a SS 0.25 mm wall transition is 0.8° C/W/cm$^2$ and 0.63° C/W/cm$^2$ for columbium.

From this data one concludes that a heat pipe-to-heat pipe transition is feasible and that the method used to calculate the interface thermal resistance is accurate within the limits of the ability to characterize the components.

The transition from the annular collector heat pipe to the cylindrical tangential arm heat pipe is harder to evaluate than was the heat pipe-to-heat pipe transition. This is attributed to the 45° bend which the cylindrical tangential arm heat pipe makes as it emanates from the annulus, and the fact that the calorimeter prevents placement of thermocouples directly on the condenser. The placement of the thermocouples were on the annular portion of the heat pipe near the tangential arm penetration and on both sides of the 45° bend in the adiabatic zone.

The test data for the collector heat pipe is seen in Table XI and XII. Table XI shows the data and correlation for the pressure drop from the annular evaporator to circular condenser (adiabatic) portion of the heat pipe. The measured temperature drop varied with temperature and

power as it should be. The last two columns in Table XI compare the measured pressure/temperature gradient to the theoretical, as calculated from the Clausius-Clapergram equation. The discrepancy between the measured and theoretical pressure/temperature gradient is attributed to temperature measuring error.

The model used to calculate the inertial pressure drop is

$$\Delta P_I = \rho v^2 = \frac{Q^2}{\rho A^2 L^2}$$

$\Delta P_I$ = Inertial pressure drop - $dy/cm^2$

$\rho$ = Vapor density - gm/cc

v = Vapor velocity - cm/sec

Q = Power transferred - watts

A = Area of vapor flow - $cm^2$

L = Latent heat of evaporation - Joules/gram

The area is that of the vapor flow in the circular portion where the temperature was measured.

TABLE XI

EXPERIMENTAL VS THEORETICAL TEMPERATURE

PRESSURE DROP FROM ANNULAR TO CIRCULAR HEAT PIPE

| Measured or Calculated from Measured | | | | | | Theoretical |
|---|---|---|---|---|---|---|
| Q | $T_1$ | $T_2$ | $\Delta T$ | $\Delta P$ | $\Delta P/\Delta T$ | $\Delta P/\Delta T$ |
| Watts | °C | °C | °C | $dy/cm^2$ | $dy/cm^2$-°C | $dy/cm^2$-°C |
| 408 | 574 | 589 | 5 | 188 | 37.6 | 264 |
| 1482 | 610 | 605 | 5 | 1675 | 355 | 388 |
| 2070 | 629 | 624 | 5 | 2247 | 449 | 563 |
| 2312 | 717 | 715 | 2 | 903 | 452 | 2100 |

$T_1$ = Temperature on annular pipe

$T_2$ = Temperature on tangential arm

$\Delta P$ = $\rho v^2$ - Assumed model for inertial pressure drop for two dimensional vapor flow from annular evaporator to circular condenser (adiabatic)

Table XII shows the temperature as measured in the 45° bend of the condenser (adiabatic). In three of the four cases, a temperature recovery was seen. The observed recovery was greater than the corresponding temperature drop seen from the annular to circular portion of the heat pipe. Accordingly, since the placement of the thermocouples did not allow for a complete thermal mapping of the heat pipe, one concludes that the thermal measurements were biased which in addition to experimental error created the apparent anomalies. This is not to say that the measured temperature drops and recovery are not real, but that the absolute magnitudes of them may be in error.

As part of the observed temperature recovery in the tangential arm, a visual dark spot was seen on the convex side of the 45° bend. This dark spot appeared to be temperature and power dependent; however, insufficient time precluded exploring the phenomenon further.

TABLE XII

MEASURED TEMPERATURES THROUGH A HEAT PIPE WITH A 45° BEND IN THE CONDENSER (ADIABATIC)

| Q (Watts) | $T_2$ (°C) | $T_3$ (°C) | T (°C) |
|---|---|---|---|
| 408 | 569 | 575 | - 6 |
| 1482 | 605 | 612 | - 7 |
| 2070 | 624 | 621 | + 3 |
| 2312 | 715 | 725 | -10 |

$T_2$ = Temperature at the beginning of 45° bend

$T_3$ = Temperature at the end of 45° bend

The measured performance of the collector heat pipe was lower than the design point. This was due to several reasons including hot spots in the driver heat pipe at higher temperatures, and more importantly the weld failure in the gas gap calorimeter. Notwithstanding the problems, the testing of the collector heat pipe did show that flexible artery construction can be used for complex geometries such as the annular to circular of the collector heat pipe, and that current heat pipe vapor flow models provide a reasonable prediction of heat pipe performance for nonstandard geometrics.

## 5. SYSTEM EVALUATION AND REDESIGN

During the time when the collector heat pipe was being demonstrated, the overall NEP system was re-evaluated in terms of size (electrical output) and type of energy conversion system. As a result of this evaluation, the size was targeted at 120 $kW_e$ beginning of life and 100 $kW_e$ end of life. Brayton, thermionic and thermoelectric energy conversion systems were considered. The Brayton system was eliminated for several reasons leaving thermoelectrics and thermionics. Accordingly, the heat pipe heat rejection system was redesigned for the new NEP system such that thermionic or thermoelectric elements could be employed.

### 5.1. System Definition

As part of the system redesign, a minimum OD radiator was to be evaluated, i.e. have the radiator heat pipes on a 2.44 M diameter rather than the 4.5 M diameter which is the maximum allowable that will fit the Shuttle bay. This system outline is seen in Figure 36.

Also during the period the system was being redefined, Thermacore looked at a means of increasing the reliability by redundancy of the heat rejection system. Figure 37 shows the initial concept. The collector heat pipe has a flat extension to one side which has four holes in it to allow for the insertion of the radiator heat pipes. The radiator heat pipes go through the lower collector heat pipe into the upper collector heat pipe of the two converters on the same emitter heat pipe.

This mechanical interface between the two heat pipes is filled with NaK and sealed off. As part of the NaK enclosure there is a bellows

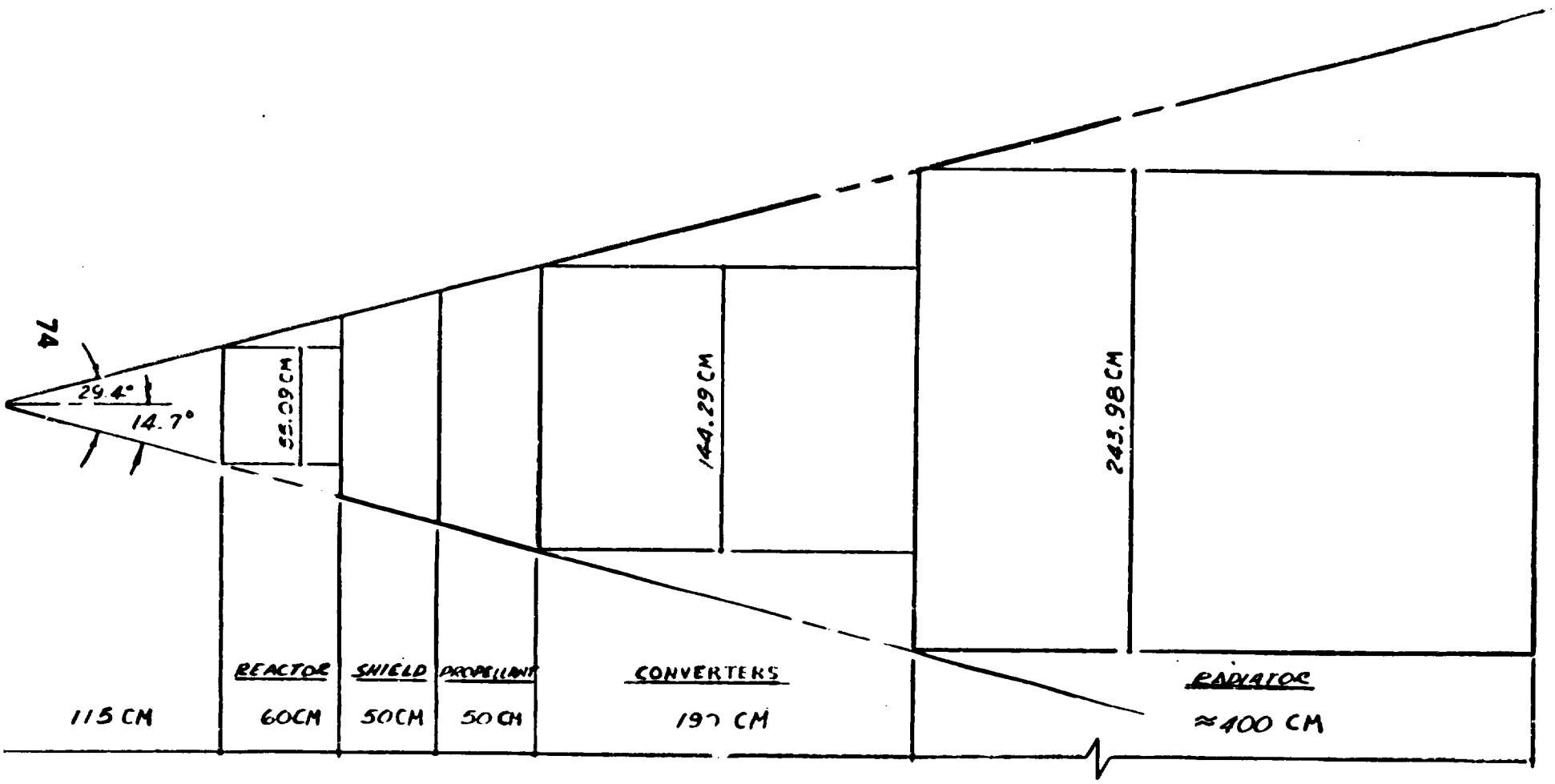
74
29.4°
14.7°
55.09 CM
144.29 CM
243.98 CM
REACTOR
SHIELD
PROPELLANT
CONVERTERS
RADIATOR
115 CM
60CM
50CM
50 CM
197 CM
≈400 CM

FIGURE 36

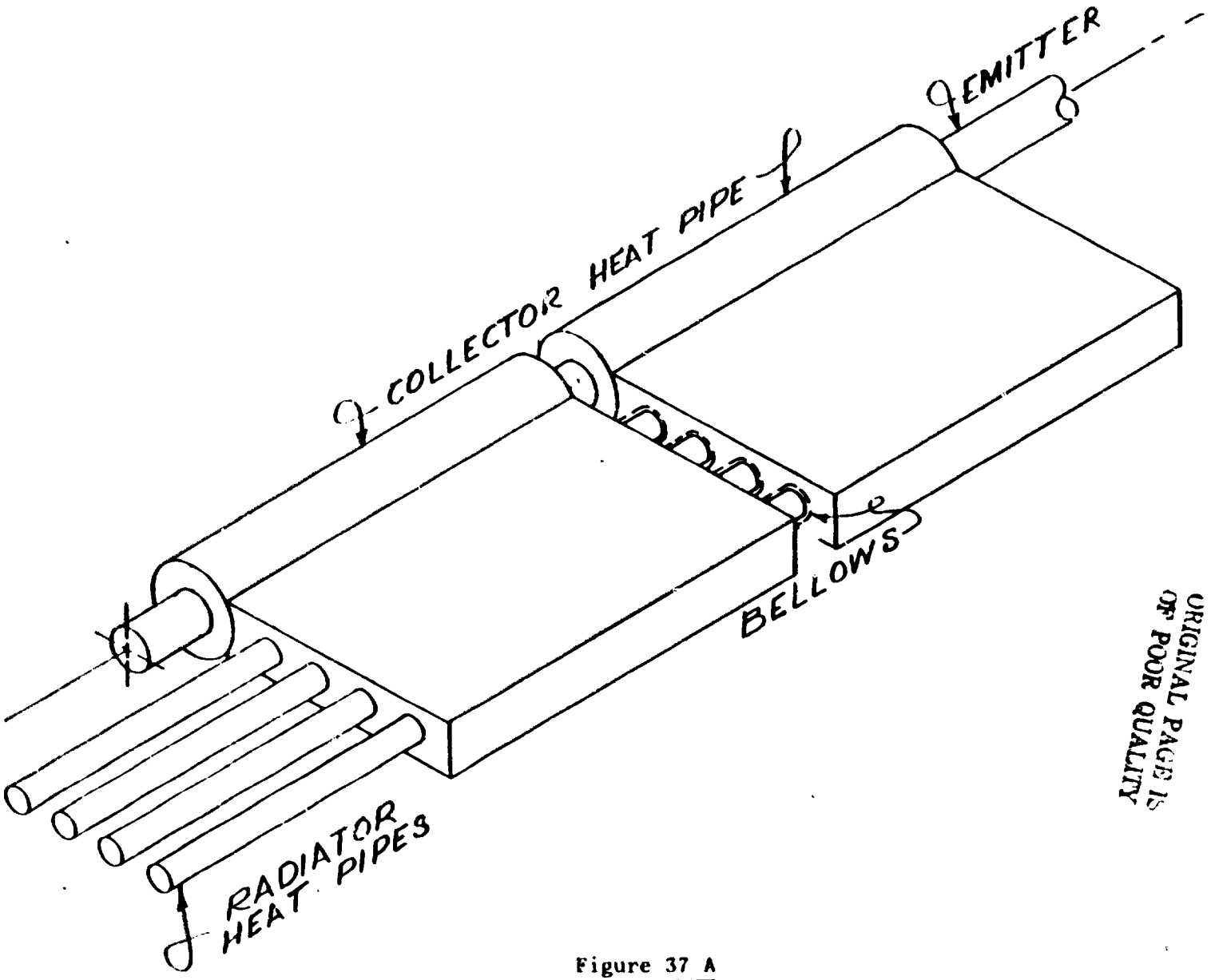


ORIGINAL PAGE IS
OF POOR QUALITY

Figure 37 A

Isometric View of Collector Heat Pipe Radiator
Heat Pipe Joint Design

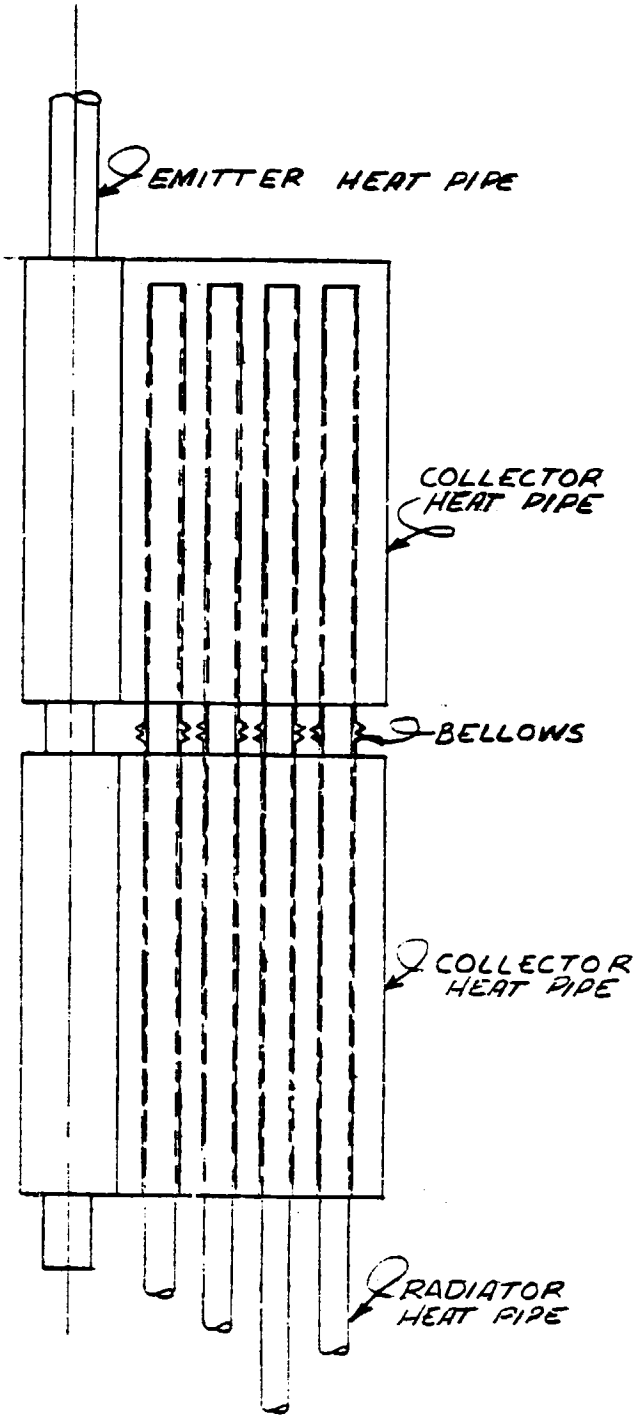


Figure 37 B

Cross-Section of Collector Heat Pipe to Radiator Heat Pipe Joint

ORIGINAL PAGE IS OF POOR QUALITY

between the two collector heat pipes to allow for thermal expansion. The thermal resistance of the NaK-filled interface is on the same order of that for a heat pipe-to-heat pipe transition which was shown in Section 4 to be acceptable for radiator service.

This concept provides the much needed redundancy for the radiator heat pipes. Initially this design was for a system with 256 thermionic converters, two of each on 128 reactor heat pipes. Thus four radiator heat pipes tied together two collector heat pipes.

Further redesign used 384 converters each having an average of 2607 watts of waste heat to be dissipated; there were three converters on each of 128 reactor heat pipes. The surface temperature of the collector was 934°K; thus the reactor temperature was a few degrees less due to the $\Delta$T's in the heat rejection system. For initial evaluation a total $\Delta$ T of 34°C was assumed; thus the radiator surface was taken to be 900°K.

In order to fit 384 single radiator heat pipes on a 244 cm diameter, each heat pipe must be 1.996 cm in diameter. Accordingly, a base line of 2 cm for the single radiator heat pipe system was chosen. As discussed above, increased reliability can be achieved with four radiator heat pipes servicing two converters. However, this creates several problems which needed to be examined. They were the heat flux (Q/A) at the 11.2 cm long evaporator of the radiator heat pipe where it is coupled to the collector heat pipe and the axial Q/A of the radiator heat pipe. Table XIII details four radiator heat pipe possibilities.

Initial calculations showed that the sonic limit for sodium at 900°K is 1590 W/cm$^2$ of vapor space. Thus since the vapor cross-sectional area will be less than the total area, one sees from Table XIII

ORIGINAL PAGE IS
OF POOR QUALITY

that only the 1.5 cm or 2 cm diameter radiator heat pipes are possible, unless the evaporator and adiabatic zones are increased in diameter or potassium is used.

TABLE XIII

POSSIBLE RADIATOR HEAT PIPE COMBINATIONS

| # Radiator HP/ Converter | # Radiator HP/3 Converters | Dia. of Rad. HP @ 244 cm | Radial Q/A Watts/$cm^2$ | Axial Q/A Watts/$cm^2$ | Total Q/HP Watts |
|---|---|---|---|---|---|
| 1 | 3 | 2.0 cm | 37 | 830 | 2607 |
| 1 1/3 | 4 | 1.5 cm | 37 | 1106 | 1955 |
| 1 2/3 | 5 | 1.2 cm | 37 | 1383 | 1564 |
| 2 | 6 | 1.0 cm | 37 | 1660 | 1304 |

Further evaluation led to the thermionic array seen in cross-section in Figure 38. This array has 123 thermionic modules as shown in Figure 39. A cross-section of the radiator heat pipe array is seen in Figure 40.

This design has three thermionic converters on an emitter heat pipe forming a thermionic module. These thermionic modules are assembled in two groups of four on a radius within the 1.44 meter diameter portion of the spacecraft allotted to the power conversion subsystem.

This arrangement allows for parallel connection of the four converters in each grouping. Also, by sizing the OD of the collector heat pipe properly, all of the thermionic modules can be on the same axial position of the spacecraft, thus reducing the number of bends required in the emitter heat pipes.

The size of the outside diameter of the collector heat pipes as seen in Figure 38 is 8.5 cm. This diameter allows for the use of six

Figure 38

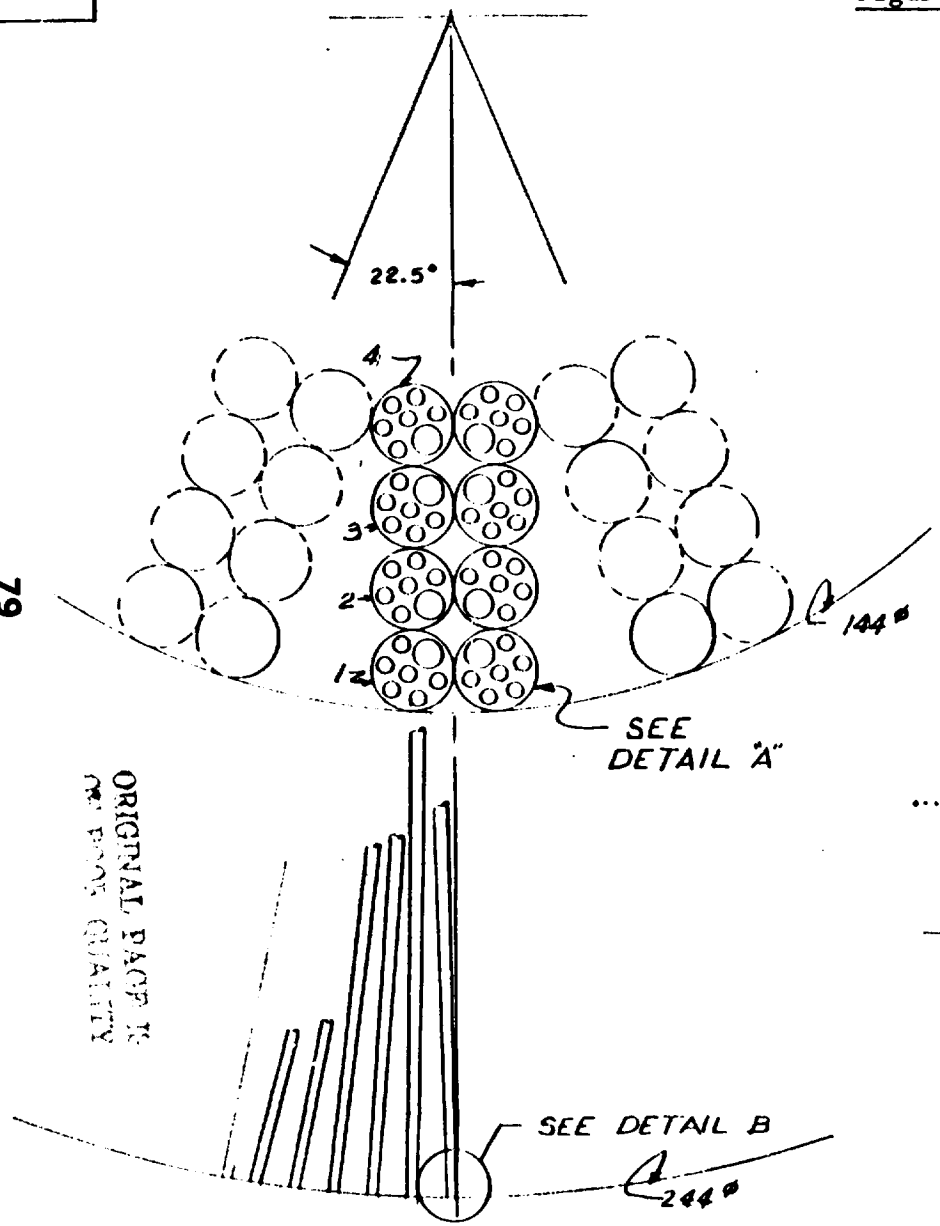


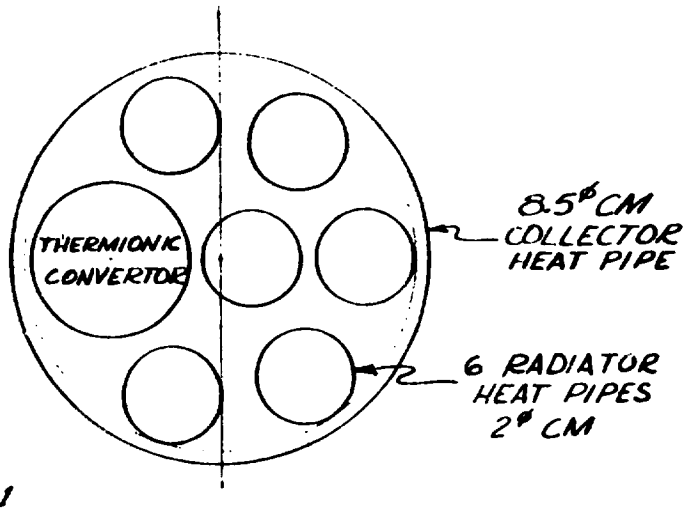


DETAIL "A"

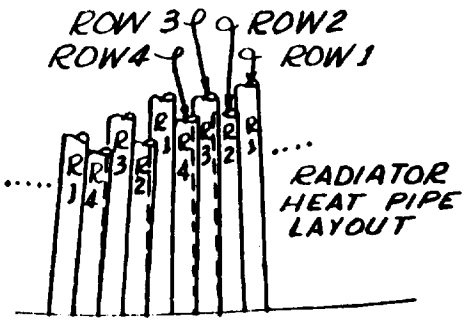


DETAIL B

| KEY | REVISION NOTE | INITIAL | DATE |
|---|---|---|---|
| | | | |

TITLE THERMIONIC ARRAY

NAME

DRAWN DATE

APPROVED AMF 4/5/80

SCALE MATL.

ASS'Y or BILL

STD. TOLERANCES

DECIMAL

FRACTION ± 1/64

ANGULAR

THERMACORE, INC.
HEAT TRANSFER SPECIALISTS

DWG. NO. B-59-106

ORIGINAL PAGE IS OF POOR QUALITY

Figure 39

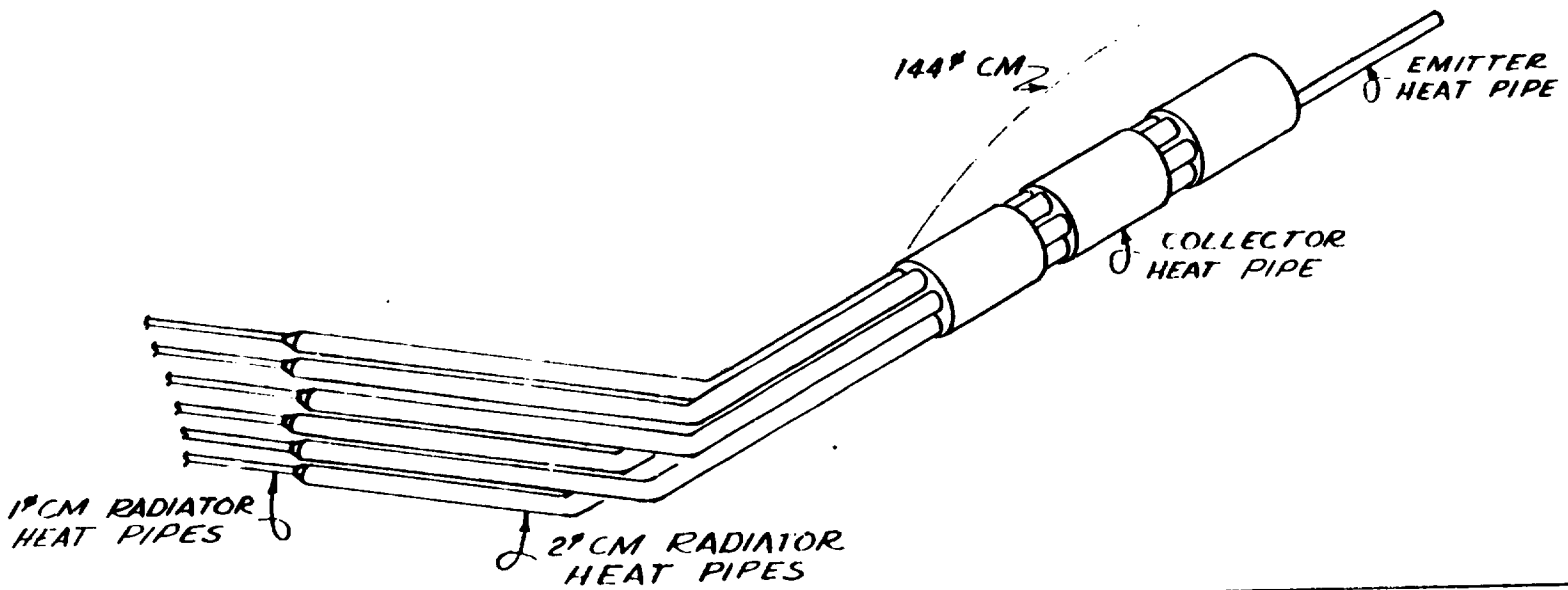


| REV | REVISION NOTE | INITIAL | DATE |
|---|---|---|---|
| | | | |

TITLE THERMIONIC MODULE

NAME

DRAWN

APPROVED DHE 4/8/80

SCALE MATL.

ASS'Y or DR.L.

U.S. TOLERANCES
DECIMAL .XX = ±.010 .XXX = ±.005
FRACTION ± 1/64
ANGULAR ± .005 PER IN. MAX LENGTH

THERMACORE, INC.
HEAT TRANSFER SPECIALISTS

DWG. NO. B-59-107

ORIGINAL PAGE IS
OF POOR QUALITY

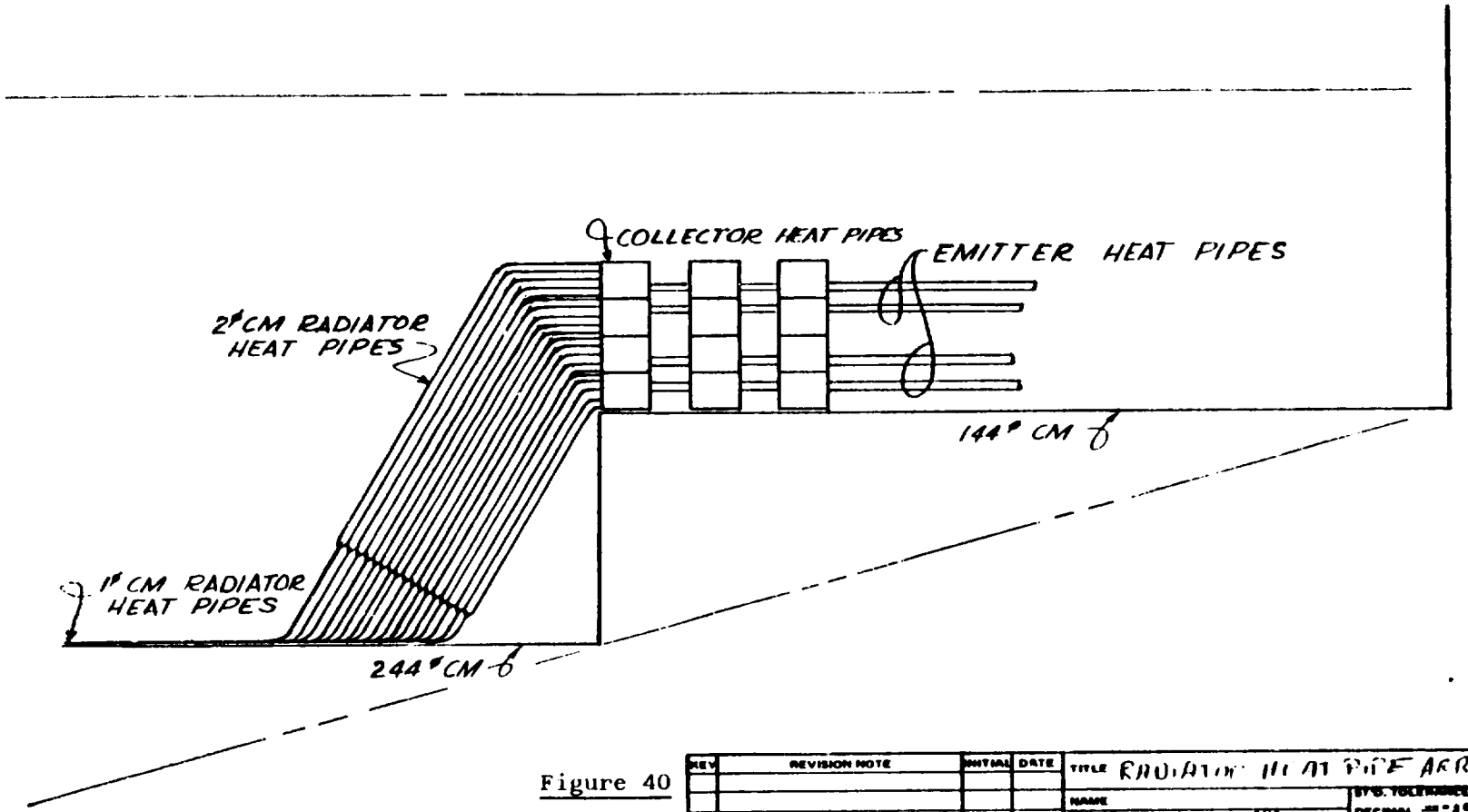


Figure 40

| REV | REVISION NOTE | INITIAL | DATE |
|---|---|---|---|
| | | | |

TITLE RADIATOR HEAT PIPE ARRAY
NAME
DRAWN
APPROVED 4/5/80
SCALE MATL
ASS'Y or BILL
THERMACORE, INC.
HEAT TRANSFER SPECIALISTS
DWG. NO. B-59-108

2 cm diameter radiator heat pipes extending through each of the three collector heat pipes of a given thermionic module. The evaporator and adiabatic diameter would be 2 cm in diameter, and the radiator portion of the heat pipe would be 1 cm in diameter. This is reflected in the drawings.

With this design each radiator heat pipe would transport 1.3 kW thermal power. Although this is a relative low absolute power level, the long ($\approx$ 300 cm), small diameter (1 cm) condenser preceeded by a long ($\approx$ 200 cm) adiabatic zone produced too large of a temperature drop, and the effectiveness of the radiator decreased.

Accordingly, since the maximum diameter of the radiator heat pipe is limited to 2 cm, which is the diameter of 384 - 2 cm heat pipes nested on the 2.44 meter diameter of the spacecraft, then the optimum number of heat pipes per thermionic converter is 1. This is so since 1 1/3, 1 1/2 or 2 heat pipes per converter (4, 5, or 6 heat pipes per three converters) have condenser diameters of 1.5 cm, 1.2 cm, and 1 cm respectively, which for the 400 cm long radiator portion of the heat pipe produces a heat pipe which will either not operate or will have an unacceptably large thermal gradient associated with it.

Therefore a decision was made to define a radiator heat pipe based on a 2 cm OD design. This heat pipe would then be suitable for a system which has 384 radiator heat pipes (3 per three thermionic converters) on a 2.44 meter diameter radiator, or for 768 radiator heat pipes ( 6 per three thermionic converters) on a 4.5 meter diameter radiator.

## 6. RADIATOR HEAT PIPE

As shown in Section 5 the radiator heat pipe element to be designed, fabricated, and tested was again a "snap shot" of the then applicable design with several alternatives.

### 6.1. Radiator Heat Pipe Design

An average radiator heat pipe was defined with a 2 cm OD, a 70 cm evaporator, a 200 cm adiabatic and a 400 cm condenser, with a 30 degree bend at each end of the adiabatic zone. Table XIV shows the details and performance of several wick designs. From Table XIV one concludes that the heat pipe with four wraps of 325 mesh wick in the evaporator is a reasonable design with respect to performance and mass, as it has a higher ultimate limit for both cases.

In order to design, fabricate and test a radiator heat pipe several concessions were necessary. The vacuum system under construction was designed for an earlier radiator heat pipe which had a 25 cm evaporator, 2 meter long adiabatic zone and 2 meter long condenser. The maximum length available was 4.6 meters. Accordingly, a test radiator heat pipe was selected to have a 4 meter long radiator-condenser, with a 25 cm evaporator and 15 cm adiabatic zone. Table XV shows the details and performance of the simulated radiator test heat pipe. It was felt that a straight heat pipe would initially validate the design, following which a second generation heat pipe with bends could be tested.

Comparison of Tables XIV and XV shows that the simulated radiator heat pipe is a fairly good representation of the actual radiator heat pipe.

TABLE XIV

RADIATOR HEAT PIPE DESIGN

1. Standard - Evaporator-70cm - Adiabatic-200 cm - Condenser 400 cm

2. Worst Case - Evaporator-25 cm - Adiabatic-270 cm - Condenser 400 cm

Diameter - 2 cm

Wall - 0.02 cm Niobium

Wick/Artery - 325 mesh stainless steel

Evaporator Temperature - 650°C - 923°K

Fluid - Sodium

Bends - 2-30° at each end of adiabatic

| Heat Pipe Type | Power Watts | $\Delta T$ °C | #Wall Wick Wraps E-A-C | No. of Arteries 0.3 cm Dia. | Mass kg |
|---|---|---|---|---|---|
| 1 | 2600 | 13.5 | 1-1-1 | 2 | .964 |
| 1 | 4125* | 88.9 | 1-1-1 | 2 | .964 |
| 2 | 2600 | 16.0 | 1-1-1 | 2 | .964 |
| 2 | 3550* | 59.3 | 1-1-1 | 2 | .964 |
| 2 | 2600 | 17.9 | 4-1-1 | 2 | .974 |
| 2 | 3800* | 117.9 | 4-1-1 | 2 | .974 |
| 1 | 2600 | 14.6 | 4-1-1 | 2 | .992 |
| 1 | 4150* | 124.2 | 4-1-1 | 2 | .992 |

*Limit

## TABLE XV

## SIMULATED RADIATOR TEST HEAT PIPE

Evaporator-10" - Adiabatic-5" - Condenser-158"

Diameter - 1.05" (3/4" IPS Sch. 40)

Wall - .113  304L - SS

Wick/Artery - 200 Mesh  304 SS

Evaporator Temperature - 650 Equivalent

Fluid - Sodium

| External Evap. Temp. °C | Power Watts | Total ΔT °C | Internal ΔT °C | Wraps Wall Wick | # Arteries 0.125" Diameter |
|---|---|---|---|---|---|
| 667 | 2600 | 25.9 | 8.9 | 2 | 2 |
| 667 | 4775* | 101.9 | 70.7 | 2 | 2 |
| 685 | 5400 | 84.7 | 49.4 | 2 | 2 |

*Limit

The use of the heavy walled stainless steel tubing provided an inner diameter which is very close to the ID of the actual radiator heat pipe, thus a direct comparison of power versus diameter was obtainable. To accommodate the different adiabatic length between the simulate test heat pipe and actual radiator heat pipe, the wick material was chosen to be 200 mesh rather than 325 mesh. The 200 mesh wick in the test heat pipe provides a maximum performance similar to the actual radiator element.

6.2. Radiator Heat Pipe Fabrication

The fabrication of a 4.42 meter long 2 cm ID heat pipe capable of transporting 2600 watts at 923°K required some development. The wick structure consisted of two layers of 200 mesh wick on the wall of the heat pipe to provide circumferential liquid flow and two -200 mesh arteries, .125" ID x .156" OD, inserted between the two layers of wall wick to provide axial flow.

Fabrication of 15 foot long arteries was solved by using a forming tool. This forming tool or extruder is seen in Figure 41. The 1" wide by 15' long strip of 200 mesh stainless screen was fed in from the large end of the conical extruder and formed into a loosely wound artery. This artery was then tightened up and fed into the spot welding saddle where the seam was welded, thus completing the artery.

The finished artery was sealed at one end by twisting it into a tight strand covered with a 0.150" OD stainless steel tube and the end welded shut. The arteries were pressure checked by immersing them in methanol and observing at what pressure the pressurizing gas breaks through.

Thermacore uses the conservative value for the effective pore

DWG. NO. B 59-161

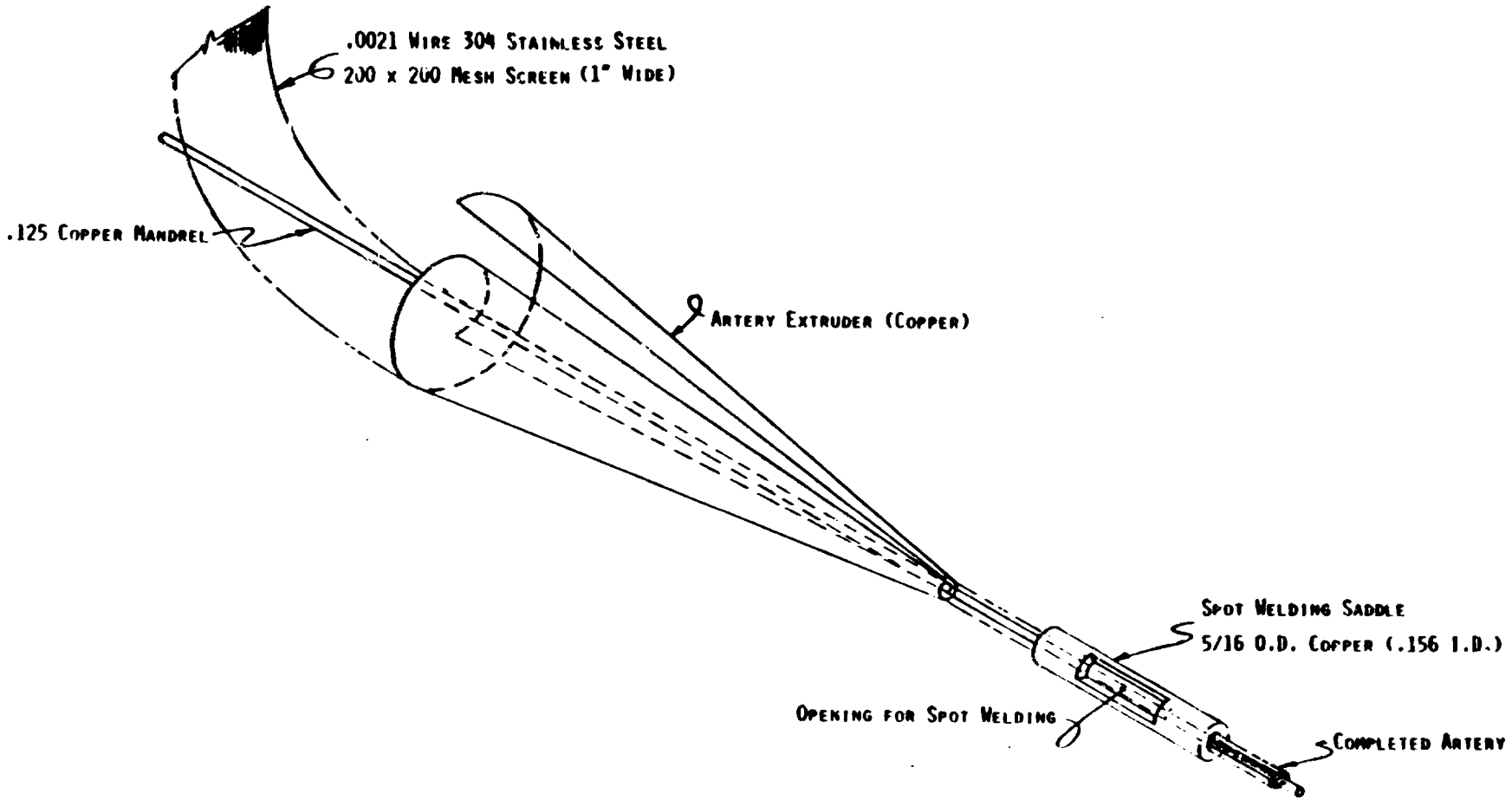


Figure 41

| REV | REVISION NOTE | APPVD | DATE |
|---|---|---|---|
| | | | |

TITLE ARTERY MANUFACTURING METHOD

FINISH

DRAWN R.J.C. 5/30/60

APPROVED

SCALE — MATL. —

ASSY or DRILL

THERMACORE, INC.
HEAT TRANSFER SPECIALISTS

STD. TOLERANCES
DECIMAL
FRACTION ± 1/64
ANGULAR

DWG. NO. B-59-161

radius of screen wicks, i.e. one over twice the mesh number, or one half of the sum of the wire diameter and the mesh opening. This value is $6.35 \times 10^{-3}$ cm for 200 mesh. The surface tension of methanol at 28°C is 21.7 dy/cm, thus the minimum capillary pressure which the 200 mesh artery should generate is 6834 dy/cm$^2$ which corresponds to 2.74 inches of water gauge.

Tests of the arteries showed values in excess of 3.2 inches WG for the capillary strength in methanol. Thus, the arteries showed an effective capillary radius equivalent to the conservative value of 233 mesh, $5.44 \times 10^{-3}$ cm.

The wick was assembled by wrapping one layer of 200 mesh on a mandrel, with two longitudinal grooves machine in it. Into these grooves the two arteries were inserted, forming the layer of mesh to the contour of the mandrel. Following this, a second layer of 200 mesh was wrapped around the mandrels covering the arteries. This structure was then inserted into the heat pipe and the mandrel pulled out. Following this, several perforated SS clips were formed to the proper shape and inserted into the ID of the wicked heat pipe to hold the wick in its proper place. Figure 42 shows the arterial wick structure in the condenser.

The heat pipe assembly was thoroughly washed, fitted with end caps and welded shut. The heat pipe was shown to be vacuum tight by a helium mass spectrometer leak checker following which the assembly was placed in the test stand, fitted with thermocouples, electrical heaters and the entire assembly put into the vacuum system. Figure 43 shows the heat pipe in the test fixtures prior to installation into the vacuum system. Figure 44 shows a close up of the evaporator portion of the heat pipe, the RF coil and instrumentation.

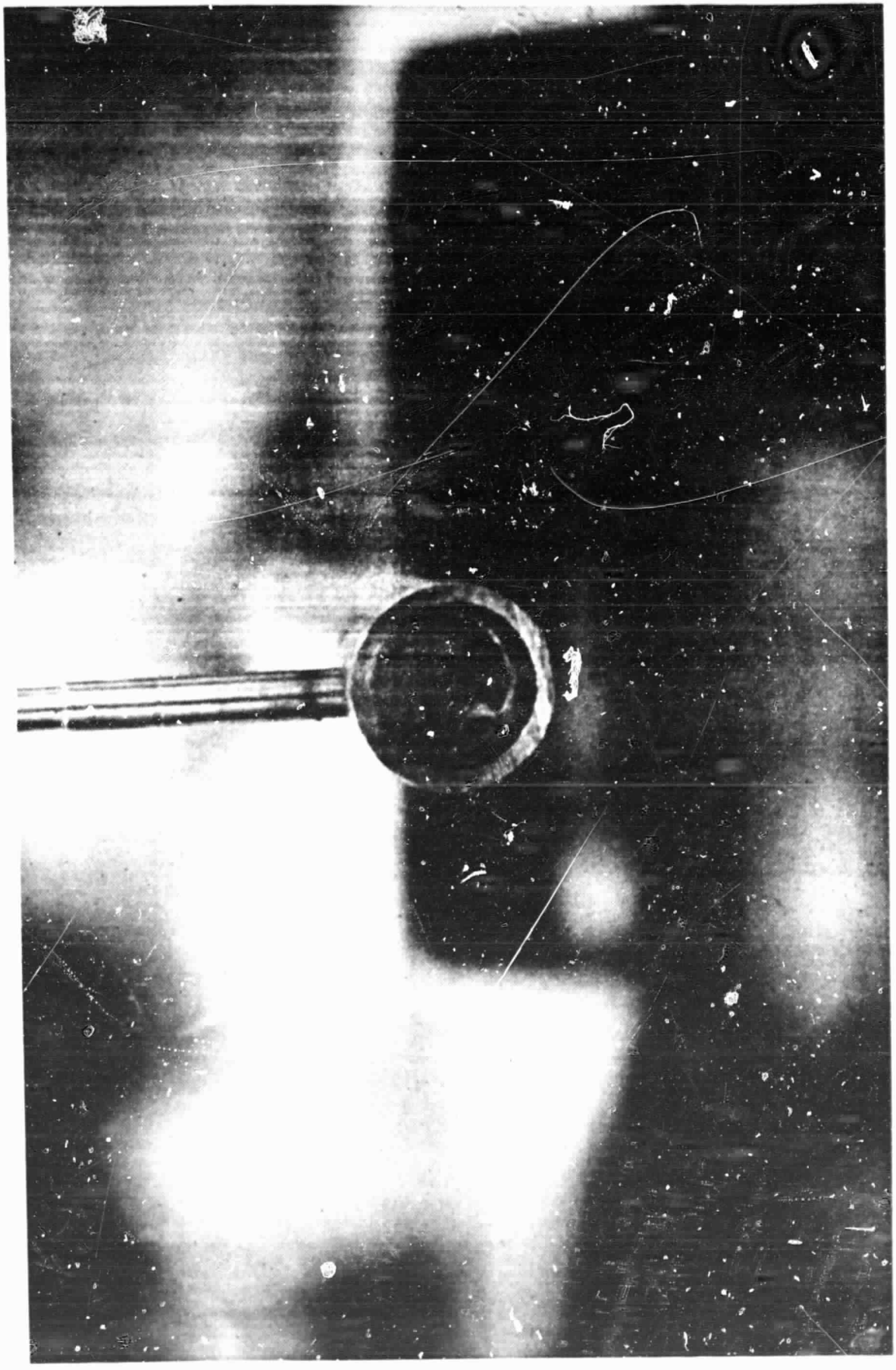

FIGURE 42

ARTERIES IN CONDENSER OF RADIATOR HEAT PIPE



ORIGINAL PAGE IS
OF POOR QUALITY

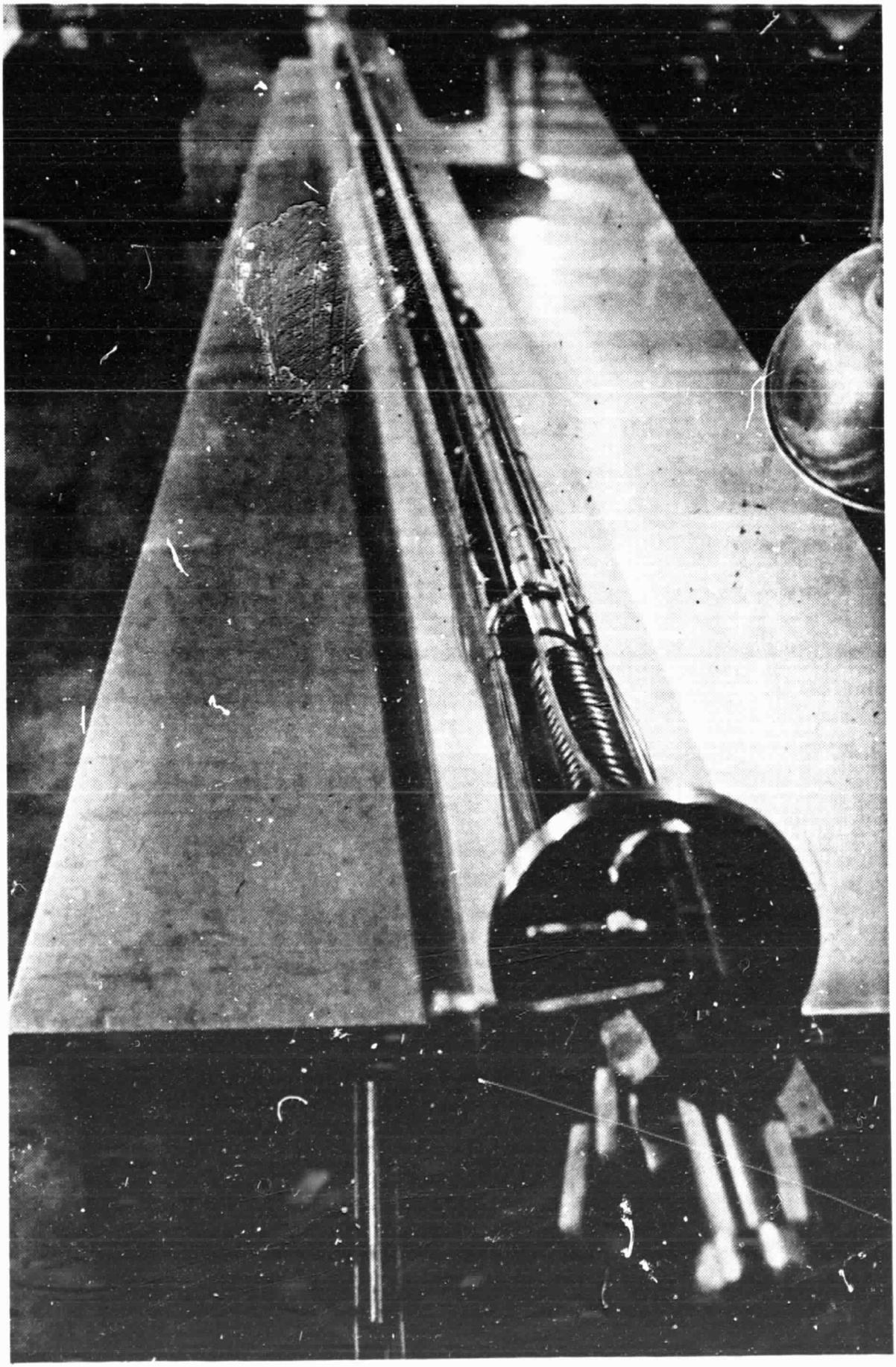

FIGURE 43

4.42 METER LONG HEAT PIPE READY FOR TESTING

ORIGINAL PAGE IS
OF POOR QUALITY



C - 2

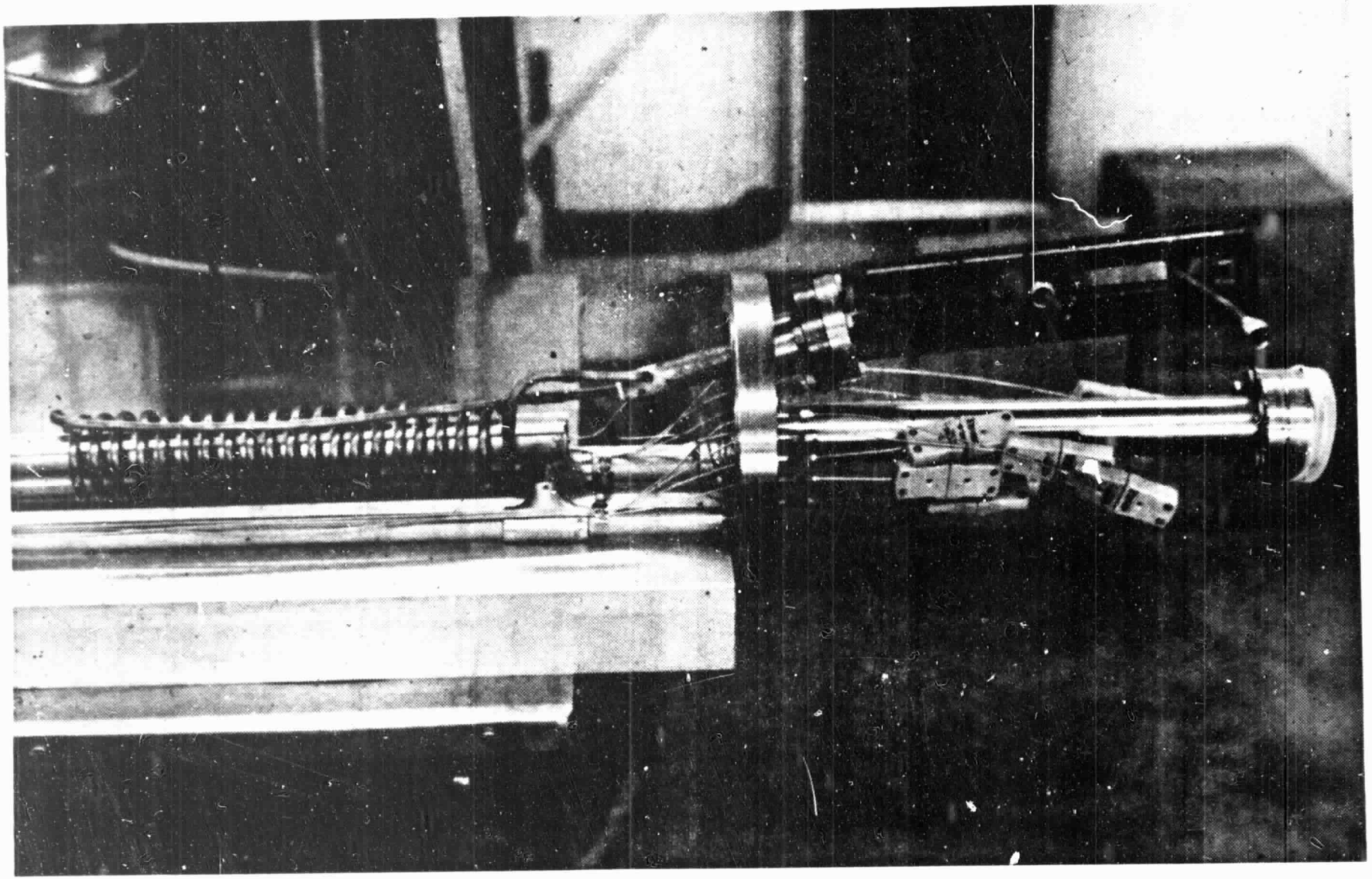

FIGURE 44

EVAPORATOR OF 4.42 M LONG RADIATOR HEAT PIPE



ORIGINAL PAGE IS
OF POOR QUALITY

Following the installation of the heat pipe, the entire vacuum system was checked and found to be free of any leaks, and the heat pipe was vacuum outgassed. The pipe temperature was held near 400°C with a vacuum of $10^{-5}$ Torr or better for twenty-four hours.

During the vacuum outgassing of the heat pipe, the sodium distillation pot was prepared for loading in an inert atmosphere. The distillation pot was loaded with 400 grams of sodium and several grams of hafnium foil. The hafnium was for gathering of oxygen, which may be present during the loading into the distillation pot.

Following the outgassing of the heat pipe, it was cooled and back filled with ultra pure argon. The sodium distillation pot was installed in the vacuum system in its position over the heat pipe, connection made and the system pumped down. When the system pressure was less than $1 \times 10^{-5}$ the distillation of sodium into the heat pipe was begun.

Figure 45 is a drawing showing the sodium distillation and processing arrangement. Figure 46 shows the actual setup and Figure 47 shows the heat pipe during processing.

## 6.3. Radiator Heat Pipe Test

Following distillation, the heat pipe was found to be operational. However, prior to a final seal off, the heat pipe was temporarily sealed off with a sodium seal by freezing sodium in the evacuation tube. This procedure allowed for final checkout of the heat pipe.

With the heat pipe temporarily sealed off, performance tests were carried out. The results of these tests are seen in Table XVI and Figure 43 along with computer predictions. These results were encouraging but posed as many questions as answers. The temperatures on the heat pipe were obtained from thermocouples placed along the heat pipe. These

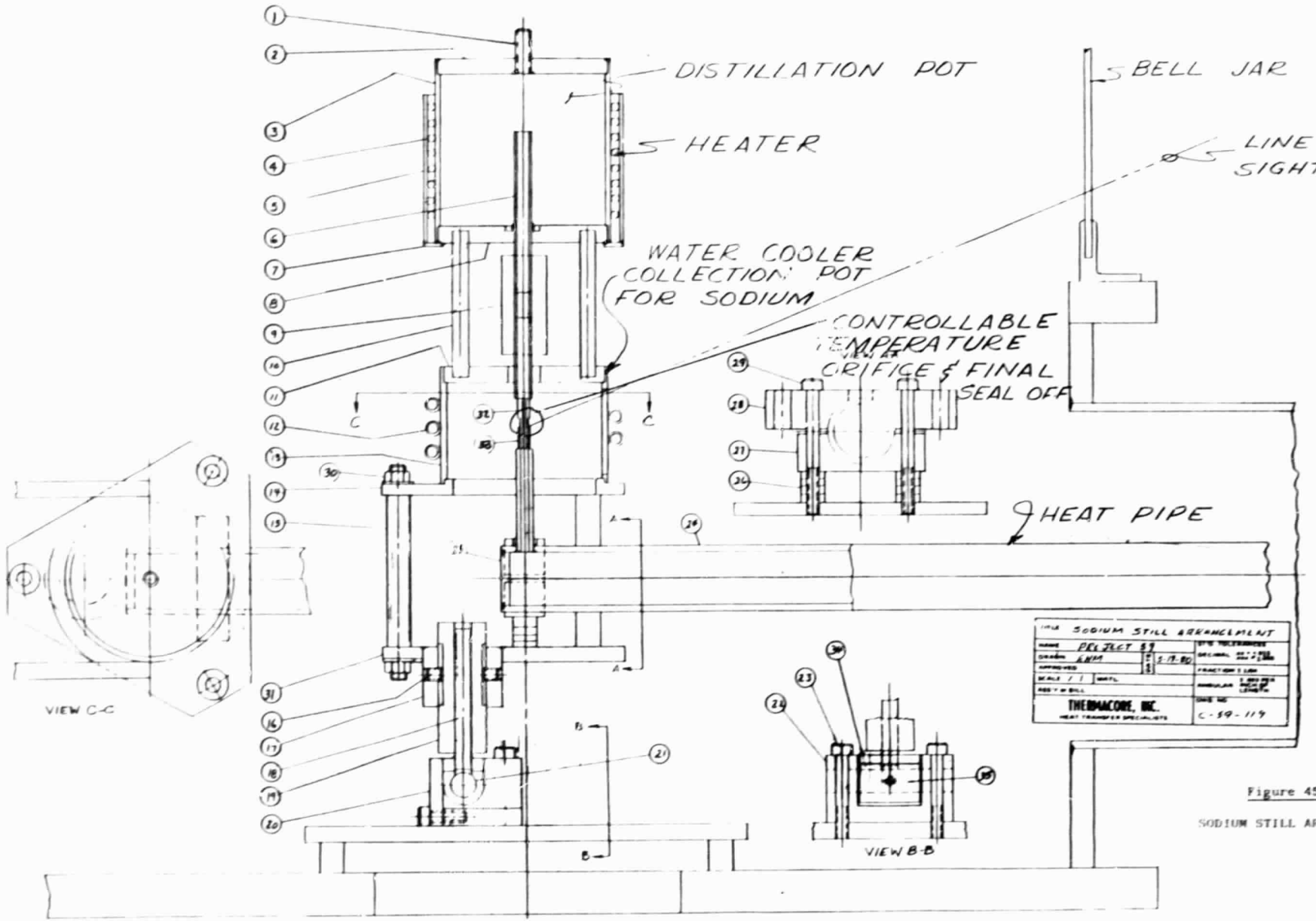


Figure 45

SODIUM STILL ARRANGEMENT

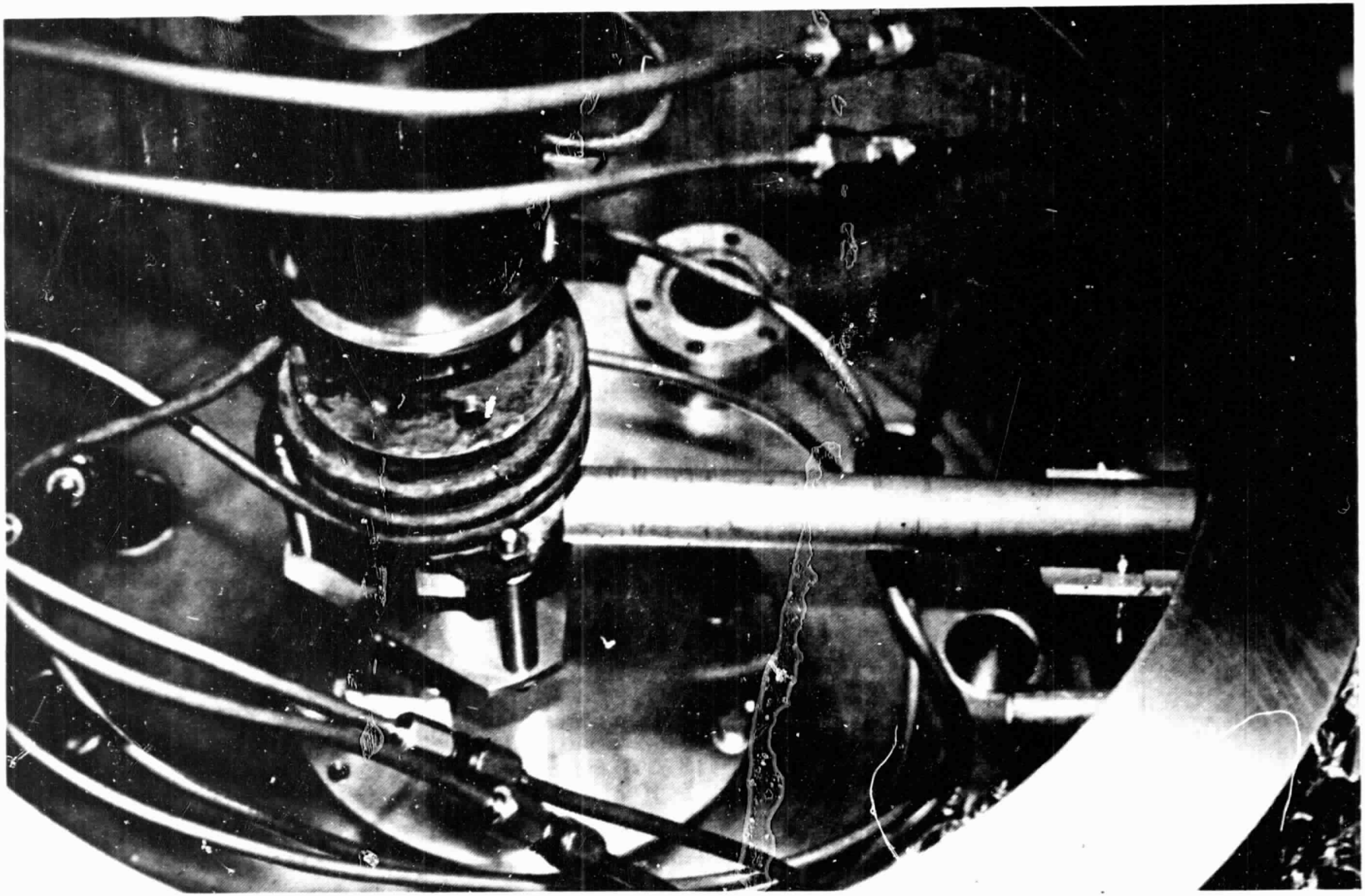

FIGURE 46

DISTILLATION POT, AND SODIUM CATCH POT INSTALLED ON 4.42 M LONG HEAT PIPE



ORIGINAL PAGE IS
OF POOR QUALITY

FIGURE 47
PROCESSING OF RADIATOR HEAT PIPE



ORIGINAL PAGE IS
OF POOR QUALITY

## RADIATOR HEAT PIPE TEST DATA

| DATE | RF AMPS | POWER(W) | THERMOCOUPLE LOCATION FROM EVAPORATOR - CM | | | | | | | | | | | | |
|---|---|---|---|---|---|---|---|---|---|---|---|---|---|---|---|
| | | | 1 | 1 | 52 | 53 | 100 | 104 | 200 | 208 | 300 | 304 | 405 | 420 | 435 |
| | | | TEMPERATIIRE $^{0}C$ | | | | | | | | | | | | |
| 10/17 | 190 | - | 563 | - | 563 | 576 | 558 | 580 | 568 | 570 | 551 | 568 | - | - | - |
| 10/28 | 190 | - | 604 | - | 552 | 571 | 542 | 563 | 572 | 558 | 558 | 544 | 557 | 536 | 558 |
| 10/28 | 190 | 2635 | 612 | - | 562 | 579 | 551 | 570 | 580 | 565 | 564 | 556 | 564 | 540 | 558 |
| 10/28 | 200 | 2698 | 627 | - | 573 | 588 | 564 | 588 | 574 | 579 | 580 | 578 | 578 | 558 | 580 |
| 10/17 | 210 | - | 573 | - | 579 | 572 | 598 | 572 | 594 | 580 | 574 | 594 | - | - | - |
| 10/17 | 220 | - | 602 | - | 606 | 622 | 624 | 624 | 625 | 613 | 608 | 624 | - | - | - |
| 10/28 | 220 | 3312 | 656 | - | 620 | 635 | 606 | 635 | 642 | 630 | 627 | 617 | 622 | 600 | 627 |

TABLE XVI

readings were taken at various RF current settings. Likewise, the power transferred by the heat pipe was found by calorimetric measurements of the radiated heat from the heat pipe at several RF settings.

The actual power transferred by the heat pipe was obtained by ratioing the measured heat removal from 365 cm of condenser length to the total 415 cm long condenser. This was required as 20 cm of condenser was radiating to the water cooling jacket around the evaporator, and 30 cm of the condenser was radiating to a non-water cooled portion of the system.

Figure 48 shows the predicted temperature profile for the radiator heat pipe similarity design at 3312 and 2698 watts. At the 3312 watt performance, the similarity design has an evaporator temperature of 641°C, adiabatic temperature of 635°C and a condenser temperature of 627°C. From the best fit straight line of the data, the measured heat pipe temperature at 3312 watts is an adiabatic zone temperature of 635°C and a condenser temperature of 627°C. The measured evaporator temperature was in error, as the thermocouples were loose, one of which was completely off the heat pipe and read low, the other still on the heat pipe but was picking up direct RF heating. The thermocouples on the end of the evaporator had worked loose due to the 3 inch thermal expansion experienced by the heat pipe. The condenser was fixed, accordingly, the evaporator moved the entire three inches thus working the thermocouples loose after a few thermal cycles.

Discounting the loose thermocouples one sees from Figure 48 that the heat pipe did perform as predicted. However, the inability to fully describe the condenser temperature profile, with respect to the observed temperature recovery, is a function of the computer program rationale.

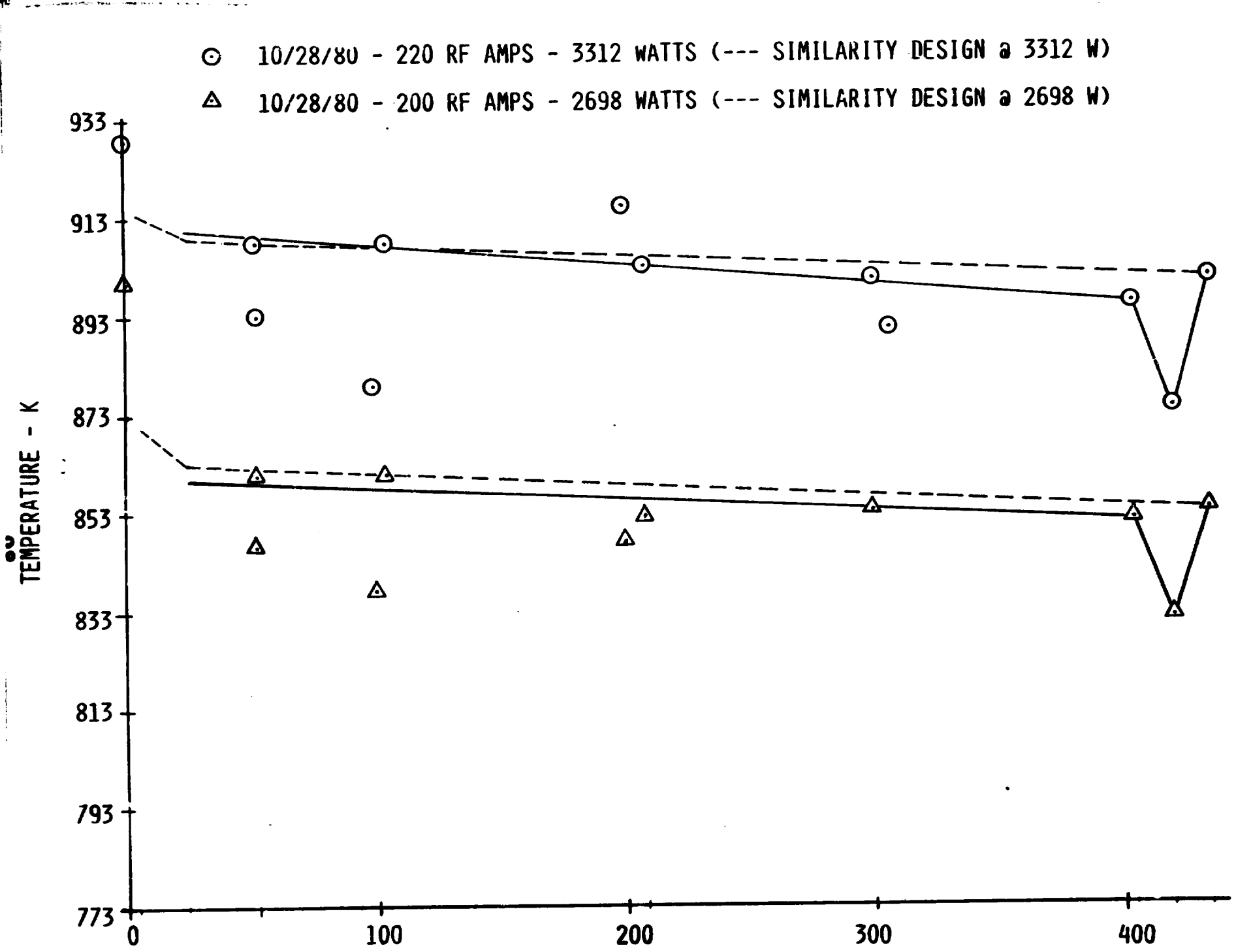
⊙ 10/28/80 - 220 RF AMPS - 3312 WATTS (--- SIMILARITY DESIGN @ 3312 W)
△ 10/28/80 - 200 RF AMPS - 2698 WATTS (--- SIMILARITY DESIGN @ 2698 W)
933
913
893
873
853
833
813
793
773
TEMPERATURE - K
0
100
200
300
400
THERMOCOUPLE LOCATION
ALONG HEAT PIPE - CM

FIGURE 4

The ongoing work on JPL Contract 955535 is addressing this problem. The ability to predict the temperature profile of a heat pipe is of great importance for radiators. A 5°K temperature error at 900°K effects the mass of the radiator by 2.2%, and a 25°K error increases the mass of the radiator by 11.9%.

Further examination of the temperature profiles shows that the thermocouples at the 50 and 100 cm locations are at lower temperatures than one would expect. This is probably due to the fact that the evaporator and first part of the condenser experienced more thermal cycles than the entire heat pipe, thus increasing the probability of having the thermocouples become loose. The other anomaly is the apparent high thermocouple reading at the 200 cm location. This was thought to be due to a loose thermocouple picking up RF that was progated down the vacuum system as in a resonant cavity or co-axial wave guide. The fact that the thermocouple is at the approximate mid-point of the system was a further indication of resonance.

During these tests there were occasions when the evaporator experienced a hot spot. This hot spot could be made to go away by lowering the evaporator end of the heat pipe. However, when the tilt of the pipe was returned to normal the hot spot would not necessarily reappear. In some cases it would reappear upon increasing the power input to the heat pipe, but again it could be made to go away.

It is felt that the hot spot was due to poor wetting of the sodium in a portion of the evaporator. Normally a heat pipe works best if it can be "wet" in by an isothermal bake at or above the desired operating temperature. Because of the length of the heat pipe, this was not done. It was also noticed that the longer the heat pipe operated, the less

problem the hot spot was. Accordingly, the heat pipe was to be operated at or above the desired operating temperature for a few days prior to final seal off to try and improve wetting. Wet-ins was to be followed by additional testing of the heat pipe on the continuation contract.

The successful operation of this 4.42 meter long 2 cm ID heat pipe is a significant step in the use of heat pipes for the NEP heat rejection system. Likewise, the reasonable agreement between the measured and calculated end to end heat pipe temperature profile along with the anticipated improvement in the condenser calculation rationale, gives a new degree of validity to the heat pipe computer codes thus providing the designer of thermal systems a new and useful tool.

## 7. NEW CONCEPTS

Through the course of the NEP heat rejection system design and evaluation covered in the preceding sections, one can see how the entire NEP system design is strongly affected by the radiator design and placement of the power subsystem components within the spacecraft. Accordingly, some time was spent looking at new concepts. These concepts included radiatively coupling the reactor heat pipes to the energy conversion devices as well as new radiator designs, including see-through radiators, and changes in the arrangement of the entire spacecraft.

As new concepts were developed, it became evident that in order to be able to evaluate the various ideas that a computer program was necessary. Accordingly, several computer programs were written. Each program was based on the previous program and provides different information. These programs are Radiator, RAD4 and RAD7.

### 7.1. Radiant Interchange Program

Radiator is a very simple program used to calculate the view factor between any number of heat pipes of a given diameter uniformly placed on a circle of a larger diameter.

This program calculates the view factor as though all of the radiation was emanating from the center of each of the heat pipes, i.e. it takes into account only the normal radiation, and computes that which is not intercepted by another heat pipe. The geometry is assumed symmetrical and that there is no net radiant interchange of heat between the heat pipes.

The program computes the net radiation from each heat pipe and

calculates an effective heat pipe perimeter. This effective perimeter is a multiplier times the actual heat pipe diameter, and when multiplied times the heat pipe length calculates the effective radiating area of the radiator heat pipe. The effective perimeter is always larger than the heat pipe diameter, even when the heat pipes are perfectly nested as in a radiator. The effective perimeter is a 2.76 for 540-2.6 cm diameter heat pipes perfectly nested on a 4.5 M circumference. This increase is only six percent but it does have the effect of reducing the required radiator length and, therefore, mass by 6%. Figure 49 shows a family of curves for multipliers of 90 radiator heat pipes for different heat pipe diameters. It is interesting to note that the straight line projection of the perfectly nested heat pipes approaches a value slightly above 1. This may be real, or a consequence of rounding off of the numbers, or that the perfect nesting curve is not a straight line.

Replotting of Figure 49 in Figure 50 shows for the see-through radiator that the radiator length increases as the heat pipe diameter is decreased, however, the mass of the heat pipe decreases and asymptotically approaches zero for small diameter heat pipes. Accordingly for a see-through type of configuration, the smallest number of small diameter infinitely long heat pipes will provide the lowest mass.

Obviously there is a trade off on the number and length of the radiator heat pipes which is constrained by the available length (shuttle bay) and the actual heat pipe capability, and the mass of the required armor for meteoroid protection. When see-through radiation is allowed the entire heat pipe must be protected. To a first approximation one could assume a doubling of the mass for an un-nested heat pipe radiator.

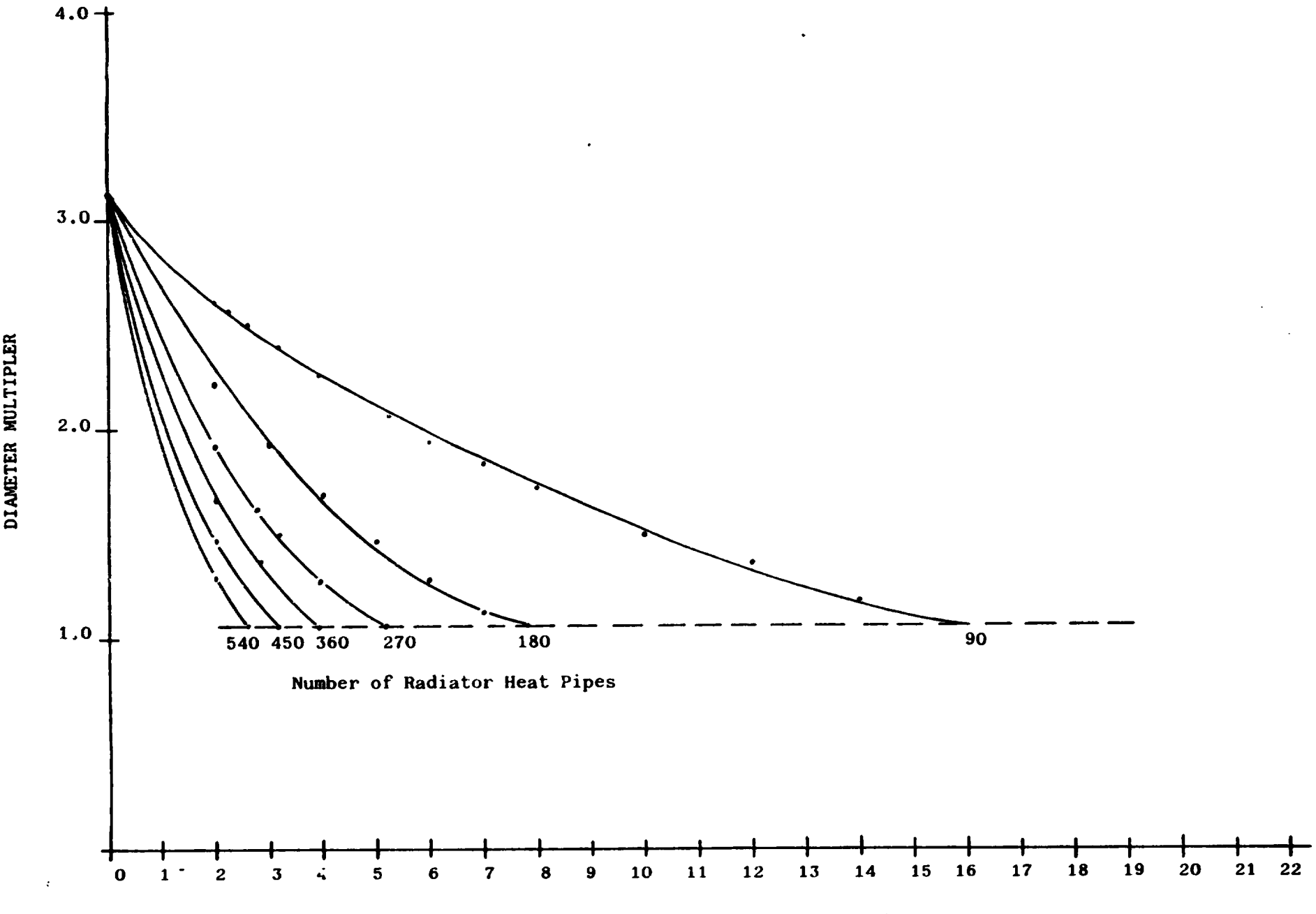
4.0
3.0
2.0
1.0
DIAMETER MULTIPLIER
540 450 360 270 180 90
Number of Radiator Heat Pipes
0 1 2 3 4 5 6 7 8 9 10 11 12 13 14 15 16 17 18 19 20 21 22
HEAT PIPE DIAMETER - CM

Figure 49

FIGURE 50

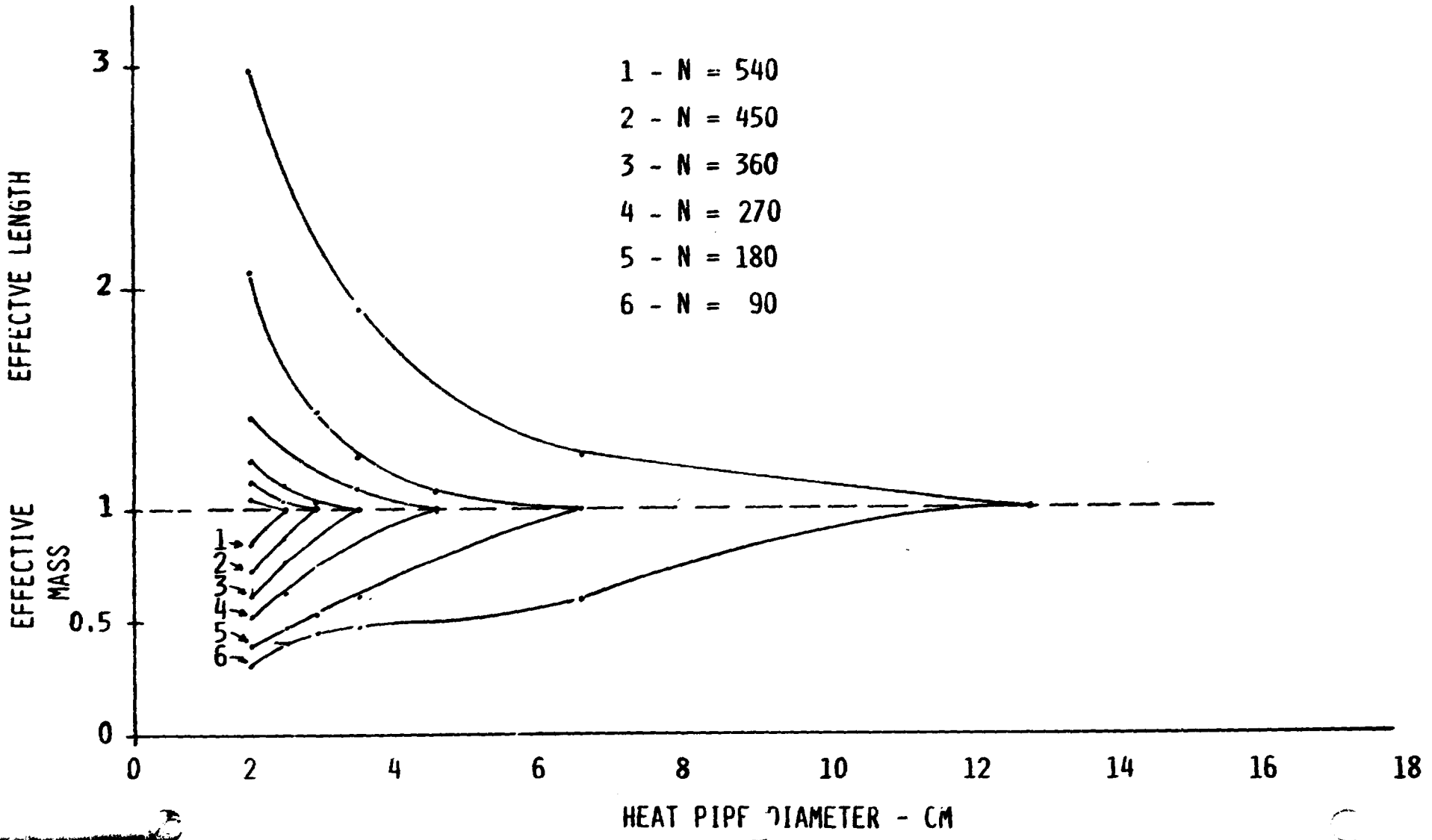
N = Number of Radiator Heat Pipes
1 - N = 540
2 - N = 450
3 - N = 360
4 - N = 270
5 - N = 180
6 - N = 90
EFFECTIVE LENGTH
EFFECTIVE MASS
10⁴
3
2
1
0.5
0
0
2
4
6
8
10
12
14
16
18
HEAT PIPE DIAMETER - CM

Thus only those heat pipes with an effective mass near 0.5 could be considered. From Figure 50, one sees that this is achievable for radiators which have 270 heat pipes or less.

A full interacting computer program to take all system constraints into consideration was beyond the scope of the work carried out. However, program Radiator forms a base from which the necessary program can be derived. Also program Radiator, with minor modifications, can be used to design a radiation coupled system for the reactor heat pipes to the thermoelectric energy conversion modules, which is another concept that needs a more detailed interaction computer program.

## 7.2. Heat Pipe Radiator Design Program

The design program for the heat pipe radiator has two versions, RAD4 and RAD7. RAD4 gives a more detailed printout of the individual grouping of the thermoelectrics and heat pipes as compared to RAD7, which parametrically looks at the radiator mass for varying input parameters.

These programs incorporate a system design layout as seen in Figure 51. The biggest single difference between the design of Figure 51 and previous NEP system designs is the repositioning of the ion propulsion engines. By moving them, it is possible to place the thermoelectric elements on the imaginary surface of the system angle cone. Thus the reactor heat pipes are as short as possible and the T/E elements begin on the reactor heat pipes as soon as the reactor heat pipes penetrate or circumnavigate the reactor shielding.

Each T/E module has a single cold side heat pipe which is accessed by a user specified number of radiator heat pipes. The radiator to cold side heat pipe joint is via a NaK filled gap. The computer program

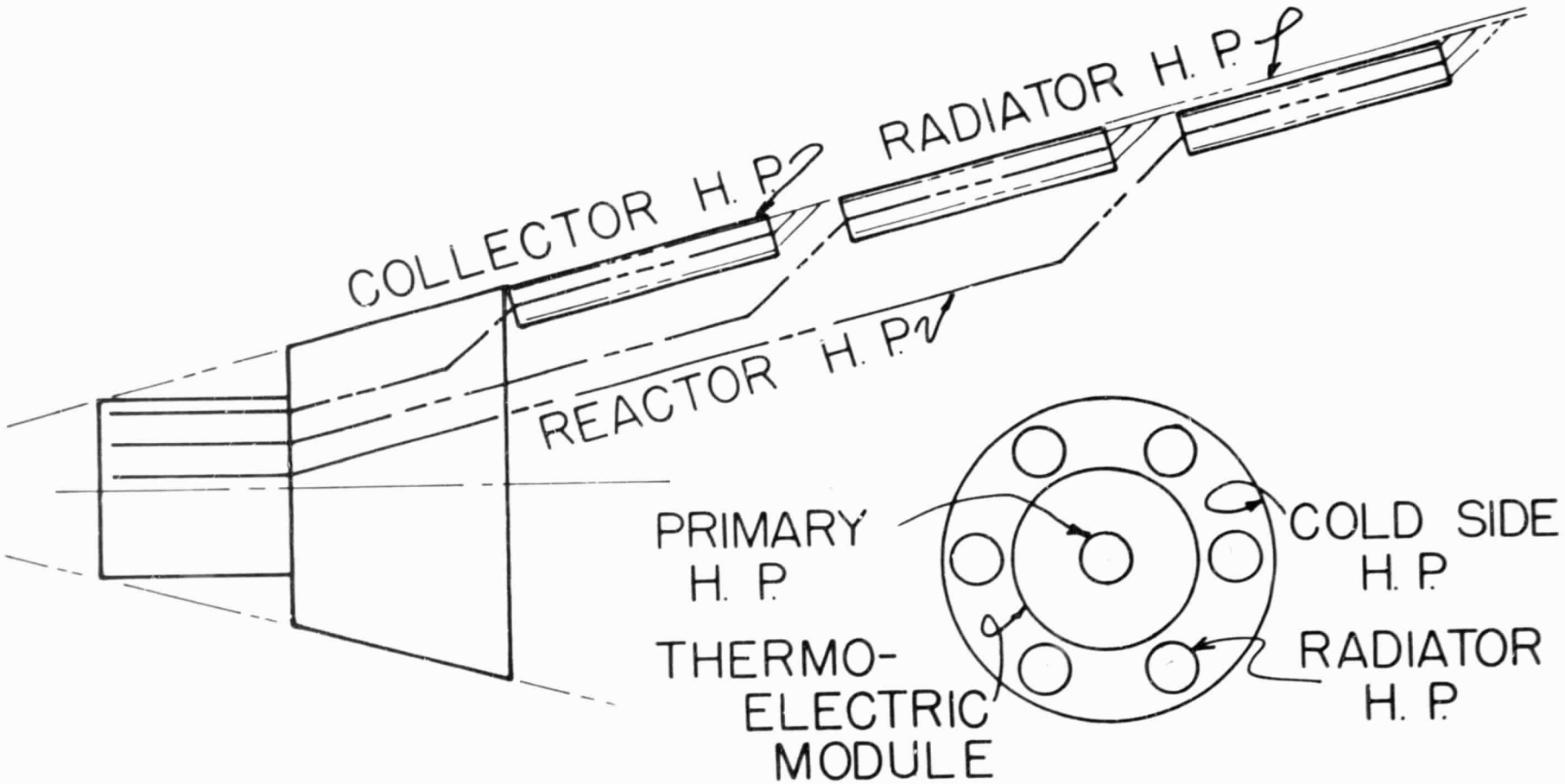


# NEP HEAT REJECTION CONCEPT

FIGURE 51

automatically calculates the number of T/E's which can nest at the given diameter on the surface of the cone. The radiator heat pipes are allowed to nest on the surface of the cone as soon as they emerge from the cold side of the T/E's. Thus, the radiator heat pipes act as meteoroid armor for the second and succeeding sets of T/E's.

Several input-output printouts for RAD7 are found in Appendix C. The input to the program is as follows: dimensions are in centimeters, angles in degrees, electrical power in watts, efficiency in decimal form and temperature in $^{o}K$. On line one the maximum allowable length and diameter and cone angle are entered. On line two the reactor diameter, length and shield length are entered. Line three calls for the output electrical power, T/E efficiency and T/E thickness. On line four, the number of radiator heat pipes, and the first and last number of radiator heat pipes per T/E element are entered. The emissivity and radiator temperature of the radiator is put in on line five and on line six the initial increment and last diameter of the radiator heat pipe is entered.

The program calculates the total thermal input from the efficiency and desired electrical output. From this and the number of reactor heat pipes, the diameter of the reactor heat pipe is calculated based on an axial pipe power density of 5 $kW/cm^2$. The required length of the T/E is then calculated based on a thermal input of 25 $watts/cm^2$. The cold side heat pipe is then calculated based on the reactor heat pipe diameter, T/E thickness, and radiator heat pipe diameter. From this the number of T/E elements which can nest at the given diameter is calculated. The dimensions along the cone are calculated and a second set of T/E's are found to nest at the new diameter. This continues until all T/E's are used.

The spacing between the succeeding sets of T/E is based on the cold side heat pipe diameter. The radiator heat pipes are then nested on the cone as soon as they emerge from the cold side. A non see-through view factor is calculated which is allowed to change for increasing cone diameter and number of radiator heat pipes. From this the required heat pipe length and mass are calculated. The heat pipe mass is based on the use of stainless steel and a wall thickness of 1% of the diameter. This is derived from the buckling constraint. For diameter less than 2.5 cm the program will show less mass than what real heat pipes will be, since a wall thickness less than .025 is too thin.

The wick structure and working fluid is assumed to have a combined mass equivalent to the wall. Accordingly, for heat pipe diameters greater than 2.5 cm the mass as calculated by RAD7 is probably too large as the fluid filled wick does not have to increase proportionally to the diameter.

The program limits the length of the heat pipe to the overall maximum available and to the number of heat pipes which will perfectly nest on the maximum diameter.

From the printouts found in Appendix C, one sees for a non see-through radiator that the lowest mass radiator occurs when the number of radiator heat pipes per T/E is one or the minimum number, which is achievable at the smallest diameter and longest length. However, one must consider the axial heat flux requirement of the heat pipe. For instance, for a 900°K radiator the lowest mass is seen to occur for one 1.5 cm diameter heat pipes per T/E for a total of ninety heat pipes. However, the required heat flux is 5.7 kW/cm$^2$ and from the test data presented in Section 6 a reasonable heat flux at 900°K is 1.1 kW/cm$^2$.

Thus the lowest mass radiator which is achievable would be that for 270-2 cm diameter heat pipes, which is very similar to the test heat pipe design.

Also included in Appendix C is a printout of RAD4 which calculates the total capability of a radiator extending the full length of the spacecraft and the heat pipe lengths for the desired radiator design.

These programs and the heat pipe model are the first step in generating a full interaction program for the NEP power subsystem design.

## CONCLUSIONS AND RECOMMENDATIONS

Specific conclusions and recommendations are found within the text of the report where they were made in the chronological sequence of events. In summary they are:

### Materials

- Beryllium should not be used for the envelope material for a low mass, self-armored, sodium or potassium radiator heat pipe.
- Titanium can be used as the low mass, self-armored radiator heat pipe material for temperatures below 800°K.
- At 920°K pure niobium and nickel do not have sufficient creep strength to be used as the envelope material for a potassium radiator heat pipe.
- The lower limit for the wall thickness of radiator heat pipes is determined by the need to withstand buckling from the earth's atmospheric pressure rather than by long term creep at operating temperature. With a safety factor of 2, the wall thickness ranges from 0.009 times the diameter for niobium 1% Zr, 0.008 times the diameter for the austenitic stainless steels, to 0.007 times the diameter for the molybdenum alloys.
- Niobium 1% Zr and the austenitic stainless steels are acceptable for the 920°K radiator heat pipes. Preliminary heat pipe evaluation should be carried out with the stainless steels, with the final choice of material coming from the actual system design and integration requirements of the energy converter.
- During the course of heat pipe evaluation extra low carbon 316 stainless steel was found to exhibit an inordinate amount of carbide

precipitation, thus removing it as a candidate envelope material. Tests continued with 304 EL stainless steel with no apparent problems.

Heat Pipe Fluids

- At 920°K sodium should be the working fluid for radiator heat pipes, at lower temperatures sodium should also be used unless the overall heat pipe $\Delta T$ becomes unacceptable. This is based on sodium's higher boiling limit and its higher latent heat of vaporization and surface tension at a given temperature, as compared to potassium. Potassium should be used only when the temperature, and therefore, absolute vapor pressure of sodium, is so low that a particular heat pipe design will not allow the use of sodium. Even then if the design can be altered to allow the use of sodium, it should be done provided the rest of the system is not adversely affected.

Heat Rejection System Design

- Heat pipe-to-heat pipe joints should be kept to a minimum within the constraints of system design, redundancy and reliability.
- Mechanically clamped or brazed heat pipe-to-heat pipe joints should be avoided.
- Heat pipe-to-heat pipe joints should be integrally built if the system design permits.
- For multiple heat pipe joints with full pretest capability for individual components, joints should be a slip fit with a sealable gap that is back filled with NaK or other suitable conductive fluid.
- The final system design for the 120 $kW_e$ thermionic system consisted of 128 reactor heat pipes each with three thermionic converters forming a module. The converters each have an integrally built collector heat pipe which is collectively accessed by three radiator

heat pipes 2 cm in diameter for a radiator diameter of 2.44 meters. Alternatively when the radiator diameter is 4.5 M, the three converters would be collectively accessed by six radiator heat pipes, 1.8 cm in diameter. In both designs, the radiator heat pipe-to-collector heat pipe joint utilized the NaK filled conductive gap.

- The overall heat rejection system design was shown to be flexible and capable of interfacing with thermoelectric as well as thermionic converters.
- Computer design analysis of the radiator system showed that without consideration for meteoroid armor and heat pipe performance, the smallest number of small diameter, long heat pipes produced the lowest mass radiator.
- A low mass armor design which has an intrinsically high emissivity may be possible.

Component Development

- Complex shapes, transitions, and bends for sodium heat pipe designs were shown to be capable of fabrication and operation. Reasonably good prediction of complex heat pipe performance was demonstrated.
- An integral heat pipe-to-heat pipe joint was demonstrated and shown to be a feasible means of connecting heat pipes. The analytical treatment of the joint falls within the experimental measurement.
- Flexible and long arteries were fabricated and shown to be capable of performing as designed for complex shapes and long heat pipes.
- Long radiator heat pipes using arteries can be designed, and fabricated. End to end temperature prediction was demonstrated within several degrees Kelvin. Additional analytical work is needed to improve prediction of the actual temperature profile in the condenser portion of the heat pipe.

The significant conclusion of the work presented here is that liquid metal heat pipes can be used for spacecraft radiator service.

Additional work is recommended on development of the computer program for the prediction of the temperature profile in the condenser (radiator) portion of the heat pipe and that experimental verification be carried out. A full scale radiator heat pipe, complete with bends and adiabatic zone, should be designed, fabricated and tested, along with the cold side heat pipe-to-radiator heat pipe NaK filled joint. Following verification of the design of the individual components, the entire heat rejection side of an assembly module should be designed, fabricated, and tested with the chosen materials of construction.

The computer design and analysis of the radiator system should be enlarged to allow for calculation of heat pipe performance, meteoroid protection and system changes resulting from failures.

Additional work should be carried out on meteoroid armor design, coupled with experimental evaluation of thermal performance and impact studied.

## NEW TECHNOLOGY

Title: Meteoroid Armor for Spacecraft Radiators

Inventors: Donald M. Ernst

G. Yale Eastman

Initital Disclosure: Progress Report #3

October 1978 - Page 13

Thermacore Drawing A59-3

Subsequent Disclosure: Final Report JPL Contract 955437

September 1979 - Pages 13-38

Current Disclosure: Final Report JPL Contract 955100

March 1981 - Pages 48-51

## REFERENCES


1. Bett, F.L. and Draycott, A., Proceedings of the Second United Nations Conference on the Peaceful Uses of Atomic Energy, Geneva, 1958, Paper 1091.

2. The Metal Beryllium, the American Society for Metals, Cleveland, Ohio, 1955.

3. LA-3881-MS, Quarterly States Report on the Space Electric Power R&D Program for the Period Ending January 31, 1968, Part I.

4. Volume 1, Properties and Selection of Metals, 8th Edition, Metals Handbook, The American Society for Metals, Metal Park, Ohio, Page 529.

5. Design and Analysis of the Radiator Structure for Space Power Systems, W. H. Dauterman and L. D. Montgomery, Atomics Internal Division, Rockwell International. AI-AEC-13093, NASA-CR-121222.

6. Progress Report, Thermionic Energy, Conversion Technology Development Program, July 15, 1978, JPL #73-24.

7. Roark, Raymond S., Formulas for Stress and Strain, McGraw-Hill, 1954.

8. Progress Report, Thermionic Energy Conversion, Technology Development Program, March 1, 1978, JPL #730-12.

9. Personal Results, RCA, 1962-1967.

10. D. M. Ernst and P. K. Shefsiek, Heat Pipe Development for Thermionic Applications, 4th Intersociety Energy Conversion Engineering Conference, September 22-26, 1969, Washington, D.C., Page 879, 699107.

11. Hsu, Y. Y., On the Size Range of Active Nucleation Cavities on a Heating System, J. of Heat Transfer, Trans A.S.M.E., August 1962.

## APPENDIX A

Appendix A consists of the following Thermacore drawings:

C-59-500

B-59-501

D-59-502

C-59-503

D-59-504

C-59-505

B-59-506

C-59-507

B-59-508

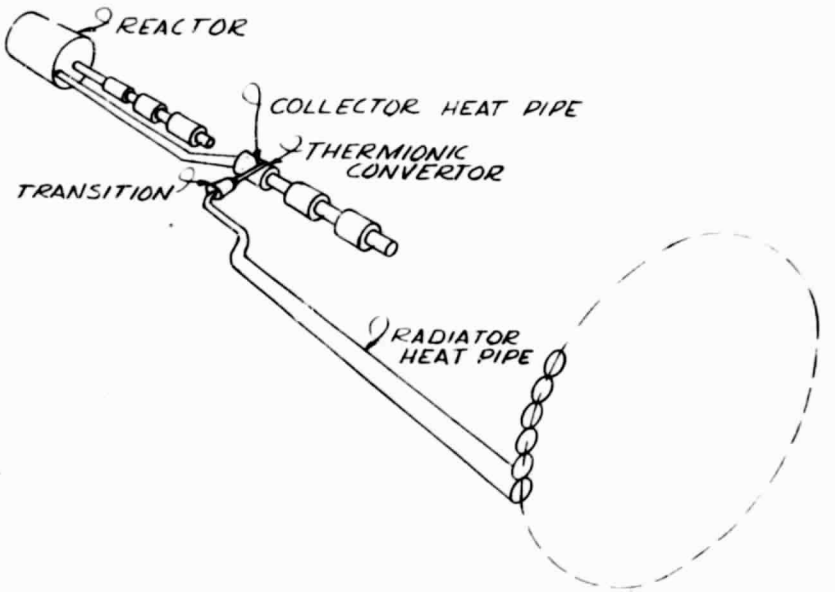


N.E.P. HEAT REJECTION CONCEPT

ORIGINAL PAGE IS
OF POOR QUALITY

| KEY | REVISION NOTE | INITIAL | DATE |
|---|---|---|---|
| | | | |

TITLE: NEP HEAT REJECTION CONCEPT

NAME

DRAWN R.L.C. DATE 3/1/79

APPROVED

SCALE NONE MATL.

ASS'Y or BILL

THERMACORE, INC.
HEAT TRANSFER SPECIALISTS

ST'D. TOLERANCES

DECIMAL

FRACTION ± 1/64

ANGULAR

DWG. NO. C-59-500

ORIGINAL PAGE IS
OF POOR QUALITY

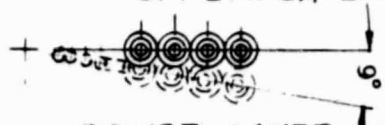


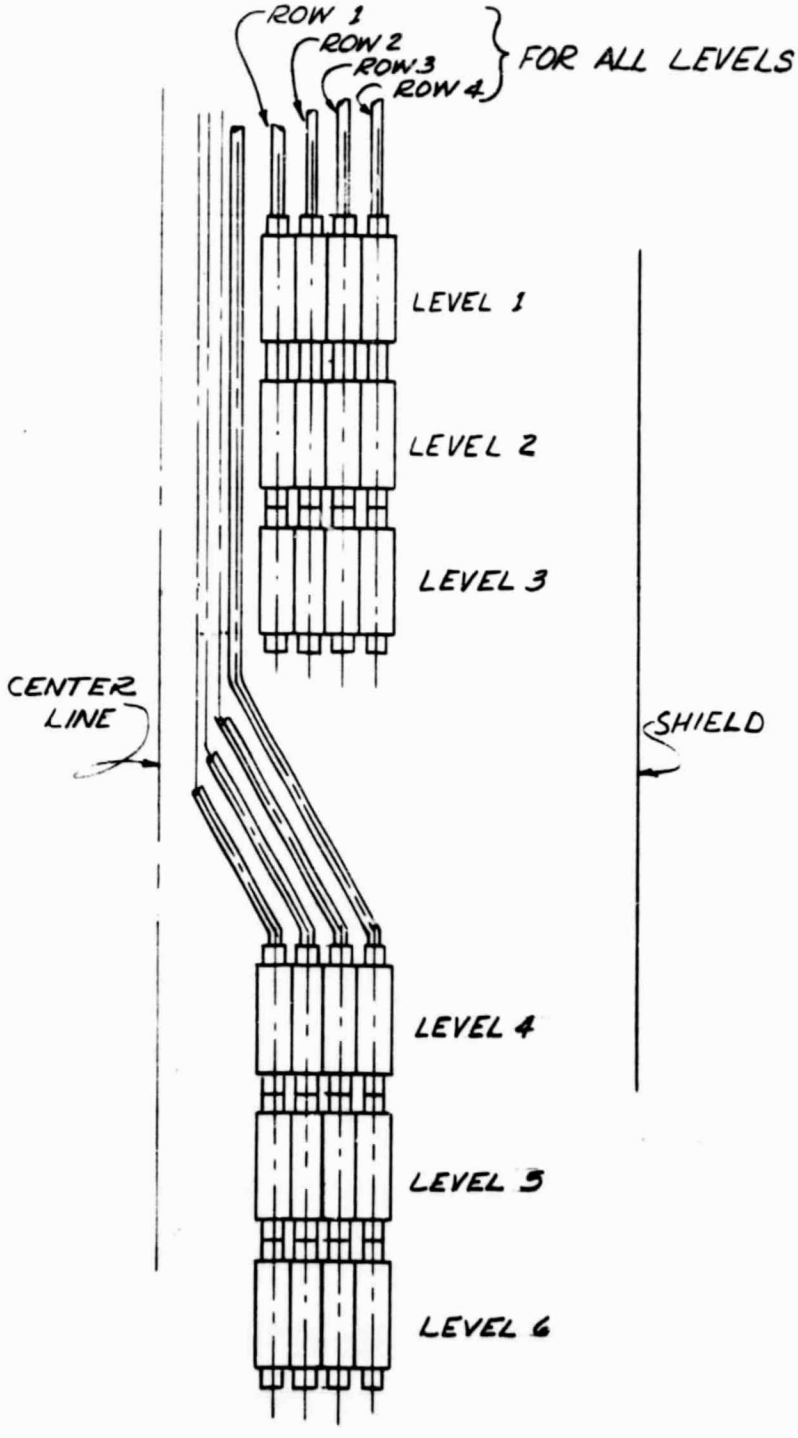


LEVEL & CONVERTOR NUMBER SYSTEM FOR MATRIX

| | | | | | |
|---|---|---|---|---|---|
| | | | | | KEY |
| | | | | | REVISION NOTE |
| | | | | | INITIAL |
| | | | | | DATE |
| | | | | | TITLE |
| | | | | | NAME |
| | | | | | DRAWN |
| | | | | | APPROVED |
| | | | | | DATE |
| | | | | | SCALE |
| | | | | | MATL. |
| | | | | | ASSY or BILL |
| | | | | | THERMACORE, INC. HEAT TRANSFER SPECIALISTS |
| | | | | | DWG. NO. B-59-5 |
| | | | | | ANGULAR |
| | | | | | FRACTION ± |
| | | | | | DECIMAL ± |
| | | | | | DWG. NO. |

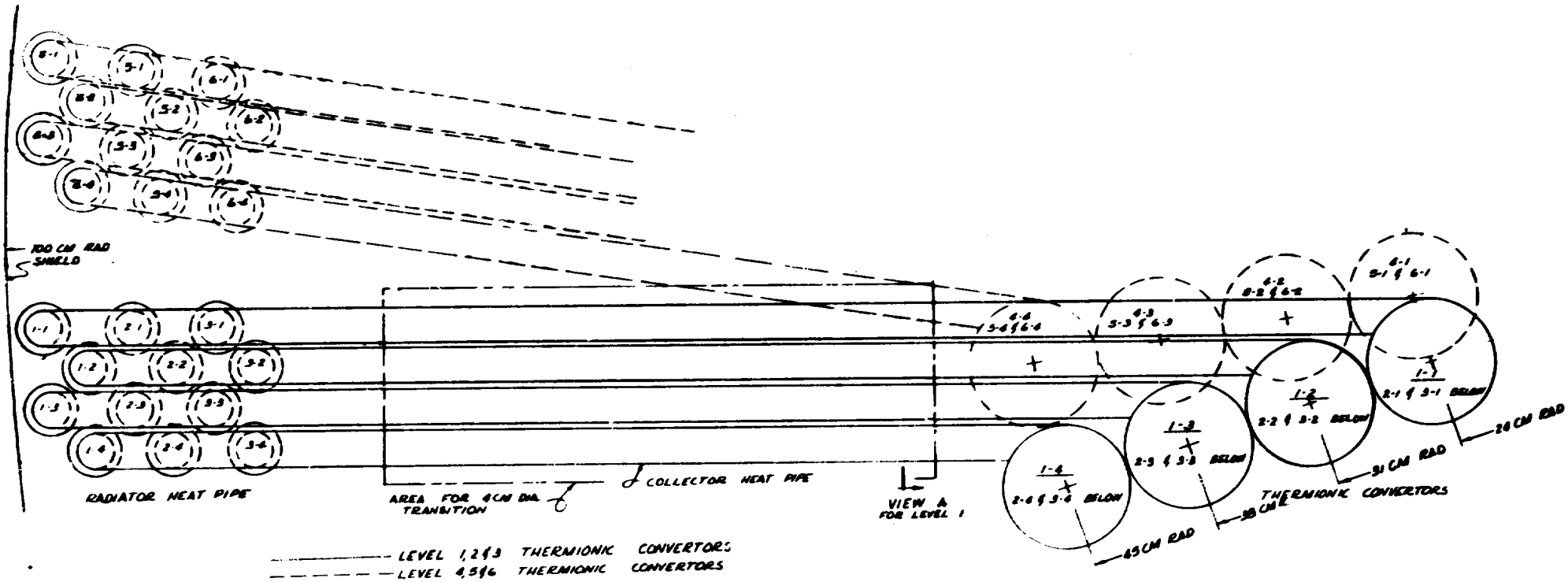


LAYOUT DESIGN NO. 1
PLAN VIEW OF
COLLECTOR HEAT PIPES

D-59-502
5/1/79 RLC

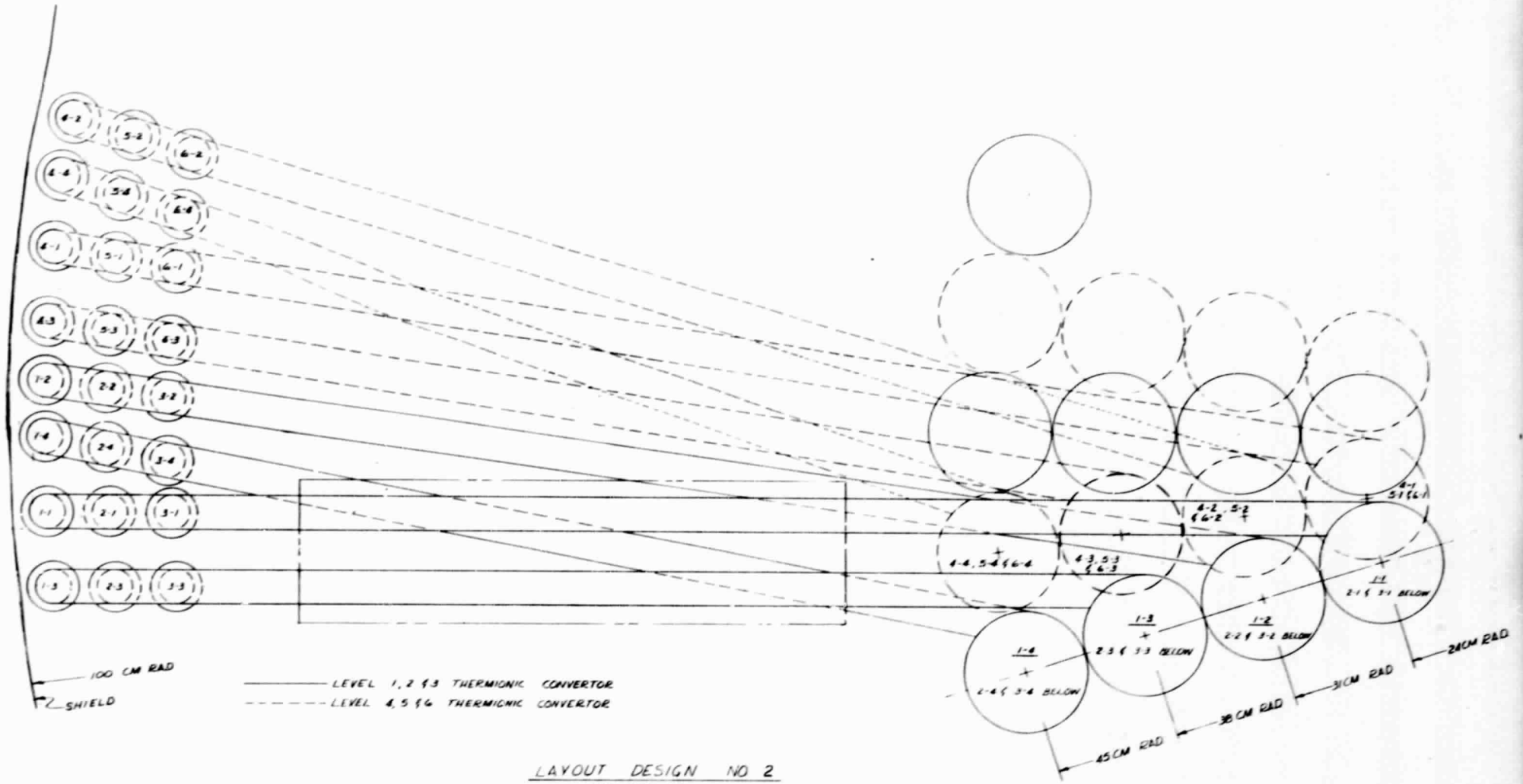


LAYOUT DESIGN NO 2

PLAN VIEW OF COLLECTOR HEAT PIPES

D-59-503
5/11/79 RLC

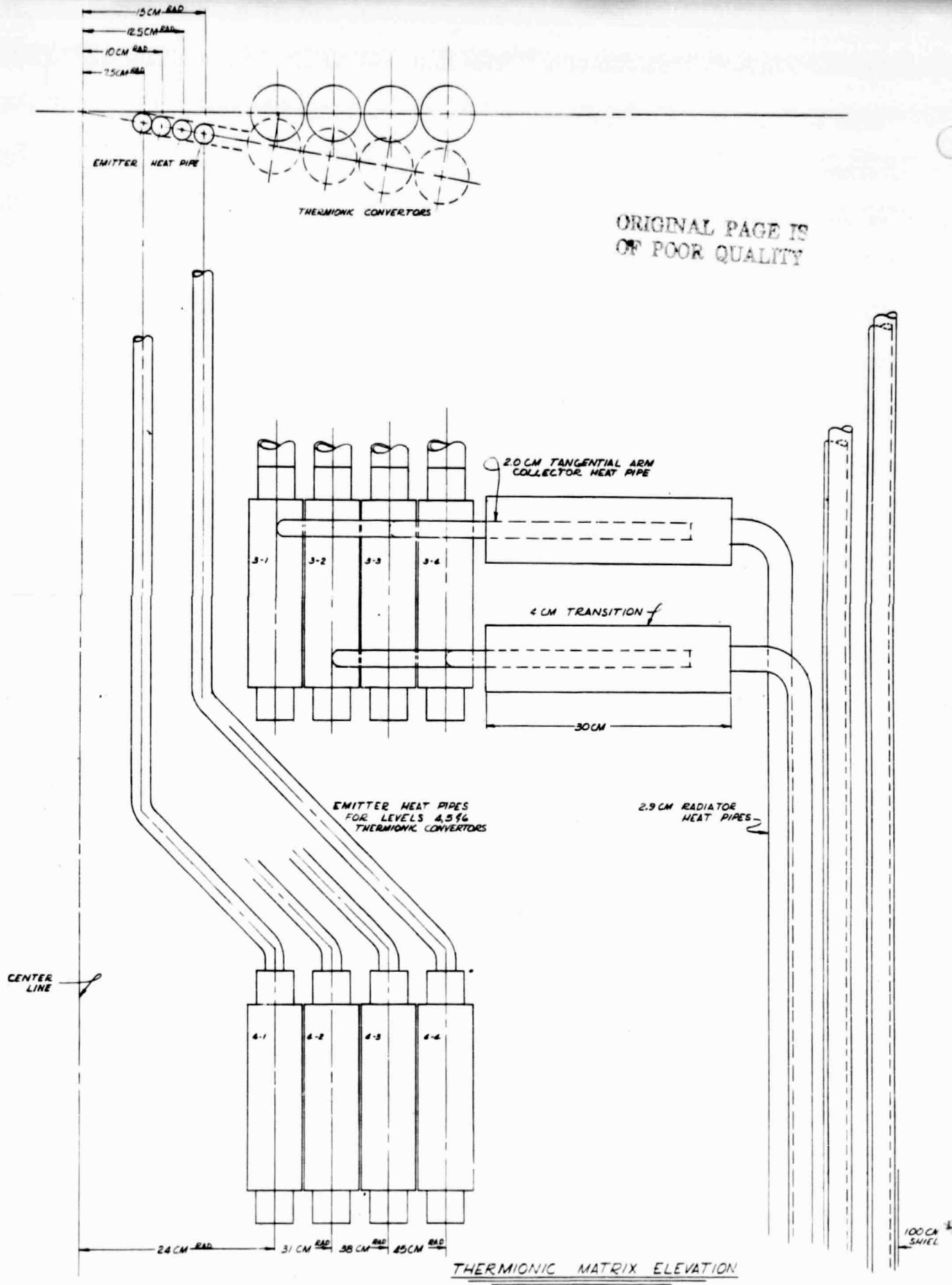


ORIGINAL PAGE IS
OF POOR QUALITY

THERMIONIC MATRIX ELEVATION

REFERENCE LAYOUT DESIGN NO. 1 D-59-502

D-59-504
5/1/79 P.L.C

405-65-D

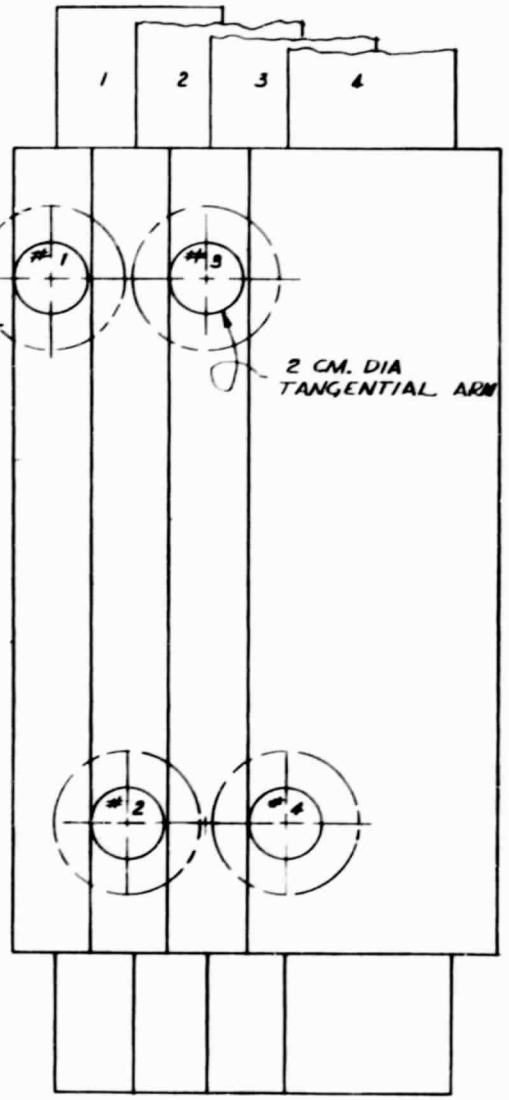


4 CM DIA TRANSITION FROM 2.9 CM DIA RADIATOR HEAT PIPE TO THE 2.0 CM TANGENTIAL ARM OF COLLECTOR HEAT PIPE

2 CM. DIA TANGENTIAL ARM

TYPICAL VIEW "A" FROM ASSEMBLY D-59-501 SHOWING POSTION OF COLLECTOR HEAT PIPES #1 & #3 HIGH & #2 & #4 LOW

| REV | REVISION NOTE | INITIAL | DATE |
|---|---|---|---|
| | | | |

TITLE

NAME

DRAWN R.L.C. 5/1/79

APPROVED

SCALE MATL.

ASSY or SELL

THERMACORE, INC.

DWG. NO. C-59-505

DWG. NO.

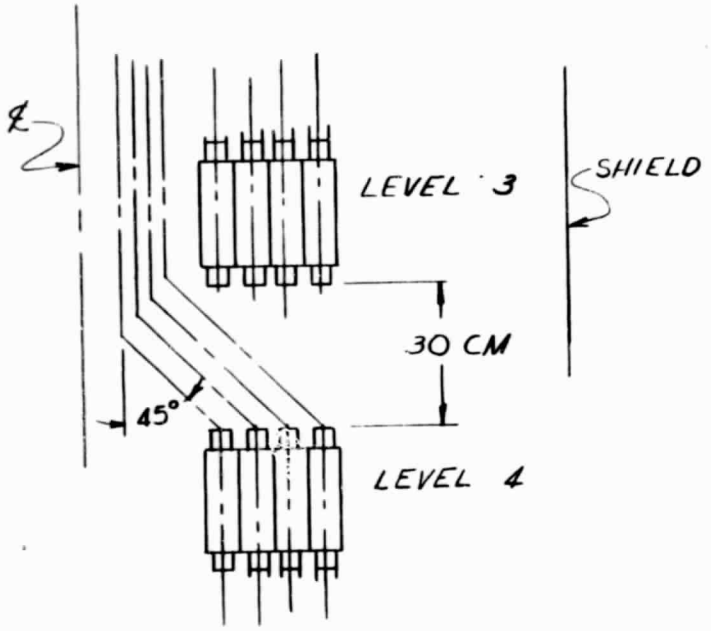


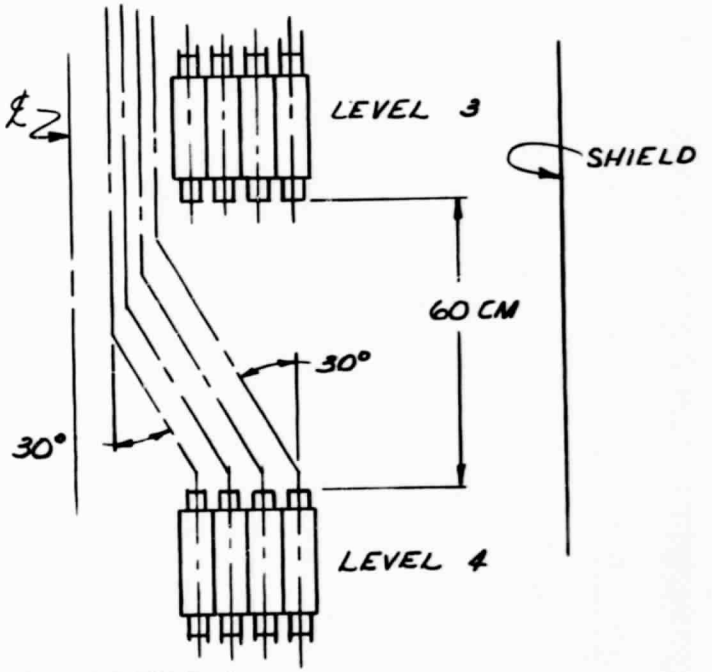


# THERMIONIC MATRIX SEPERATION
## FOR 30° & 45° EMITTER HEAT PIPE ANGLES

| KEY | REVISION NOTE | INITIAL | DATE |
|---|---|---|---|
| | | | |

TITLE

NAME

DRAWN R.L.C. DATE 5/1/79

APPROVED

SCALE MATL.

ASS'Y or BILL

BY'S TOLERANCES

DECIMAL .xx ± .010 .xxx ± .005

FRACTION ± 1/64

ANGULAR ± .003 PER INCH OF LENGTH

THERMACORE, INC.
HEAT TRANSFER SPECIALISTS

DWG. NO. B-59-506

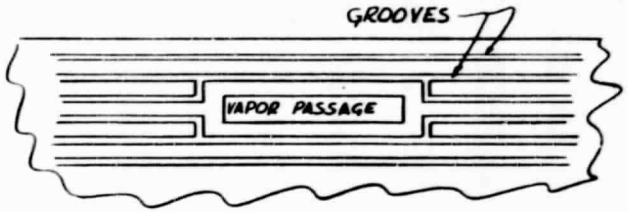


DETAIL OF GROOVES
AROUND VAPOR PASSAGE

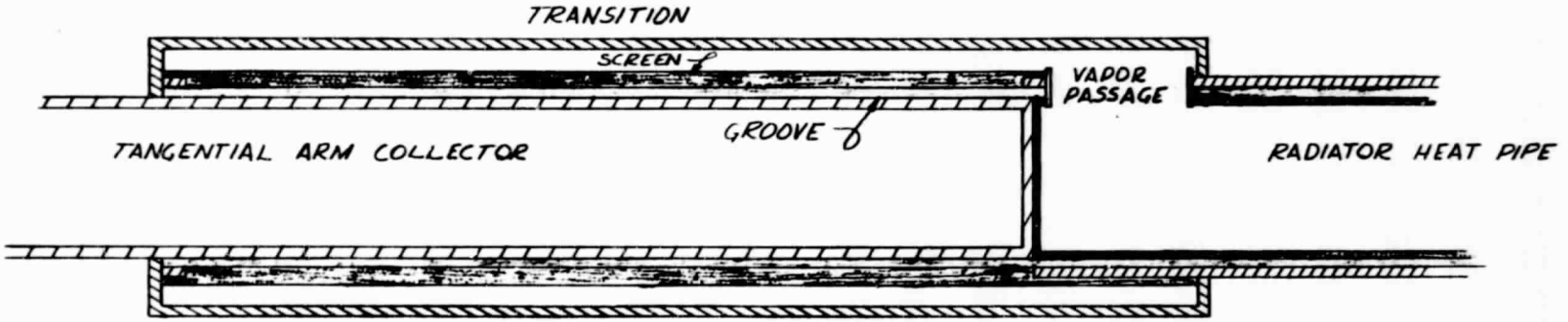


HEAT PIPE GROOVE GEOMETRY
IN TRANSITION ZONE

| REV | REVISION NOTE | INITIAL | DATE |
|---|---|---|---|
| | | | |

TITLE

NAME

DRAWN R.L.C. 5/1/77

APPROVED

SCALE MATL.

ASS'Y or BILL

GENERAL TOLERANCES
DECIMAL ±.1 ±.01 ±.005
FRACTION ± 1/64
ANGULAR ± .005 PER INCH OF LENGTH

DWG. NO. C-59-507

NACORE, INC.
WICK SPECIALISTS

## APPENDIX B

### Super Heat Considerations

Ernst and Shefsiek show the super heat limit to be:

$$T = \frac{2\gamma T}{\rho_v L r_b}$$

where $r_b$ = the half width of the wire mesh - cm

$\gamma$ = surface tension - dy/cm

T = absolute temperature - $^oK$

$\rho_v$ = vapor pressure of fluid - $gm/cm^3$

L = latent heat - cal/gram

Hsu's correlation shows the super heat limit to be:

$$T = \frac{3.06\Delta T}{\rho_v L r_b}$$

where $r_b = 2.5 \times 10^{-3}$ cm

Accordingly, one can calculate the $\Delta T$ through a liquid filled wick to determine if the super heat limit is being approached.

$$W/A = \frac{K\Delta T}{\ell}$$

where W/A = heat flux through wick - $watt/cm^2$

K = thermal conductivity of liquid filled wick - $\frac{watts\text{-}cm}{cm^o\text{-}^oK}$

$\Delta T$ = super heat limit - $^oK$

$\ell$ = wick thickness - cm

## APPENDIX C

Listing of computer programs RAD7 and RAD4.

## PROGRAM RAD4

```
INPUT DATA

XXXXX LINE 1, MAX LENGTH, MAX DIAMETER, CONE ANGLE
?1800,450,30

XXXXX LINE 2, REACTOR DIA, REACTOR LENGTH, SHIELD LENGTH
?50,53,60

XXXXX LINE 3, ELEC PWR, T/E EFF, T/E THICKNESS
?120000,.08,2.54

XXXXX LINE 4, # OF REAC. HP, # OF RAD HP PER T/E, DIA OF RAD HP
?90,3,2

XXXXX LINE 5, EMISSIVITY, RADIATOR TEMPERATURE
?.9,800

 CHANGE WHICH LINE (0 TO RUN, STOP TO QUIT)
?
```

# RAD4 OUTPUT

LAYER 1 HAS 23 T/E, 69 ADDITIONAL RAD HPS FOR A TOTAL OF 69 HPS
LAYER 1 HAS 69 NESTED HEAT PIPES
LAYER 1 HPS ARE 1709 CM LONG AND CARRY 9227 WATTS

LAYER 2 HAS 36 T/E, 108 ADDITIONAL RAD HPS FOR A TOTAL OF 177 HPS
LAYER 2 HAS 177 NESTED HEAT PIPES
LAYER 2 HPS ARE 1593 CM LONG AND CARRY 8497 WATTS

LAYER 3 HAS 31 T/E, 93 ADDITIONAL RAD HPS FOR A TOTAL OF 270 HPS
LAYER 3 HAS 270 NESTED HEAT PIPES
LAYER 3 HPS ARE 1477 CM LONG AND CARRY 7834 WATTS

LAYER 1 HPS HAVE 232 CM OVER THE T/E. 307 CM ON THE CONE.
AND 1053 CM AT THE MAXIMUN DIAMETER
ESTIMATED SS RADIATOR HP MASS IS 86.54 KG

LAYER 2 HPS HAVE 116 CM OVER THE T/E. 307 CM ON THE CONE.
AND 1053 CM AT THE MAXIMUN DIAMETER
ESTIMATED SS RADIATOR HP MASS IS 80.66 KG

LAYER 3 HPS HAVE 0 CM OVER THE T/E. 307 CM ON THE CONE.
AND 1053 CM AT THE MAXIMUN DIAMETER
ESTIMATED SS RADIATOR HP MASS IS 74.78 KG

RADIATOR HAS THE CAPABILITY OF SERVICING 182642 WATTS ELECTRICAL POWER AT 8 PERCENT EFFICIENCY
270 RADIATOR HPS 2.0 CM IN DIA DISSIPATE 2283020 WATTS AT 800 K

## HEAT PIPE RADIATOR DESIGN

REQUIRED POWER IS 5111 WATTS

LAYER 1 HEAT PIPES HAVE A 103 CM LONG EVAPORATOR, 13 CM LONG ADABATIC AND A 884 CM LONG CONDENSER (RADIATOR) AND CARRY 5111 WATTS
ESTIMATED SS RADIATOR HP MASS IS 50.66 KG

LAYER 2 HEAT PIPES HAVE A 103 CM LONG EVAPORATOR, 13 CM LONG ADABATIC AND A 893 CM LONG CONDENSER (RADIATOR) AND CARRY 5111 WATTS
ESTIMATED SS RADIATOR HP MASS IS 51.14 KG

LAYER 3 HEAT PIPES HAVE A 103 CM LONG EVAPORATOR, 13 CM LONG ADABATIC AND A 892 CM LONG CONDENSER (RADIATOR) AND CARRY 5111 WATTS
ESTIMATED SS RADIATOR HP MASS IS 51.04 KG

RADIATOR HPS HAVE AN AXIAL HEAT FLUX OF 1626 WATTS/CM**2
270 RADIATOR HPS 2.0 CM IN DIA DISSIPATE 1380000 WATTS AT 800 K
TOTAL ESTIMATED SS RADIATOR MASS IS 13766.30 KG

```
1000 REM PROGRAM RAD4
1010 DIM L(20,20)
1020 P0=10
1030 P$=CHR$(P0)
1040 PRINT P$;P$;
1050 PRINT P$;TAB(32);"PROGRAM RAD4"
1060 PRINT TAB(29);"------------"
1070 PRINT P$
1080 PRINT P$;"INPUT DATA"
1090 S=0
1100 PRINT P$;"XXXXX LINE 1, MAX LENGTH, MAX DIAMETER, CONE ANGLE"
1110 INPUT L,D,A
1120 A=A/57.29577951
1130 IF S=0 THEN 1150
1140 GOTO 3590
1150 PRINT P$;"XXXXX LINE 2, REACTOR DIA, REACTOR LENGTH, SHIELD LENGTH
"
1160 INPUT D1,L1,L2
1170 IF S=0 THEN 1190
1180 GOTO 3590
1190 PRINT P$;"XXXXX LINE 3, ELEC PWR, T/E EFF, T/E THICKNESS"
1200 INPUT P,E0,T0
1210 IF S=0 THEN 1230
1220 GOTO 3590
1230 PRINT P$;"XXXXX LINE 4, # OF REAC. HP, # OF RAD HP PER T/E, DIA O
F RAD HP"
1240 INPUT N0,N,D4
1250 IF S=0 THEN 1270
1260 GOTO 3590
1270 PRINT P$;"XXXXX LINE 5, EMISSIVITY, RADIATOR TEMPERATURE"
1280 INPUT E1,T
1290 DEF FNS(X)=ATN(X/SQR(1-X**2))
1300 S=1
1310 P1=3.141592654
1320 S1=5.67E-12
1330 T=T-273.16
1340 S2=S1*E1*(T+273.16)**4
1350 GOTO 3590
1360 REM BEGIN CALCULATIONS
1370 FOR I=0 TO K+1
1380 FOR J=0 TO 13
1390 L(J,I)=0
1400 NEXT J
1410 NEXT I
1420 FOR I=0 TO K+1
1430 P(1,I)=P(2,I)=Q(1,I)=Q(2,I)=X(1,I)=D(1,I)=0
1440 K(1,I)=0
1450 K(2,I)=0
1460 NEXT I
1470 FOR I=0 TO K+1
1480 FOR J=0 TO 7
1490 N(J,I)=0
1500 NEXT J
1510 NEXT I
1520 REM CALC REACTOR HP PWR & DIA AT 5 KW/CM**2
1530 P2=P/(N0*E0)
1540 D0=SQR(4*P2/(5000*P1))
1550 REM CALCULATR COLD SIDE T/E DIA
1560 D6=D0+2*T0+2*(D4+1)
1570 REM CALCULATE DIAM AT BEGINING OF T/E
1580 D3=D1+2*(L1+L2)*TAN(A/2)
1590 REM CALCULATE T/E LENGTH AT  AT 25W/CM**2
1600 L0=P2/(25*P1*D0)
1610 REM CALC PLANT LENGTH OF T/E
```

```
1620 L3=D3
1630 L4=L3+L0
1640 REM CALCULATE HORZ LENGTH OF T/E
1650 REM CALC INCREASE IN DIA OVER LENGTH OF T/E
1660 D7=2*L4*SIN(A/2)
1670 D(1,0)=D3
1680 L(2,0)=L1+L2
1690 REM HOW MANY T/E AT EACH DIA
1700 K=1
1710 K1=0
1720 N(1,K)=INT(P1/FNS(D6/(D(1,K-1)-D6-(2*K1*D4))))
1730 N(2,0)=N0
1740 N(2,K)=N(2,K-1)-N(1,K)
1750 L(1,K)=L4*COS(A/2)
1760 D(1,K)=D(1,K-1)+D7
1770 L(2,K)=L(2,K-1)+L(1,K)
1780 IF N(2,K)>0 THEN 1800
1790 GOTO 1830
1800 K=K+1
1810 K1=1
1820 GOTO 1720
1830 N(1,K)=N(2,K-1)
1840 REM PERFECT NESTING OF RAD HP AROUND T/E
1850 N1=INT(P1/FNS(D4/(D6-D4-1)))
1860 IF N1>N THEN 1890
1870 PRINT P$;N;"RADIATOR HPS WILL NOT NEST AT T/E";N1;"HEAT PIPES WILL
 "
1880 GOTO 3590
1890 REM PERFECT NESTING OF RAD HP ON OD
1900 FOR I=1 TO K
1910 N(3,I)=INT(P1/FNS(D4/(D(1,I)-D4)))
1920 NEXT I
1930 FOR I=1 TO K
1940 N(4,0)=0
1950 N(4,I)=N(4,I-1)+N*N(1,I)
1960 N(6,I)=N(6,I-1)+N*N(1,I)
1970 N(7,I)=N*N(1,I)
1980 IF N(4,I)<=N(3,I) THEN 2020
1990 N(5,I)=N(6,I)-N(3,I)
2000 N(4,I)=N(3,I)
2010 K(1,I)=I
2020 NEXT I
2030 REM PERFECT NESTING OF RAD HPS ON MAXIMUN DIAMETER
2040 N2=INT(P1/FNS(D4/(D-D4)))
2050 IF N(6,K)<=N2 THEN 2080
2060 PRINT USING 2070,N(6,K),D4,N2
2070 ###### RAD HPS ##.## CM IN DIA WILL NOT NEST AT MAX DIA.  ### HPS W
ILL
2080 REM CALC EFFICTIVE PIES
2090 FOR I=1 TO K-1
2100 C=D4/(2*(D(1,I)-D4)*SIN(P1/N(4,I)))
2110 C=2*FNS(C)
2120 C=P1+(2*P1/N(4,I))-C
2130 P(1,I)=C/2
2140 C1=D4/(2*(D(1,I+1)-D4)*SIN(P1/N(4,I)))
2150 C1=2*FNS(C1)
2160 C1=P1+(2*P1/N(4,I))-C1
2170 P(2,I)=C1/2
2180 REM CALC EFFECTIVE PIES AT BEGINING OF CONE
2190 C3=D4/(2*(D(1,K)-D4)*SIN(P1/N(4,K)))
2200 C3=2*FNS(C3)
2210 C3=P1+(2*P1/N(4,K))-C3
2220 P(2,K)=C3/2
2230 NEXT I
2240 REM CALC REAMING CONE AND RADIATOR LENGTHS
```

```
2270 L7=L-L6-L(2,K)
2280 REM CALC SLANT LENGTH OVER T/E
2290 FOR I=1 TO K
2300 L(3,I)=L(1,I)/COS(A/2)
2310 NEXT I
2320 REM CALC POWER REQUIRED / HP
2330 P3=((P/E0)-P)/(N0*N)
2340 REM CALC NECESSARY LENGTH FOR RAD HP
2350 A1=P3/(S1*E1*(T+273.16)**4)
2360 L9=A1/D4
2370 REM CALC EFFECTIVE PIE AT MAX DIAMETER
2380 C2=D4/(2*(D-D4)*SIN(P1/N(4,K)))
2390 C2=2*FNS(C2)
2400 C2=P1+(2*P1/N(4,K))-C2
2410 P4=C2/2
2420 REM CALC RAD HP LENGTH
2430 FOR I=1 TO K-1
2440 L(4,I)=((P(1,I)+P(2,I))/2)*L4
2450 NEXT I
2460 L(4,K)=((P(2,K)+P4)/2)*L8
2470 L(4,K+1)=P4*L7
2480 FOR I=1 TO K+1
2490 L(5,0)=0
2500 L(5,I)=L(5,I-1)+L(4,I)
2510 NEXT I
2520 FOR I=1 TO K
2530 L(7,0)=L(5,K+1)
2540 L(7,I)=L(7,I-1)-L(4,I-1)
2550 NEXT I
2560 FOR I=1 TO K
2570 L(6,I)=L7+L8+((K-I)*L4)
2580 NEXT I
2590 FOR I=1 TO K+1
2600 L(8,I)=L(5,K+1)-L(5,K+1-I)
2610 NEXT I
2620 REM MAX Q/ HP
2630 FOR I=1 TO K
2640 Q(1,I)=L(7,I)*D4*S1*E1*(T+273.16)**4
2650 Q(2,0)=0
2660 Q(2,I)=Q(2,I-1)+Q(1,I)*N(7,I)
2670 NEXT I
2680 FOR I=1 TO K
2690 S3=0
2700 FOR J=1 TO K+1
2710 K(2,I)=J
2720 IF S3=1 THEN 2790
2730 S3=1
2740 IF L9>L(7,I) THEN 2760
2750 GOTO 2790
2760 PRINT USING 2770,L9,L(7,I)
2770 :REQUIRED RADIATOR LENGTH #### EXCEEDES MAXIMUN AVAILABLE LENGTH #
###
2780 GOTO 3590
2790 L(9,I)=L(5,K+1)-L(5,I-1)-L(8,J)
2800 IF L(9,I)>L9 THEN 2820
2810 GOTO 2830
2820 NEXT J
2830 X(1,I)=(L9-L(9,I))/(L(8,J)-L(8,J-1))
2840 NEXT I
2850 L(10,K)=L8
2860 L(10,K+1)=L7
2870 FOR I=1 TO K-1
2880 L(10,I)=L4
2890 NEXT I
2900 FOR I=1 TO K
```

ORIGINAL PAGE IS

```
2920 L(11,J)=L(11,J-1)+L(10,J)
2930 NEXT J
2940 L(12,I)=L(11,J)-(I-1)*L4
2950 NEXT I
2960 FOR I=1 TO K
2970 L(13,I)=L(12,I)+X(1,I)*L(10,K+1-(K(2,I)-1))
2980 NEXT I
2990 PRINT P$;P$;
3000 PRINT P$;P$;TAB(35);"RAD4 OUTPUT"
3010 PRINT TAB(29);"-----------"
3020 PRINT P$;P$;
3030 FOR I=1 TO K
3040 PRINT USING 3050,I,N(1,I),N(1,I)*N,N(6,I)
3050 :LAYER ## HAS ### T/E, ### ADDITIONAL RAD HPS FOR A TOTAL OF ####
HPS
3060 IF K(1,I)=0 THEN 3090
3070 PRINT USING 3080,I,N(5,I)
3080 :LAYER ## HAS ### UN-NESTED HEAT PIPES
3090 PRINT USING 3100,I,N(4,I)
3100 :LAYER ## HAS ### NESTED HEAT PIPES
3110 PRINT USING 3120,I,L(6,I)+L4,Q(1,I)
3120 :LAYER ## HPS ARE ##### CM LONG AND CARRY ##### WATTS
3130 PRINT
3140 NEXT I
3150 PRINT
3160 FOR I=1 TO K
3170 PRINT USING 3180,I,(K-I)*L(3,I),L8
3180 :LAYER ## HPS HAVE #### CM OVER THE T/E.  #### CM ON THE CONE.
3190 PRINT USING 3200,L7
3200 : AND #### CM AT THE MAXIMUN DIAMETER
3210 PRINT USING 3220,P1*1.02*D4*(L(6,I)+L4)*7.9/1000
3220 : ESTIMATED SS RADIATOR HP MASS IS ###.## KG
3230 PRINT
3240 NEXT I
3250 PRINT USING 3260,Q(2,K)*E0
3260 :RADIATOR HAS THE CAPABILITY OF SERVICING ######### WATTS ELECTRIC
AL
3270 :POWER AT ## PERCENT EFFICIENCY
3280 PRINT USING 3270,E0*100
3290 PRINT USING 3300,N(6,K),D4,Q(2,K),T+273.16
3300 :### RADIATOR HPS ##.# CM IN DIA DISSIPATE ####### WATTS AT ####
K
3310 PRINT P$;P$;TAB(24);"HEAT PIPE RADIATOR DESIGN"
3320 PRINT TAB(22);"------------------------"
3330 P3=INT(P3)
3340 PRINT P$;
3350 PRINT P$;"REQUIRED POWER IS ";P3;"WATTS"
3360 PRINT
3370 FOR I=1 TO K
3380 PRINT
3390 PRINT USING 3400,I,L0,L3
3400 :LAYER ## HEAT PIPES HAVE A ### CM LONG EVAPORATOR, ### CM LONG A
DABATIC,
3410 PRINT USING 3420,L(13,I),P3
3420 : AND A #### CM LONG CONDENSER (RADIATOR) AND CARRY ##### WATTS
3430 PRINT USING 3220,P1*1.02*D4*(L0+L3+L(13,I))*7.9/1000
3440 IF K(1,I)=0 THEN 3470
3450 PRINT USING 3460,I,N(5,I)
3460 : *NOTE LAYER ### HAS #### UN-NESTED HEAT PIPES.
3470 NEXT I
3480 PRINT P$;P$
3490 PRINT USING 3500,P3/(P1*D4**2/4)
3500 :RADIATOR HPS HAVE AN AXIAL HEAT FLUX OF ##### WATTS/CM**2
3510 PRINT USING 3520,N(6,K),D4,(P/E0)-P,T+273.16
3520 ### RADIATOR HPS ##.# CM IN DIA DISSIPATE ####### WATTS AT ####
```

ORIGINAL PAGE IS
OF POOR QUALITY

```
3530 FOR I=1 TO K
3540 M(1,I)=M(1,I-1)+(L(13,I)+L0+L3)*P1*1.02*D4*7.9*N(1,I)*N/1000
3550 NEXT I
3560 PRINT USING 3570,M(1,K)
3570 : TOTAL ESTIMATED SS RADIATOR MASS IS ######.## KG
3580 PRINT P$;P$
3590 PRINT P$;" CHANGE WHICH LINE (0 TO RUN, STOP TO QUIT)"
3600 INPUT X
3610 IF X=0 THEN 3630
3620 ON X GOTO 1100,1150,1190,1230,1270
3630 PRINT P$;P$;
3640 GOTO 1360
3650 IF X>5 THEN 3590
3660 END
```

*

## PROGRAM RAD7

```
INPUT DATA

XXXXX LINE 1, MAX LENGTH, MAX DIAMETER, CONE ANGLE
?1800,450,30

XXXXX LINE 2, REACTOR DIA, REACTOR LENGTH, SHIELD LENGTH
?50,53,60

XXXXX LINE 3, ELEC PWR, T/E EFF, T/E THICKNESS
?120000,.08,2.54

XXXXX LINE 4, # OF REAC HPS, # OF RAD HPA PER T/E 1&LAST
?90,1,6

XXXXX LINE 5, EMISSIVITY, RADIATOR TEMPERATURE
?.9,800

XXXXX LINE 6, FIRST DIAMETER, INCREMENT, LAST DIAM OF RAD HP
?1,.5,5

 CHANGE WHICH LINE (0 TO RUN, STOP TO QUIT)
?0
```

# RAD7 OUTPUT

| LAY | TEMP | T/E | HP-T/E | THP | DIA | LENGTH | MASS | Q/A | Q |
|---|---|---|---|---|---|---|---|---|---|
| N | K | N | N | N | CM | CM | KG | W/CM**2 | W |
| 3 | 800 | 90 | 4 | 360 | 1.00 | 1386 | 12641 | 4880 | 3833 |
| 3 | 800 | 90 | 5 | 450 | 1.00 | 1160 | 13233 | 3904 | 3066 |
| 3 | 800 | 90 | 6 | 540 | 1.00 | 1012 | 13852 | 3253 | 2555 |
| 3 | 800 | 90 | 3 | 270 | 1.50 | 1257 | 12894 | 2892 | 5111 |
| 3 | 800 | 90 | 4 | 360 | 1.50 | 1009 | 13807 | 2169 | 3833 |
| 3 | 800 | 90 | 5 | 450 | 1.50 | 864 | 14784 | 1735 | 3066 |
| 3 | 800 | 90 | 6 | 540 | 1.50 | 771 | 15840 | 1446 | 2555 |
| 3 | 800 | 90 | 2 | 180 | 2.00 | 1377 | 12560 | 2440 | 7666 |
| 3 | 800 | 90 | 3 | 270 | 2.00 | 1006 | 13766 | 1626 | 5111 |
| 3 | 800 | 90 | 4 | 360 | 2.00 | 825 | 15069 | 1220 | 3833 |
| 3 | 800 | 90 | 5 | 450 | 2.00 | 723 | 16514 | 976 | 3066 |
| 3 | 800 | 90 | 6 | 540 | 2.00 | 632 | 17324 | 813 | 2555 |
| 3 | 800 | 90 | 2 | 180 | 2.50 | 1150 | 13119 | 1561 | 7666 |
| 3 | 800 | 90 | 3 | 270 | 2.50 | 858 | 14691 | 1041 | 5111 |
| 3 | 800 | 90 | 4 | 360 | 2.50 | 720 | 16451 | 780 | 3833 |
| 3 | 800 | 90 | 5 | 450 | 2.50 | 611 | 17430 | 624 | 3066 |
| 3 | 800 | 90 | 6 | 540 | 2.50 | 534 | 18293 | 520 | 2555 |
| 3 | 800 | 90 | 2 | 180 | 3.00 | 1000 | 13701 | 1084 | 7666 |
| 3 | 800 | 90 | 3 | 270 | 3.00 | 762 | 15681 | 723 | 5111 |
| 3 | 800 | 90 | 4 | 360 | 3.00 | 626 | 17179 | 542 | 3833 |
| 3 | 800 | 90 | 5 | 450 | 3.00 | 533 | 18271 | 433 | 3066 |
| 3 | 800 | 90 | 5 | 450 | 3.12 | 518 | 18463 | 401 | 3066 |
| 4 | 800 | 90 | 2 | 180 | 3.50 | 891 | 14255 | 796 | 7666 |
| 4 | 800 | 90 | 3 | 270 | 3.50 | 690 | 16607 | 531 | 5111 |
| 4 | 800 | 90 | 4 | 360 | 3.50 | 558 | 17935 | 398 | 3833 |
| 4 | 800 | 90 | 4 | 360 | 3.89 | 522 | 18644 | 322 | 3833 |
| 4 | 800 | 90 | 2 | 180 | 4.00 | 811 | 14829 | 610 | 7666 |
| 4 | 800 | 90 | 3 | 270 | 4.00 | 631 | 17343 | 406 | 5111 |
| 4 | 800 | 90 | 3 | 270 | 5.18 | 524 | 18713 | 242 | 5111 |
| 4 | 800 | 90 | 1 | 90 | 4.50 | 1231 | 12653 | 964 | 15333 |
| 4 | 800 | 90 | 2 | 180 | 4.50 | 748 | 15409 | 482 | 7666 |
| 4 | 800 | 90 | 3 | 270 | 4.50 | 583 | 18062 | 321 | 5111 |
| 4 | 800 | 90 | 3 | 270 | 5.18 | 524 | 18713 | 242 | 5111 |
| 4 | 800 | 90 | 1 | 90 | 5.00 | 1130 | 12912 | 780 | 15333 |
| 4 | 800 | 90 | 2 | 180 | 5.00 | 697 | 15992 | 390 | 7666 |
| 4 | 800 | 90 | 3 | 270 | 5.00 | 538 | 18549 | 260 | 5111 |
| 4 | 800 | 90 | 3 | 270 | 5.18 | 524 | 18713 | 242 | 5111 |

```
1000 REM PROGRAM RAD7
1010 DIM L(20,20)
1020 P0=10
1030 P$=CHR$(P0)
1040 PRINT P$;P$;
1050 PRINT P$;TAB(32);"PROGRAM RAD7"
1060 PRINT TAB(29);"------------"
1070 PRINT P$
1080 PRINT P$;"INPUT DATA"
1090 S=0
1100 PRINT P$;"XXXXX LINE 1, MAX LENGTH, MAX DIAMETER, CONE ANGLE"
1110 INPUT L,D,A
1120 A=A/57.29577951
1130 IF S=0 THEN 1150
1140 GOTO 3340
1150 PRINT P$;"XXXXX LINE 2, REACTOR DIA, REACTOR LENGTH, SHIELD LENGTH
"
1160 INPUT D1,L1,L2
1170 IF S=0 THEN 1190
1180 GOTO 3340
1190 PRINT P$;"XXXXX LINE 3, ELEC PWR, T/E EFF, T/E THICKNESS"
1200 INPUT P,E0,T0
1210 IF S=0 THEN 1230
1220 GOTO 3340
1230 PRINT P$;"XXXXX LINE 4, # OF REAC HPS, # OF RAD HPA PER T/E 1&LAS
T"
1240 INPUT N0,N3,N4
1250 IF S=0 THEN 1270
1260 GOTO 3340
1270 PRINT P$;"XXXXX LINE 5, EMISSIVITY, RADIATOR TEMPERATURE"
1280 INPUT E1,T
1290 T1=T
1300 S1=5.67E-12
1310 S2=S1*E1*T1**4
1320 IF S=0 THEN 1340
1330 GOTO 3340
1340 PRINT P$;"XXXXX LINE 6, FIRST DIAMETER, INCREMENT, LAST DIAM OF R
AD HP"
1350 INPUT I1,I2,I3
1360 DEF FNS(X)=ATN(X/SQR(1-X**2))
1370 S=1
1380 P1=3.141592654
1390 GOTO 3340
1400 PRINT P$;P$;
1410 PRINT P$;P$;TAB(35);"RAD7 OUTPUT"
1420 PRINT TAB(29);"-----------"
1430 PRINT P$;P$;
1440 PRINT USING 1450
1450 ;LAY  TEMP   T/E  HP-T/E  THP    DIA   LENGTH   MASS     Q/A
 Q
1460 PRINT
1470 PRINT USING 1480
1480 ; N     K     N      N      N    CM      CM       KG    W/CM**2
 W
1490 PRINT P$
1500 REM BEGIN CALCULATIONS
1510 FOR D4=I1 TO I3 STEP I2
1520 FOR N=N3 TO N4
1530 IF S5=1 THEN 3260
1540 FOR I=0 TO K+1
1550 FOR J=0 TO 15
1560 L(I,J)=0
```

ORIGINAL PAGE IS
OF POOR QUALITY

```
1580 NEXT I
1590 FOR I=0 TO K+1
1600 P(1,I)=P(2,I)=Q(1,I)=Q(2,I)=X(1,I)=D(1,I)=0
1610 K(1,I)=0
1620 K(2,I)=0
1630 M(1,I)=0
1640 NEXT I
1650 FOR I=0 TO K+1
1660 FOR J=0 TO 7
1670 N(J,I)=0
1680 NEXT J
1690 NEXT I
1700 P5=0
1710 REM CALC REACTOR HP PWR & DIA AT 5 KW/CM**2
1720 P2=P/(N0*E0)
1730 D0=SQR(4*P2/(5000*P1))
1740 REM CALCULATR COLD SIDE T/E DIA
1750 D6=D0+2*T0+2*(D4+1)
1760 REM CALCULATE DIAM AT BEGINING OF T/E
1770 D3=D1+2*(L1+L2)*TAN(A/2)
1780 REM CALCULATE T/E LENGTH AT  AT 25W/CM**2
1790 L0=P2/(25*P1*D0)
1800 REM CALC SLANT LENGTH OF T/E
1810 L3=D6
1820 L4=L3+L0
1830 REM CALCULATE HORZ LENGTH OF T/E
1840 REM CALC INCREASE IN DIA OVER LENGTH OF T/E
1850 D7=2*L4*SIN(A/2)
1860 D(1,0)=D3
1870 L(2,0)=L1+L2
1880 REM HOW MANY T/E AT EACH DIA
1890 K=1
1900 K1=0
1910 N(1,K)=INT(P1/FNS(D6/(D(1,K-1)-D6-(2*K1*D4))))
1920 N(2,0)=N0
1930 N(2,K)=N(2,K-1)-N(1,K)
1940 L(1,K)=L4*COS(A/2)
1950 D(1,K)=D(1,K-1)+D7
1960 L(2,K)=L(2,K-1)+L(1,K)
1970 IF N(2,K)>0 THEN 1990
1980 GOTO 2020
1990 K=K+1
2000 K1=1
2010 GOTO 1910
2020 N(1,K)=N(2,K-1)
2030 REM PERFECT NESTING OF RAD HP AROUND T/E
2040 N1=INT(P1/FNS(D4/(D6-D4-1)))
2050 IF N1>N THEN 2080
2060 PRINT P$;N;"RADIATOR HPS WILL NOT NEST AT T/E";N1;"HEAT PIPES WIL
L"
2070 GOTO 3340
2080 REM PERFECT NESTING OF RAD HP ON OD
2090 FOR I=1 TO K
2100 N(3,I)=INT(P1/FNS(D4/(D(1,I)-D4)))
2110 NEXT I
2120 FOR I=1 TO K
2130 N(4,0)=0
2140 N(4,I)=N(4,I-1)+N*N(1,I)
2150 N(6,I)=N(6,I-1)+N*N(1,I)
2160 N(7,I)=N*N(1,I)
2170 IF N(4,I)<=N(3,I) THEN 2210
2180 N(5,I)=N(6,I)-N(3,I)
2190 N(4,I)=N(3,I)
2200 K(1,I)=I
```

```
2230 N2=INT(P1/FNS(D4/(D-D4)))
2240 IF N(6,K)<=N2 THEN 2340
2250 S5=1
2260 N=N-1
2270 IF N>0 THEN 2300
2280 PRINT P$;"# OF RAD HPS WHICH NEST AT MAX DIA < # OF T/E"
2290 GOTO 3260
2300 I5=D4
2310 I4=SIN(P1/(N*NO))
2320 D4=D*I4/(1+I4)
2330 GOTO 1540
2340 REM CALC EFFICTIVE PIES
2350 FOR I=1 TO K-1
2360 C=D4/(2*(D(1,I)-D4)*SIN(P1/N(4,I)))
2370 C=2*FNS(C)
2380 C=P1+(2*P1/N(4,I))-C
2390 P(1,I)=C/2
2400 C1=D4/(2*(D(1,I+1)-D4)*SIN(P1/N(4,I)))
2410 C1=2*FNS(C1)
2420 C1=P1+(2*P1/N(4,I))-C1
2430 P(2,I)=C1/2
2440 REM CALC EFFECTIVE PIES AT BEGINING OF CONE
2450 C3=D4/(2*(D(1,K)-D4)*SIN(P1/N(4,K)))
2460 C3=2*FNS(C3)
2470 C3=P1+(2*P1/N(4,K))-C3
2480 P(2,K)=C3/2
2490 NEXT I
2500 REM CALC REAMING CONE AND RADIATOR LENGTHS
2510 L6=((D-D1)/(2*TAN(A/2)))-L(2,K)
2520 L8=L6/COS(A/2)
2530 L7=L-L6-L(2,K)
2540 REM CALC SLANT LENGTH OVER T/E
2550 FOR I=1 TO K
2560 L(3,I)=L(1,I)/COS(A/2)
2570 NEXT I
2580 REM CALC POWER REQUIRED / HP
2590 P3=((P/E0)-P)/(N0*N)
2600 REM CALC NECESSARY LENGTH FOR RAD HP
2610 A1=P3/S2
2620 L9=A1/D4
2630 REM CALC EFFECTIVE PIE AT MAX DIAMETER
2640 C2=D4/(2*(D-D4)*SIN(P1/N(4,K)))
2650 C2=2*FNS(C2)
2660 C2=P1+(2*P1/N(4,K))-C2
2670 P4=C2/2
2680 REM CALC RAD HP LENGTH
2690 FOR I=1 TO K-1
2700 L(4,I)=((P(1,I)+P(2,I))/2)*L4
2710 NEXT I
2720 L(4,K)=((P(2,K)+P4)/2)*L8
2730 L(4,K+1)=P4*L7
2740 FOR I=1 TO K+1
2750 L(5,0)=0
2760 L(5,I)=L(5,I-1)+L(4,I)
2770 NEXT I
2780 FOR I=1 TO K
2790 L(7,0)=L(5,K+1)
2800 L(7,I)=L(7,I-1)-L(4,I-1)
2810 NEXT I
2820 FOR I=1 TO K
2830 L(6,I)=L7+L8+((K-I)*L4)
2840 NEXT I
2850 FOR I=1 TO K+1
2860 L(8,I)=L(5,K+1)-L(5,K+1-I)
```

ORIGINAL PAGE IS
OF POOR QUALITY

```
2890 FOR I=1 TO K
2900 Q(1,I)=L(7,I)*D4*S2
2910 Q(2,0)=0
2920 Q(2,I)=Q(2,I-1)+Q(1,I)*N(7,I)
2930 NEXT I
2940 FOR I=1 TO K
2950 FOR J=1 TO K+1
2960 K(2,I)=J
2970 IF L9>L(7,I) THEN 3260
2980 L(9,I)=L(5,K+1)-L(5,I-1)-L(8,J)
2990 IF L(9,I)>L9 THEN 3010
3000 GOTO 3020
3010 NEXT J
3020 X(1,I)=(L9-L(9,I))/(L(8,J)-L(8,J-1))
3030 NEXT I
3040 L(10,K)=L8
3050 L(10,K+1)=L7
3060 FOR I=1 TO K-1
3070 L(10,I)=L4
3080 NEXT I
3090 FOR I=1 TO K
3100 FOR J=1 TO K+1-K(2,I)
3110 L(11,J)=L(11,J-1)+L(10,J)
3120 NEXT J
3130 L(12,I)=L(11,J)-(I-1)*L4
3140 NEXT I
3150 FOR I=1 TO K
3160 L(13,I)=L(12,I)+X(1,I)*L(10,K+1-(K(2,I)-1))
3170 NEXT I
3180 P5=P3/(P1*D4**2/4)
3190 FOR I=1 TO K
3200 M(1,I)=M(1,I-1)+(L(13,I)+L0+L3)*P1*1.02*D4*7.9*N(1,I)*N/1000
3210 L(14,I)=L(14,I-1)+L0+L3+L(13,I)
3220 NEXT I
3230 L(15,K)=L(14,K)/K
3240 PRINT USING 3250,K,T1,N0,N,N0*N,D4,L(15,K),M(1,K),P5,P3
3250 :##   ####   ###    ##    ####  ##.##   ####    #####   #####   #
####
3260 NEXT N
3270 S5=0
3280 IF I5=0 THEN 3310
3290 D4=I5
3300 I5=0
3310 PRINT P$
3320 NEXT D4
3330 PRINT P$;P$
3340 PRINT P$;" CHANGE WHICH LINE (0 TO RUN, STOP TO QUIT)"
3350 INPUT X
3360 IF X=0 THEN 3380
3370 ON X GOTO 1100,1150,1190,1230,1270,1340
3380 PRINT P$;P$;
3390 GOTO 1400
3400 IF X>6 THEN 3340
3410 END

*
?
```